TECHNISCHE HOGESCHOOL DELFT
AFDELING DER SCHEEPSBOUW- EN SCHEEPVAARTKUNDE
LABORATORIUM VOOR SCHEEPSHYDROMECHANICA

Rapport No. 479-P

BOTTOM IMPACT PRESSURES DUE TO FORCED OSCILLATION

W. Beukelman

International Shipbuilding Progress, Volume 27
May 1980, No.309.

Report No. 479 Februari 1979
Ship Hydromechanics Laboratory - Delft.

Delft University of Technology
Ship Hydromechanics Laboratory
Mekelweg 2
Delft 2208
Netherlands

International Shipbuilding *Progress*

Vol. 27 - May 1980 - No. 309 ISSN 0020 - 868X MARINE TECHNOLOGY MONTHLY

devoted to theoretical and practical shipbuilding, marine-engine building and allied subjects; viz. ship hydrodynamics, advanced techniques in shipping and ship design, strength and hull vibration, offshore and mooring problems, ship manoeuvrability and control, unconventional ship types, marine engineering, small craft and dredgers, cargo handling.

Published by International Periodical Press
193 Heemraadssingel,
3023 CB Rotterdam, The Netherlands
Annual subscription rate Dfl. 115.00
single copy Dfl. 10.00
Telephone 010 - 773325
Telegrams Inpress - Rotterdam
Bankers RABO-Bank, Rotterdam
acc.nr. 14.15.38.678

Contributions for publication
Editors International Shipbuilding Progress
Postbox 199, 2600 AD Delft, The Netherlands

BOTTOM IMPACT PRESSURES DUE TO FORCED OSCILLATION*

by

W. Beukelman **

Abstract

Forced oscillation tests about the water surface have been carried out with a segmented ship model to measure slamming pressures on two segments.
A calculation procedure based on a two-dimensional approach has been proposed.
These analytical results, together with those of other theories have been compared with the measurements.
The results of the proposed calculation method proved to be rather satisfactory.

1. Introduction

The literature about tests and theories on slamming is rather extensive.
In most of the experiments, the object was to find a relation between the vertical impact velocity and the maximum slam pressure [1, 2, 3, 4, 5, 6]. A general form for this relation is presented by Margaret Ochi and José Bonilla-Norat in [3] as

$$p = kv^n$$

where:

p = the impact pressure
v = the impact velocity
k and n are constants.

Experimentally, these authors found that the pressure is proportional to the square of the velocity at impact and that the proportionality constant k is dependent on the section shape. Others like Takezawa et al., M.K. Ochi, L.E. Motter [1, 2, 7] used a similar relation,

$$p = \tfrac{1}{2}\rho\, k_1 v^2$$

and established experimentally the coefficient k_1 of the impact pressure dependent on the position considered as a flat bottom or stem front. For the pressure distribution on the surface of a wedge-shaped body the authors used the well-known formula of Wagner [8].
Remarkable model test results, together with theoretical results, are presented by P. Kaplan et al [9] for the case of bow slamming of SES craft in waves.
Most frequently used up to now is the procedure introduced by Tick [10] and Ochi [4] with respect to bottom impact slamming. After some evaluations, Ochi et al [4, 11] stated two conditions required for bottom impact slamming to occur viz.:

a. bow (fore foot) emergence
b. a certain magnitude of relative velocity between wave and ship bow.

*) Report 479 P.
**) Delft University of Technology, Ship Hydromechanics Laboratory, Delft, The Netherlands.

The critical relative velocity below which slamming does not occur is called the 'threshold velocity', denoted by v^*.
Ochi showed by tests on a Mariner model that the threshold velocity is nearly constant with an average of 12 fps for a ship of 520 ft length. Aertssen [12] advised that the threshold value should be 50 percent greater for the Mariner, that is 18 fps. Mostly the threshold velocity according to Ochi is accepted with an appropriate Froude scaling law for ships of different lengths.

To analyse the problem experimentally a series of drop tests with a flat plate [13, 14] or a wedge [7, 15, 16, 17] have been executed. Very often, the behaviour of the air layer between the falling body and the water surface has been taken into consideration [13, 18, 19, 20].
Chuang [21] showed that the effect of this compressible air causes a remarkable reduction of the acoustic pressure, which is frequently assumed.
Mathematical models have been developed to describe the cushioning effect of the air between the descending body and the water surface for instance by Verhagen [13] and Greenberg [20]. The predictions of Verhagen showed good agreement with experimental results. It is, however, rather complicated to apply these theories to the real problem of ship bottom impact because no account is taken of forward speed or of the three-dimensional flow caused by changes in the shape of the sections.

Model experiments in waves or full scale observations may statistically deliver rather good and useful results [1, 2, 3, 4, 6, 12, 22], but do not give a deeper insight in the phenomena slamming. This might be very important for establishment of design criteria.

Several authors have tried to formulate mathematical models describing slamming [13, 20, 22, 23, 24, 25, 26, 27].
The great majority of them accepted the rate of change of the momentum of the hull's added mass as the main cause of the arise of slamming forces. In this way they

The characteristics of the pressure transducers were as follows:

- Manufacture : Druck Ltd.
- Type : PDCR 42
- Range : 69 kPa (10 psi)
- Acceleration sensitivity : for 69 kPa: 0.002% of full scale output/*g*
- Temperature drift and thermal shock : 0.02%/°C/FSO
- Natural frequency (in air) : 15 kHz.

The output signals of the pressure transducers, situated at the bottom of the segments, were amplified and recorded simultaneously on an analog instrumentation *tape recorder* and *UV-recorder.* The latter had been used for visual observation and preliminary determination of the peak values of the impact pressures. Recording on the tape recorder took place at high speed (1.5 m/s or 60 ips) to ensure a sufficient bandwidth.

The block diagram of Figure 4 shows the instrumentation set-up for the experiments. After the measurements the slamming signals were replayed one at a time and fed via a delay line to a correlator which was used in its signal recovery mode.

By using a mechanical oscillator there is an enormous ratio between the interval time of the oscillation and the width of the impact wave form. Only a small part of the cyclus has to be isolated. Therefore the signal is sent through an analog delay line to catch both the slamming wave form and a small piece of the signal preceeding the impact.

A trigger pulse generated by the slamming wave form at the input of the delay line triggered the correlation and after 20 ms the delayed wave form entered the correlator.

The principle of signal recovery is to examine a part of the signal following the trigger pulse and by repeating this observation to extract a coherent pattern. After each triggerpulse a series of 100 samples is taken and added to the corresponding samples of the previous series. In this way the coherent pattern is reinforced at each repetition while noise present in the signal is surpressed to a degree dependent on the number of pulses that had been averaged. After a summation of 128 repetitions the result had been normalised (divided by 128) and could be displayed and reflected on an X-Y recorder.

A digital storage oscilloscope was used to monitor the slamming signals. The results obtained with the correlator had to be carefully interpreted. A time jitter

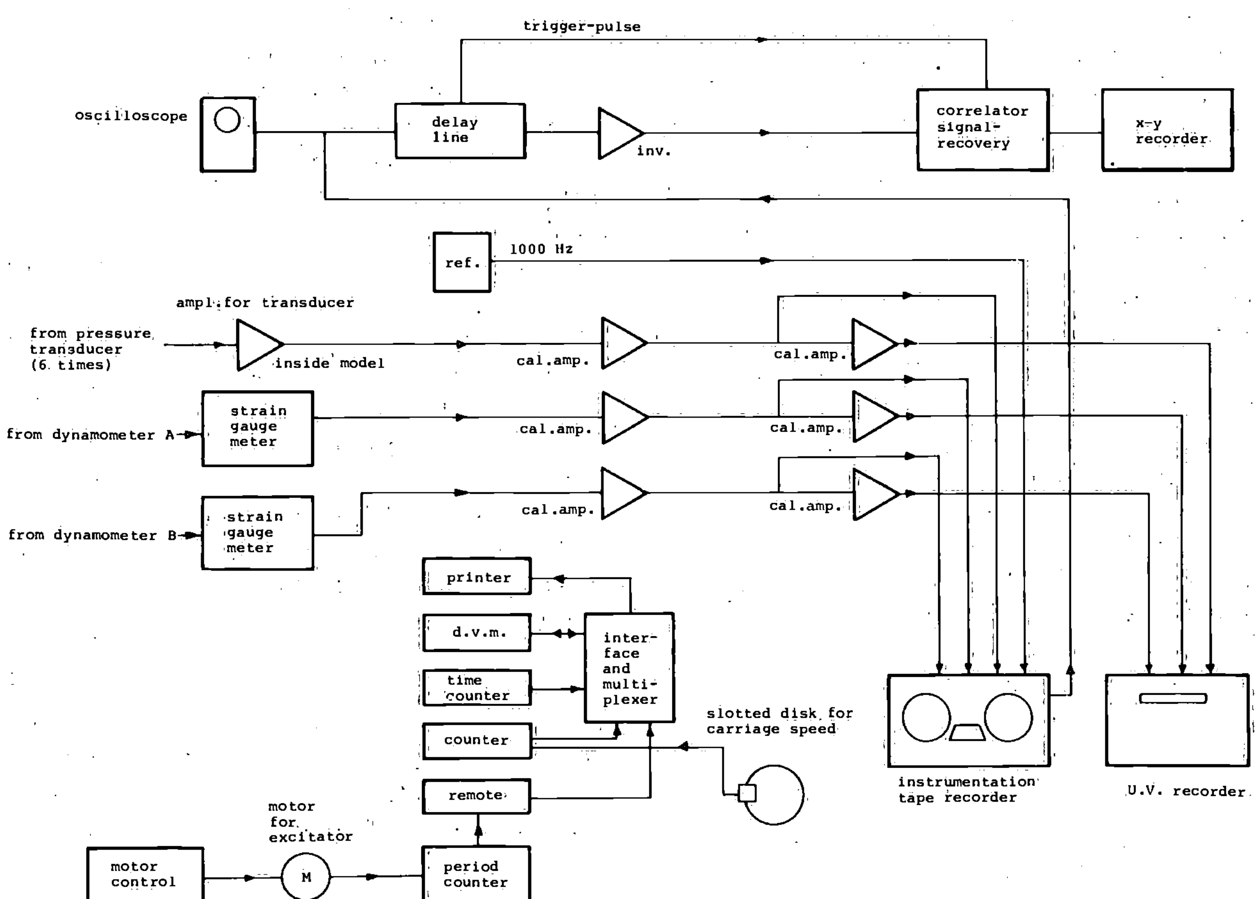

Figure 4. Block diagram.

could occur between the triggerpulse and the peak of the slamming wave form due to the great difference in both shape and amplitude of the succeeding wave forms. As a result the peak value could be somewhat too small and the width of the impact wave form too large. However the energy contained under the pulse was still correct and represented the energy of an average impact wave form.

During the experiments photo's were taken of the model bottom to obtain an impression of the behaviour of air. See Figure 2. The camera shutter was opened when the model was in the near vicinity of the camera and an electronic flash was fired at the first trigger pulse generated by an impact wave form. Therefore the photo's were made at almost the same moment that the impact took place.

3. Analysis of test results

Occasionally, the measured local slamming pressures were compared with the pressures derived from the force-measurements on the segments. Although equality could not be expected, the agreement in the order of magnitude appeared to be satisfactory. The measurements showed that the impact pulses during one run could differ a great deal in shape. Using the method as described in 2.1., it was possible with the aid of a correlator to obtain an average pulse with satisfactory consistency.

A reasonable agreement could also be established between the values of the peak pressures obtained from the UV-recorder and those derived from the correlator, although it remains as stated in 2.1. that the peak values from the correlator are somewhat less reliable.

From the peak pressures measured by the UV-recorder and shown in Figures 10-12 it is clear that with respect to the longitudinal position of the pressure gauges the most forward one, E, delivered the highest values. This effect, which might be due to the higher impact velocities or to the smaller wetted width of the section will be discussed in 4.1. and 6.

The influence of the transverse position of the pressure gauges on the slamming pressures appeared to be negligible as shown in Figure 10-12.

According to expression (7) of the proposed theory, the pressures measured by A, B and F should be equal in the cases of pitching and heaving motions with an angle between bottom and water surface. From Figures 10-12, it is obvious that this fact was confirmed satisfactorily by experiments.

The effect of forward speed appeared to be remarkably small for the cases where the bottom was parallel to the water surface. Greater forward speed effects were measured for the other cases. These results also agree with the proposed theory, as will be discussed in 4.2.3. and 6.

For heave and pure pitch, the measured peak pressures have been non-dimensionalized as $p/\frac{1}{2}\rho v^2$ and plotted versus the frequency of oscillation for the various gauges and speeds as indicated in Figure 13. This dimensionless pressure also represents the well-known proportionality constant.

From the figures, however, it is clear that such a constant, proportional to the squared vertical velocity could not be established for all frequencies of oscillation.

For a certain frequency of oscillation there was a slight indication that the peak pressures are proportional to the squared amplitude of oscillation.

It was assumed that the value of the peak pressure was not significantly influenced by the elastic characteristics of the model-bottom. The oscillations in the pressure after the peak as shown in Figure 3 might have been due to the elasticity of the bottom material.

The amount of time required to obtain the peak pressure varied greatly with an average of about 4 à 5 ms for the case with the bottom parallel to the water surface. For heaving, with an angle between bottom and water surface, there was a large reduction of this rise-time to about 1 ms. This might have been due to the greater influence of the high accelerations of the added mass, which according to the proposed theory occurred as a consequence of the arise of the forward speed component.

This time, as denoted in (18) should be shorter than the rise-time.

The photographs (Figure 2) made of the model-bottom at the moment of impact with the water-surface show that the air layer is most significant when the bottom is parallel to the water surface. As soon as there is an angle between bottom and water surface a large reduction of the amount of trapped air can be established. Concerning this observation, it should be remarked that the distribution of the air about the model bottom seemed rather random, so no consistant pattern was observed.

Finally, it is worthwhile to stress the advantages of using a PMM (Planar Motion Mechanism) for the analysis of slamming. Vertical speed, acceleration and angle with the water surface are perfectly adjustable, while the behaviour of air can be easily observed.

4. Proposed calculation method for determining slam pressures

4.1. General

It is essential for determining slam pressures to divide the velocities into two components: one component along the hull (or keel-line), and one component perpendicular to the hull. The velocities along the hull determine the so-called planing pressure which is usually small and insignificant in comparison with the impact pressure [26].

Therefore this impact pressure is mainly determined by the velocities normal to the hull. In the case of a ship with a flat bottom, the impact pressures on the bottom can be determined if the velocities normal to the bottom are known. This case will be considered here.

The calculation method is based on the strip theory as presented in [28]. The hydromechanic force per unit length on a strip of an oscillating ship in still water with respect to the coordinate system $x_b\ y_b\ z_b$ fixed to the ship at the center of gravity (Figure 5) will be

$$F' = F_1' + F_2' + F_3' \qquad (1)$$

in which:

$$F_1' = -2\rho\, g\, y_w s$$
$$F_2' = -N'\dot{s}$$
$$F_3' = -\frac{d}{dt}(m'\dot{s})$$

with:

- ρ = density of water
- g = acceleration of gravity
- y_w = half width of the cross-section at the moment of touching the water surface
- m' = the sectional added mass
- N' = the sectional damping
- s = the displacement of the strip into the z_b-direction, so perpendicular to the bottom.

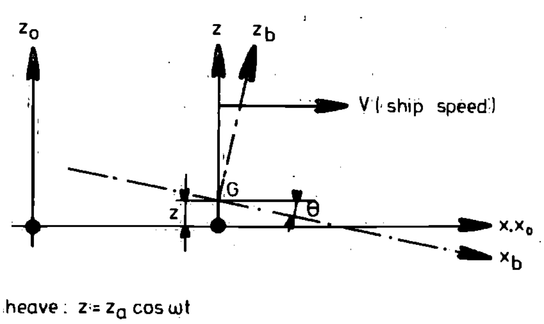

Figure 5. Coordinate systems.

For a pure heaving oscillation $z = z_a \cos\omega t$ about the waterline with the keel-line or bottom parallel to the waterline

$$s = z = z_a \cos\omega t \qquad (2)$$

while for a pure pitching oscillation $\theta = \theta_a \cos\omega t$ about the waterline

$$s = x_b \theta_a \cos\omega t \qquad (3)$$

x_b is the distance between the strip considered and the centre of gravity where the origin of the $x_b y_b z_b$ coordinate system is assumed to be located, see Figure 5.

It is possible to write the sectional hydromechanic force of (1) as follows:

$$\begin{aligned} F' &= -\left(2\rho g\, y_w s + N'\dot{s} + \frac{dm'}{dt}\dot{s} + m'\ddot{s}\right) \\ &= -\left(2\rho g\, y_w s + N'\dot{s} + \frac{dm'}{ds}\dot{s}^2 + m'\ddot{s}\right) \end{aligned} \qquad (4)$$

The total slam-force on a strip may be expressed as:

$$F' dx_b = 2p\, y_w\, dx_b \qquad (5)$$

in which:

p = the slam pressure

Substitution of (4) into (5) delivers the following expression for slam pressure:

$$p = -\left(\rho g s + \frac{N'}{2y_w}\dot{s} + \frac{dm'}{ds}\frac{1}{2y_w}\dot{s}^2 + \frac{m'}{2y_w}\ddot{s}\right) \qquad (6)$$

The first term of the right hand side may be neglected because of the very small displacement during the time that the maximum slam pressure is built up. So the general expression for the slam pressure may be written as:

$$p = -\frac{1}{2y_w}\left(N'\dot{s} + \frac{dm'}{ds}\dot{s}^2 + m'\ddot{s}\right) \qquad (7)$$

From (7) it appears that

1. the slam pressure mainly is composed of three hydro-dynamic terms.
2. the slam pressure is inversely proportional to the 'wetted width', $2y_w$.
3. the second term is proportional to the squared vertical strip velocity.

Further remarks which can be made about the slam pressure are:

1. the first hydrodynamic term containing the sectional damping will deliver a small contribution to the total slam pressure because it is proportional to only the first power of the vertical strip velocity.
2. from the second hydrodynamic term, it appears that the increase of added mass with depth is very important.
3. the third hydrodynamic term may become very significant if the vertical strip acceleration is high. This may be the case if there is a component due to the forward velocity of the ship. This phenomenon will be considered further on.

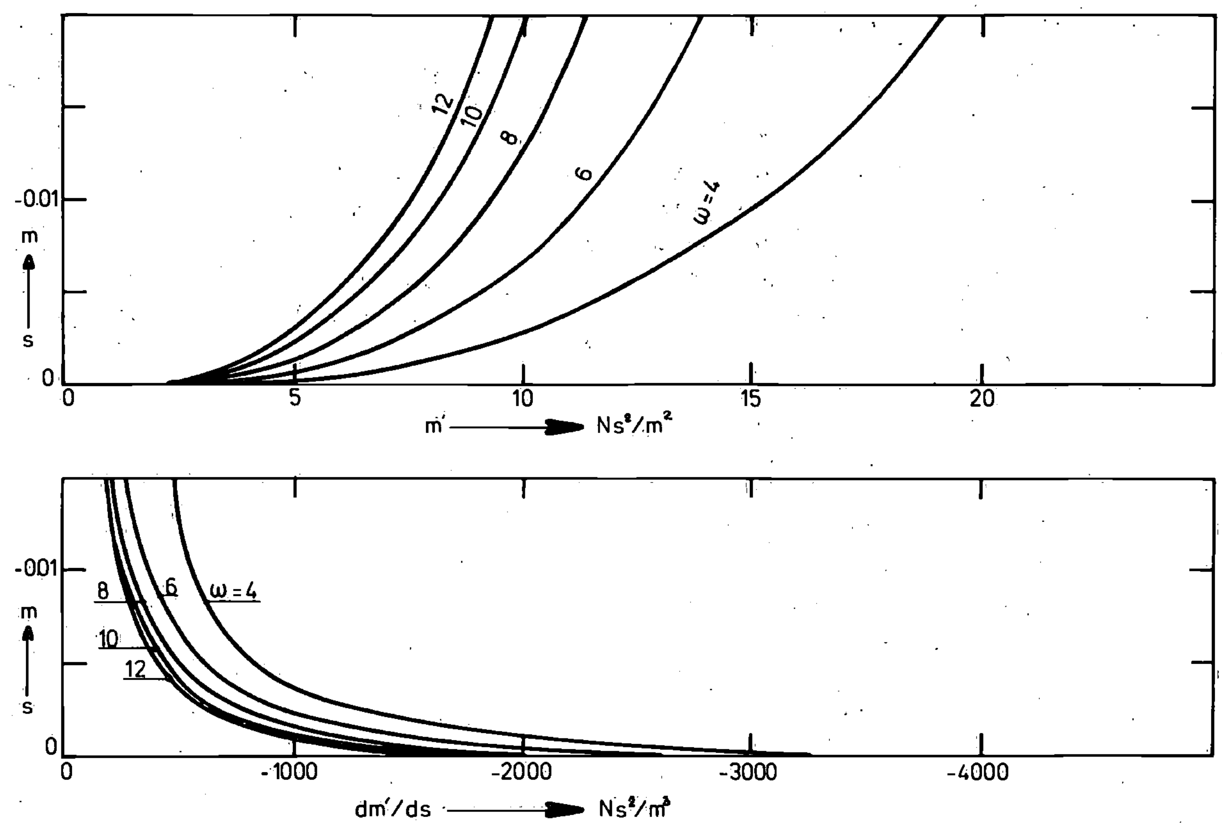

Figure 6. Added mass and rate of change of added mass with depth per unit length for the section at pressure gauge *E*.

4. the value which should be taken for the hydrodynamic mass is not clear. In this work the adjusted frequency of oscillation has been used, but there might also be reasons related to the transient character of slamming to start from infinite frequency or to consider a spectral value for the added mass.

4.2. Determination of speeds and accelerations

At first the velocities and accelerations due to oscillations will be calculated and afterwards the influence of forward speed will be considered.

4.2.1. Heave oscillation

For the heaving motion, the displacement of a strip is defined as:

$$s = z = z_a \cos \omega t \qquad (2)$$

from which follows:

the strip velocity $\dot{s} = \dot{z} = -\omega\, z_a \sin \omega t$

and (8)

the strip acceleration $\ddot{s} = \ddot{z} = -\omega^2 z_a \cos \omega t$

with:

ω = circular frequency of oscillation

z_a = amplitude of heave oscillation.

In the case of pure heaving with the bottom of the model at the water surface in the zero position of the oscillator, it is clear that at the moment of impact with the water surface the strip velocity will achieve a maximum value while the acceleration becomes zero. This means that the third hydrodynamic term of equation (7), $\frac{m'\ddot{s}}{2y_w}$, does not contribute to the slam pressure for this case.

For heaving of the bottom about the waterline with a constant angle between bottom and watersurface, the situation is different.

If a point P on the bottom is situated at a distance z_o above the waterline in the zero position of the oscillator (Figure 7) there will be contact with the water surface if:

$$z = z_a \cos \omega t = -z_o = -x_b\ tg\alpha$$

$$\text{or if arc}\left(\cos \omega t = \frac{-x_b\ tg\alpha}{z_a}\right) = \gamma \text{ and } \dot{s} < 0 \qquad (9)$$

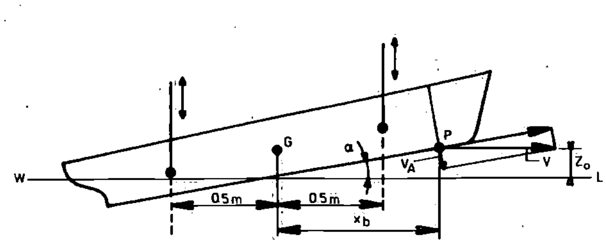

Figure 7. Heaving with an angle.

The velocity and acceleration perpendicular to the bottom due to oscillation for the section at P at the moment of contact with the watersurface are respectively:

$$\dot{s} = -z_a \omega \sin\gamma \cos\alpha$$
$$\ddot{s} = -z_a \omega^2 \cos\gamma \cos\alpha \quad (10)$$

The angle α is small (2.3 degrees) and so it may be assumed that $\cos\alpha \simeq 1$.

Another velocity component perpendicular to the bottom results from the forward speed viz.:

$$V_A = -V\sin\alpha \quad (11)$$

This influence will be discussed in 4.2.3.

4.2.2. Pitch oscillation

For the pitching motion the displacement of a strip may be expressed as:

$$s = x_b\theta = x_b\theta_a \cos\omega t \quad (3)$$

from which follows:

the strip velocity $\dot{s} = -x_b\omega\theta_a \sin\omega t$
and
the strip acceleration $\ddot{s} = -x_b\omega^2\theta_a \cos\omega t$ (12)

For pitching around the aft leg with a certain draught T' of the model the situation is different. See Figure 8.

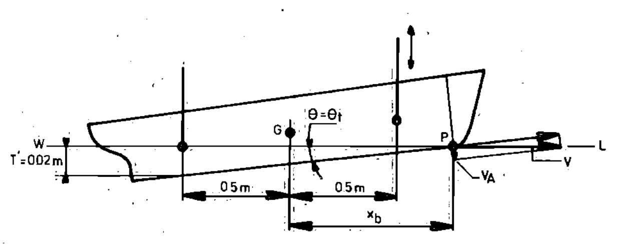

Figure 8. Pitching around the aft leg for the model with a draught $T' = 0.02$ m.

If the fore leg has a displacement $z = z_a\cos\omega t$ the vertical displacement of a point P at the bottom will be

$$z' = z_a(x_b + 0.5)\cos\omega t \quad (13)$$

The water surface will be contacted if

$$z' = T'$$

therefore holds:

$$\text{arc}\left(\cos\omega t = \frac{T'}{z_a(x_b + 0.5)}\right) = \gamma \text{ and } \dot{s} < 0 \quad (14)$$

The velocity and acceleration perpendicular to the bottom due to oscillation for the section at P at the moment of contact with the water surface are respectively:

$$\dot{s} = -z_a(x_b + 0.5)\omega \sin\gamma \cos\theta_t$$
$$\ddot{s} = -z_a(x_b + 0.5)\omega^2 \cos\gamma \cos\theta_t \quad (15)$$

θ_t is the angle between the bottom and the water surface when the point P contacts the water surface and may be characterized by:

$$\theta_t = \text{arc}\left(tg\,\theta_t = \frac{T'}{x_b + 0.5}\right) \quad (16)$$

For this case θ_t is small (up to one degree) and so it may be assumed that $\cos\theta_t \simeq 1$.

Another velocity component perpendicular to the bottom results from the forward speed viz.:

$$V_A = -V\sin\theta_t \quad (17)$$

4.2.3. Influence of forward speed

For heaving and pitching with the bottom parallel to the water surface at the moment of contact there is no component of the forward speed normal to the bottom. If the bottom makes an angle α or θ_t with the water surface, the component V_A of the forward speed normal to the bottom, will arise for a particular strip as derived in 4.2.1. and 4.2.2.

If this component V_A develops within the time that the maximum slam pressure occurs the added mass of the strip will be subjected to very high accelerations.

It is reasonable to expect that the effect of these high accelerations on the added mass is dependent on the draught of the strip or wetted part of the section and for this reason also dependent on the strip velocity $\dot{s}$ due to oscillation.

The maximum value of the acceleration for the sectional added mass will be determined in accordance with the assumptions in the appendix.

The following calculation procedure with respect to the influence of the forward speed is proposed:

1. Determine the normal strip velocity V_A which should be achieved on account of the angle of the bottom with the water surface.
2. It is first assumed that the added mass has achieved the velocity V_A if the displacement of the strip $s \doteq 0.00015$ m and the time in which this takes place is

$$t = \frac{0.00015}{\dot{s}} \quad (18)$$

3. Next the average acceleration is determined by

$$a_a = \frac{V_A}{t} \quad (19)$$

4. Furthermore, it is assumed that the peak pressure is dependent on the maximum acceleration. This maximum acceleration due to the forward speed component will be determined as proposed in the

appendix

$$a_{max} = 1.5\, a_a \qquad (20)$$

5. Finally the total maximum acceleration of the sectional added mass perpendicular to the bottom is found to be:

$$\ddot{s}' = \ddot{s} + a_{max} \qquad (21)$$

4.3. Execution of the calculations

To carry out the proposed calculations, it was first necessary to determine the sectional added mass and damping for several draughts and for the bottom of the model. The Frank-computer program [29] was used to make these calculations. For numerical reasons, it was necessary to introduce a slight deadrise in the bottom and a slight draught. A deadrise of 0.00002 m and a draught of the same value served as initial inputs.

For small draughts (below 0.00004 m) the variations in added mass and damping are negligable. All these calculations have been carried out for several sections after which added mass and damping have been determined by interpolation for the sections where the pressure-gauges were situated.

Afterwards the rate of change of added mass with depth, dm'/ds, has been determined in the same way and values have been graphically established for zero draught. See Tables 2 and 3. As an example, the results are shown in Figure 6, for pressure gauge E.

Calculations of the peak slam pressures have been executed in accordance with equation (7) for the modes of motions considered with and without the forward speed influence as proposed in 4.2.3.

Results are shown in Table 4 and Figures 10-12 where the peak pressures are plotted on the basis of the impact velocity:

$$v = \dot{s}' = \dot{s} + V_A \qquad (22)$$

Table 2

Sectional hydrodynamic characteristics for pure heave

ω	Section at pressure gauge											
	A		B		C		D		E		F	
	y_w = 0.124 m		y_w = 0.124 m		y_w = 0.124 m		y_w = 0.089 m		y_w = 0.034 m		y_w = 0.072 m	
	N'	$\frac{dm'}{ds}$	N'	$\frac{dm'}{ds}$	N'	$\frac{dm'}{ds}$	N'	$\frac{dm'}{ds}$	N'	$\frac{dm'}{ds}$	N'	$\frac{dm'}{ds}$
s^{-1}	$\frac{Ns}{m^2}$	$\frac{Ns^2}{m^3}$	$\frac{Ns}{m^2}$	$\frac{Ns^2}{m^3}$	$\frac{Ns}{m^2}$	$\frac{Ns^2}{m^3}$	$\frac{Ns}{m^2}$	$\frac{Ns^2}{m^3}$	$\frac{Ns}{m^2}$	$\frac{Ns^2}{m^3}$	$\frac{Ns}{m^2}$	$\frac{Ns^2}{m^3}$
4	148	−4542	150	−4179	150	−4316	72	−6377	16	−3051	59	−5042
6	169	−3836	171	−3257	170	−3473	86	−5435	21	−2354	71	−4179
8	175	−3237	177	−3012	176	−3090	92	−4365	23	−1874	77	−3365
10	171	−3110	173	−2796	173	−2914	94	−3875	25	−1648	79	−2992
12	162	−3090	163	−2815	163	−2914	93	−3689	26	−1511	79	−2835

Table 3

Sectional hydrodynamic characteristics for pitch and heave with an angle

ω	Section at pressure gauge											
	A, B, F			C			E			D		
	y_w = 0.0722 m			y_w = 0.053 m			y_w = 0.034 m			y_w = 0.089 m		
	N'	m'	$\frac{dm'}{ds}$	N'	m'	$\frac{dm'}{ds}$	N'	m'	$\frac{dm'}{ds}$	N'	m'	$\frac{dm'}{ds}$
s^{-1}	$\frac{Ns}{m^2}$	$\frac{Ns^2}{m^2}$	$\frac{Ns^2}{m^3}$	$\frac{Ns}{m^2}$	$\frac{Ns^2}{m^2}$	$\frac{Ns^2}{m^3}$	$\frac{Ns}{m^2}$	$\frac{Ns^2}{m^2}$	$\frac{Ns^2}{m^3}$	$\frac{Ns}{m^2}$	$\frac{Ns^2}{m^2}$	$\frac{Ns^2}{m^3}$
4	59	16	−5042	38	10	−4052	16	5	−3051	72	19	−6377
6	71	12	−4179	46	8	−3276	21	4	−2354	86	14	−5435
8	77	10	−3365	50	6	−2619	23	3	−1874	92	12	−4365
10	79	9	−2992	52	6	−2325	25	3	−1648	94	11	−3875
12	79	8	−2835	52	5	−2178	26	2	−1511	93	10	−3689

Table 4

Calculated pressures for gauge E; $r = 0.04$ m; $y_w = 0.034$ m

mode of motion	ω	$\frac{N'}{2y_w}\dot{s}$	$\frac{dm'}{ds}\frac{\dot{s}^2}{2y_w}$	v=0.706 m/s		v=1.412 ms		$\frac{m'}{2y_w}\ddot{s}$ kPa			p kPa		
				$t.10^3$	a_{max}	$t.10^3$	a_{max}	V= 0 m/s	V= 0.706 m/s	V= 1.412 m/s	V= 0 m/s	V= 0.706 m/s	V= 1.412 m/s
	s^{-1}	kPa	kPa	s	m/s²	s	m/s²						
pure heave (T' = 0 m)	4	0.04	1.15	-	-	-	-	-	-	-	1.19	1.19	1.19
	6	0.07	1.99	-	-	-	-	-	-	-	2.06	2.06	2.06
	8	0.11	2.82	-	-	-	-	-	-	-	2.93	2.93	2.93
	10	0.15	3.87	-	-	-	-	-	-	-	4.02	4.02	4.02
	12	0.19	5.10	-	-	-	-	-	-	-	5.29	5.29	5.29
pitch (T' = 0 m)	4	0.05	1.74	-	-	-	-	-	-	-	1.79	1.79	1.79
	6	0.09	3.02	-	-	-	-	-	-	-	3.11	3.11	3.11
	8	0.14	4.27	-	-	-	-	-	-	-	4.41	4.41	4.41
	10	0.18	5.88	-	-	-	-	-	-	-	6.06	6.06	6.06
	12	0.23	7.74	-	-	-	-	-	-	-	7.97	7.97	7.97
pitch (T' = 0.02 m)	4	0.04	1.45	0.83	−20	0.83	− 41	0.02	1.40	2.91	1.51	2.89	4.40
	6	0.08	2.52	0.56	−30	0.56	− 52	0.04	1.62	3.36	2.64	4.22	5.96
	8	0.13	3.56	0.42	−40	0.42	− 83	0.06	1.80	3.69	3.75	5.49	7.38
	10	0.17	4.99	0.33	−50	0.33	−104	0.08	1.95	4.01	5.14	7.01	9.07
	12	0.21	6.45	0.28	−59	0.28	−124	0.10	2.12	4.33	6.76	8.78	10.99
heave with (T' = 0 m) α = 2.3°	4	0.03	0.53	1.37	−31	1.37	− 62	−0.03	2.10	4.31	0.53	2.66	4.87
	6	0.05	0.91	0.92	−46	0.92	− 93	−0.06	2.38	4.90	0.90	3.34	5.86
	8	0.08	1.29	0.69	−61	0.69	−124	−0.08	2.58	5.35	1.29	3.95	6.72
	10	0.10	1.78	0.56	−75	0.56	−154	−0.11	2.78	5.76	1.77	4.66	7.64
	12	0.13	2.35	0.46	−91	0.46	−186	−0.15	2.97	6.19	2.33	5.45	8.67

From the calculations it appears that:

1. The sectional damping given by the first hydrodynamic term of equation (7) has very low values for all motions.
2. For oscillations with the model-bottom at the water surface in the zero position of the oscillator, only the second hydrodynamic term of equation (7) has a significant value.
3. The rate of increase of added mass with depth *dm'/ds* for zero draught is very important for all motions, but not easily established and very sensitive.
4. The correction for the influence of forward speed might be very significant for the case of an angle between bottom and water surface at the moment of contact. It is strongly dependent on the value which has been taken for the section draught necessary to achieve the vertical forward speed component.

   The correction of the forward speed as proposed in 4.2.3. influences only the third hydrodynamic term of equation (7) containing the acceleration of the sectional added mass. However, there should also be an increasing influence on the second hydrodynamic term with the increase of the vertical forward speed component.

   This influence was neglected in these calculations, but has been considered separately before with respect to the maximum value of the forward speed component without taking into account the influence of the accelerations as proposed in 4.2.3. In this way the peak slam pressures remain far too low, especially for the case of heaving with an angle of trim.

   In fact, the problem is rather complex. Both influences are working together, however the one proposed in 4.2.3. appeared to be a great deal stronger.

4.4. Units

All units in this paper are presented according to the 'Système Internationale d'Unités' (SI).

For convenience the following conversion factors with respect to the former technical or kg(force)-m-sec units and the related English units are given for:

force	: 1 N	= 1 kg m s^{-2}	(SI)
		= 0.1019 kgf	(technical units)
		= 0.225 lb	(English units)
length	: 1 m	= 3.28 ft	(English units)
		= 39.37 in	
pressure	: 1kPa	= 1000 Nm^{-2} = 1000 kg m^{-1} s^{-2}	(SI)
		= 101.937 kgf/m^2	(technical units)
		= 0.145 psi	(English units)
mass	: 1 kg	= 1 Ns^2 m^{-1}	(SI)
		= 0.1019 kgf s^2 m^{-1}	(technical units)

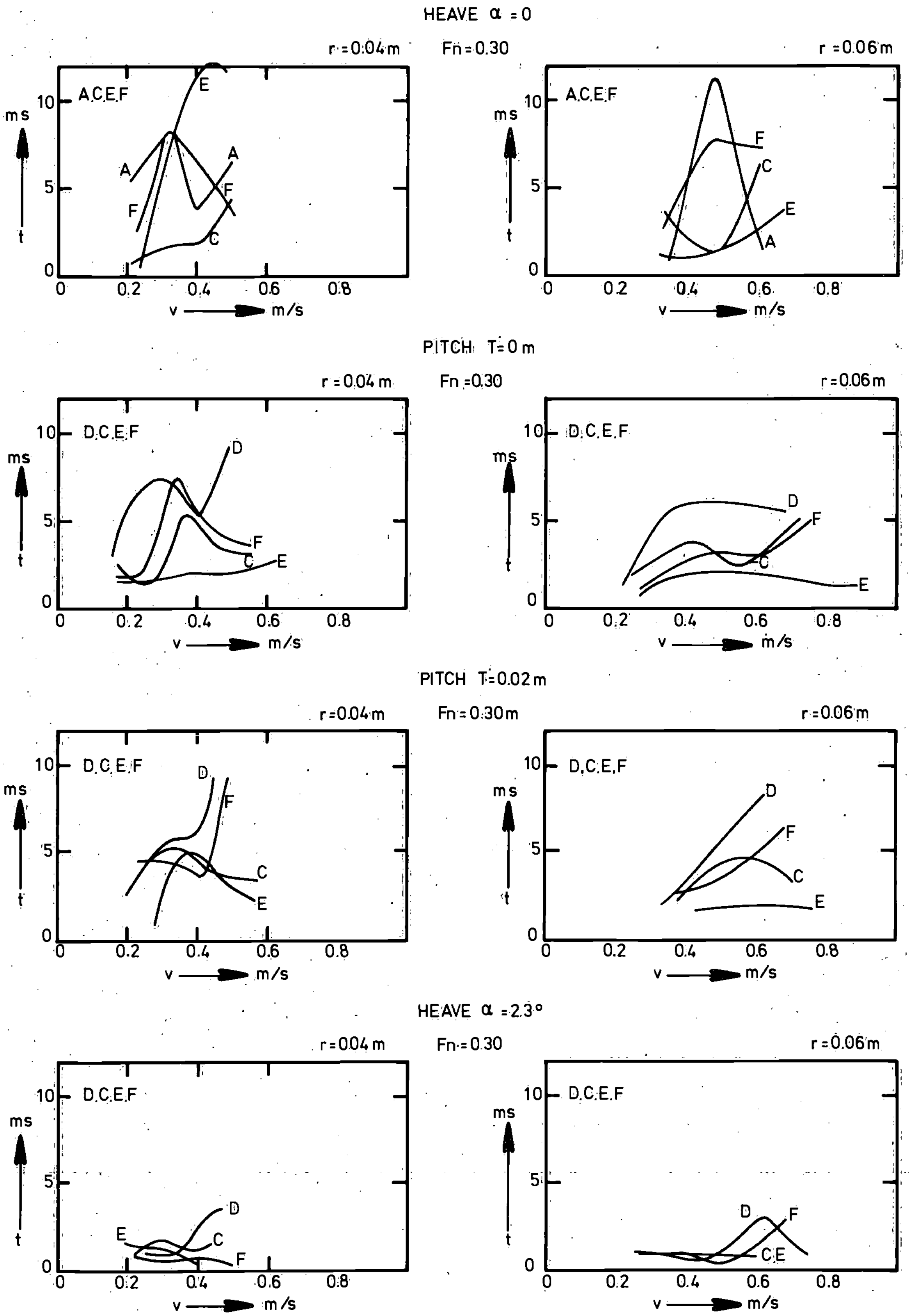

Figure 9. Time in which peak pressure develops.

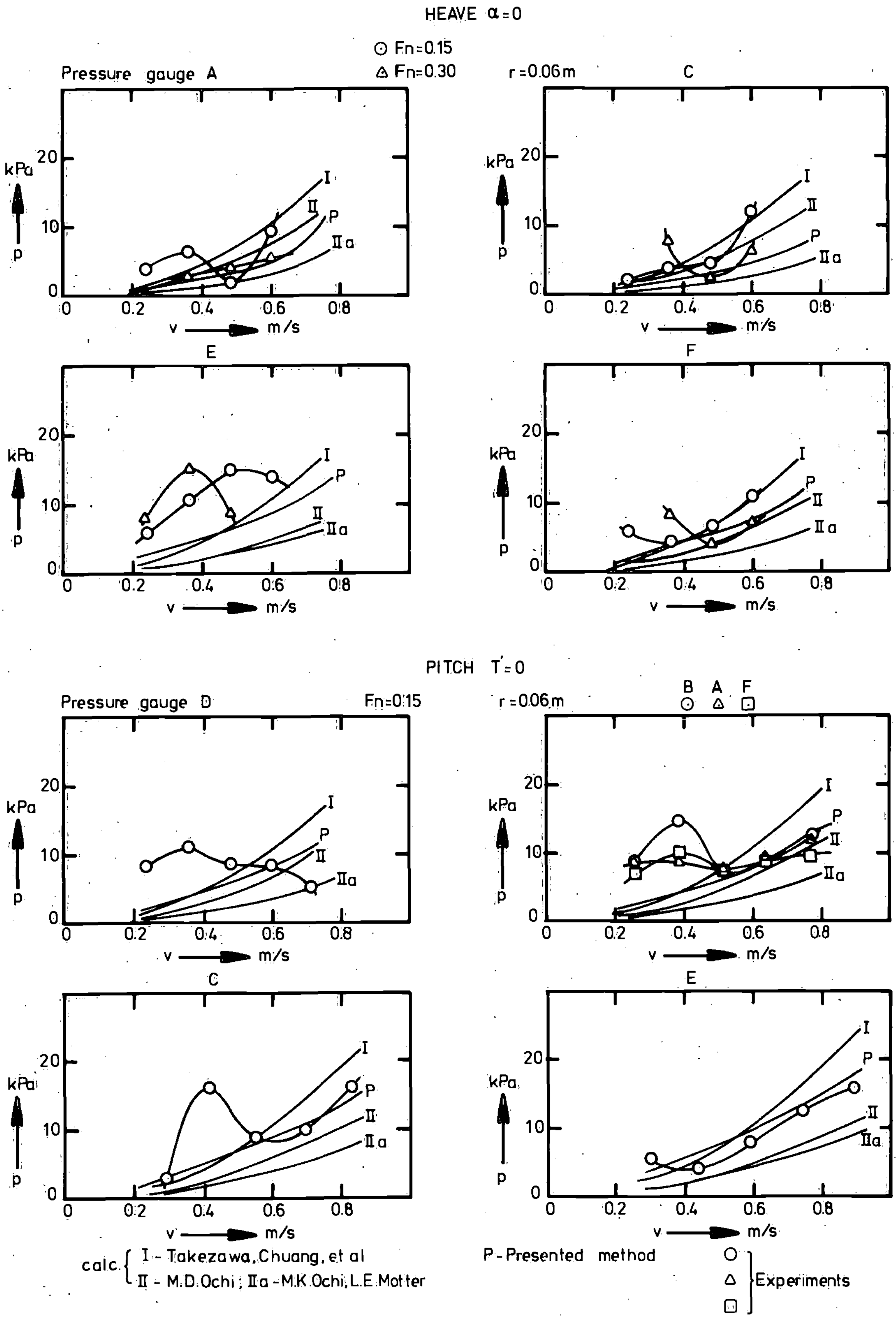

Figure 10. Test- and calculation results of peak pressure for pure heave and pitch.

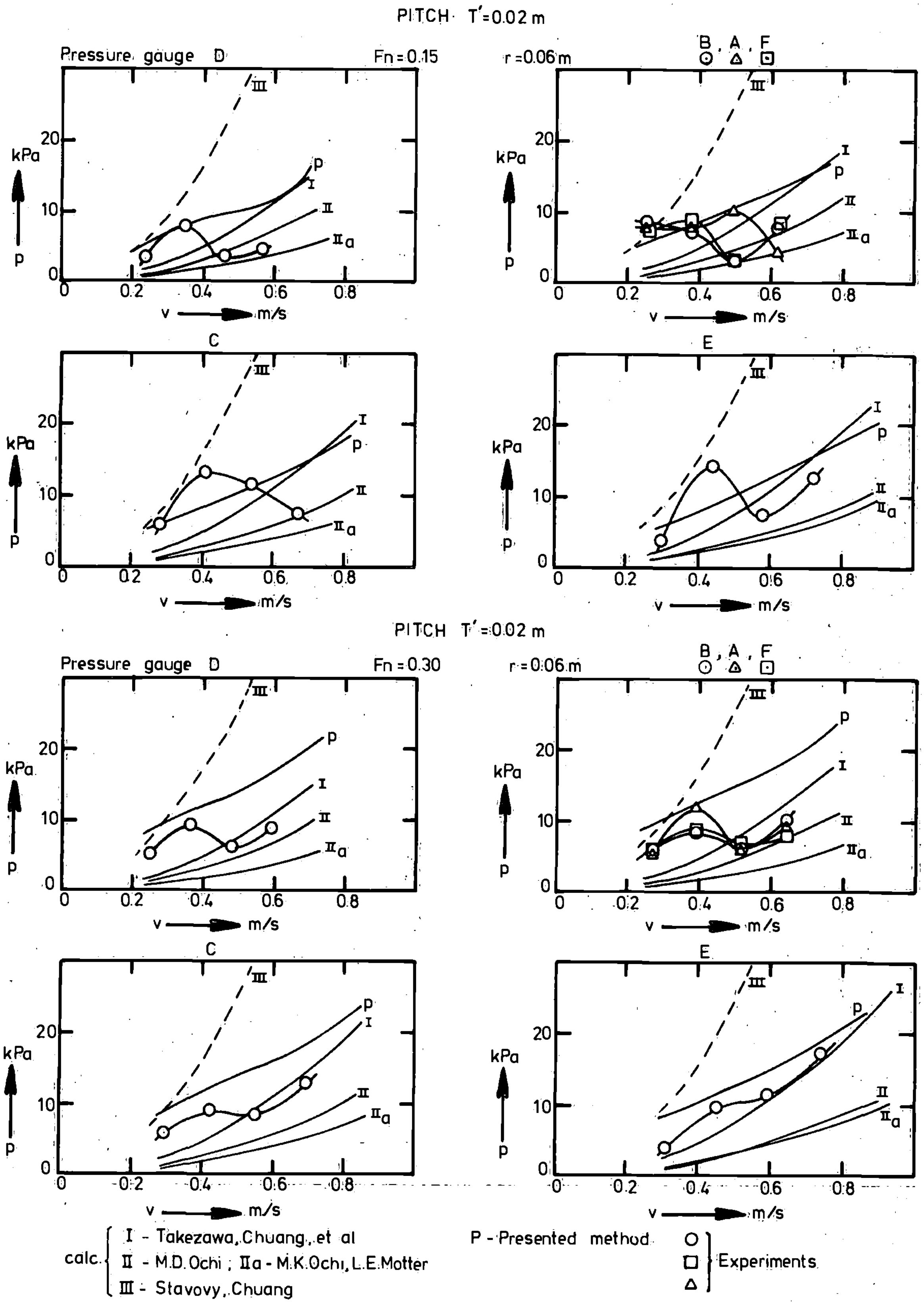

Figure 11. Test- and calculation results of peak pressure for pitch around the aft leg with $T' = 0.02$ m.

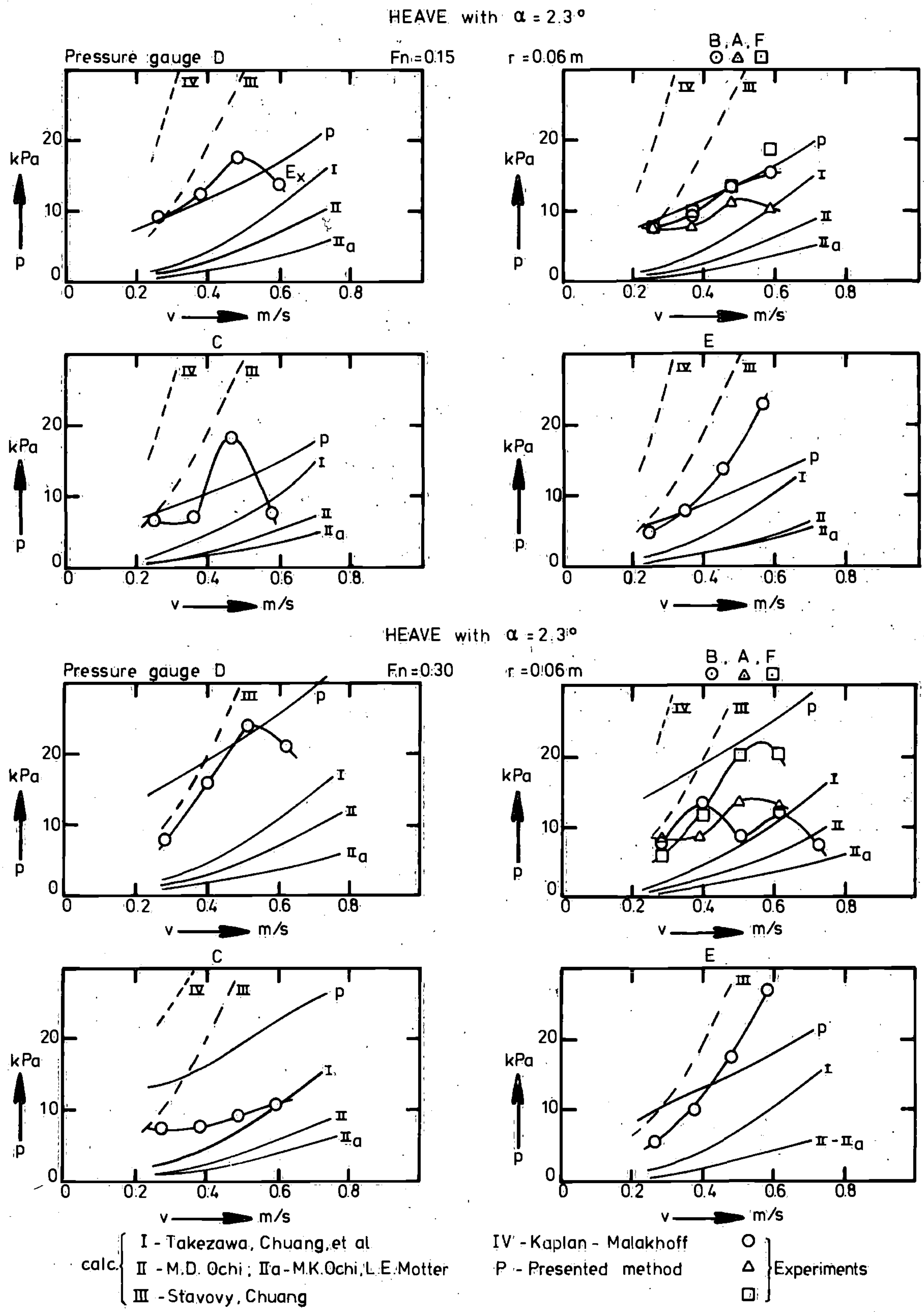

Figure 12. Test- and calculation results of peak pressure for heave with an angle between bottom and watersurface.

5. Other calculation methods

As discussed in the introduction, most of the formula's used to determine slamming pressures are based on a relation between the squared vertical velocity and the slamming pressure. There is a scattering in the value of the proportionality constant for most of the authors [1, 2, 3, 4, 5, 6, 7, 22]. However, it is possible to distinguish roughly two groups for the case of pure flat bottom impact where the angle between the bottom and water surface is almost zero. The first group found a proportionality constant $k_1 \simeq 60$ for this case, mostly by experimental methods. Proponents of this method include Takezawa [2], Lewison [19], Chuang [14] and Verhagen [13].

The peak slamming pressures are calculated and denoted in Figures 10-12 as:

$$p_{\mathrm{I}} = 30\,\rho\,v^2 \tag{23}$$

with p_{I} in N/m^2.

The second group also stated a proportional relation between the slamming pressure and the squared vertical velocity for bottom impact. To this group belong among others Margaret D. Ochi [3], who found that the proportionality constant is dependent on the width and the area of a section considered with a draught equal to 0.08 times the design draught T.

The peak pressure may be expressed, after some corrections for the dimensions, as

$$p_{\mathrm{II}} = 1480\frac{b^2}{A}\,v^2 \tag{24}$$

with p_{II} in N/m^2

and

- b = half width of the section with a draught $T' = 0.08\,T$
- A = half area of the section with a draught $T' = 0.08\,T$.
- T = design draught of the section.

As another representative of the second group may be mentioned M.K. Ochi and L.E. Motter [1]. The peak pressure is written by the following expression:

$$p_{\mathrm{IIa}} = \tfrac{1}{2}\rho\, k_1\, v^2 \tag{25}$$

in which

- k_1 = a function of the hull section shape below one tenth of the design draught T.
- $k_1 = \exp(1.377 + 2.419\,a_1 - 0.873\,a_3 + 9.624\,a_5)$ (26)
- a_1, a_3 and a_5 are the conformal transformation coefficients of the section with a draught of $0.1\,T$ when a 3-parameter transformation is applied.

The pressures calculated according to method II (Margaret D. Ochi) and method IIa (M.K. Ochi and L.E. Motter) have been determined for the sections situated at the different pressure gauges, and these results are also shown in Figures 10-12. If there is a small angle (up to about 3 degrees) between the bottom of the model and the water surface, the forward velocity component is added to the impact velocity due to oscillation. This means that the velocities normal to the bottom or keel have been taken into account and not the pure vertical velocities.

For the case of an angle between the model-bottom and the water surface it is interesting to make use of the expressions to determine bow slamming pressures for high speed vehicles as presented by Stavovy-Chuang [26] and Kaplan-Malakhoff [24].

As stated in the introduction Stavovy-Chuang define two pressure components viz.:

1. the *impact pressure* p_i due to the normal velocity component, so perpendicular to the bottom for the case considered and written in the present notation as:

$$p_i = \frac{k_1}{\cos^4\alpha}\,\rho\;144\,(\dot{s}\cos\alpha + V\sin\alpha)^2 \tag{27}$$

in which k_1 is dependent on the angle α.

For this case $k_1 = 0.8374$.

2. the *planing pressure* due to the tangential velocity component

$$p_p = \tfrac{1}{2}\rho\,(V\cos\alpha + \dot{s}\sin\alpha)^2 \tag{28}$$

The total slamming pressure according to [26] has been calculated and denoted as:

$$p_{\mathrm{III}} = p_i + p_p \tag{29}$$

in Figures 11 and 12 for the different pressure gauges.

Kaplan-Malakhoff [24] determine the slamming pressure with the equivalent planing velocity and it is denoted here as:

$$p_{\mathrm{IV}} = \tfrac{1}{2}\rho\,(V + \dot{z}\cot\alpha)^2 \tag{30}$$

The results are also shown in Figure 12 however, for heaving with an angle only. For pitching around the aft-leg with a draught $T' = 0.02$ m the angle between modelbottom and water surface achieved a value of about one degree, which delivered unreliably high values for slamming pressure when the expression of Kaplan-Malakhoff [24] was applied.

6. Comparison of experimental- and analytical results

In comparing experimental and analytical results, it should be kept in mind, that perfect agreement cannot be expected because the high sensitivity of slamming phenomena reduces the accuracy of experimental results. This is especially true for the peak values because the very short time in which a peak develops requires a steep slope in the pressure curve up to the peak. For this reason it was difficult to obtain an accurate recording of the pressure variations. Moreover, there might have been other disturbances which influenced the peak pressure such as local air-inclusion, variable influence due to the local elasticity of the material, vibrations of the model or towing carriage, etc.

On the other hand, the analytical methods also show some sensitive parameters which are not easily determined such as: the rate of increase of added mass with depth for almost zero draught, the choice of the draught which should be taken into account, the angle between hull or bottom and water surface etc.

All analytical methods take account of only the most important parameters which influence slamming.

It is hardly possible and perhaps not always necessary to include local influences and disturbances as mentioned before.

With respect to bottom impacts which occurred during pure heave and pitching motions about the water surface, it can be observed from Figures 10-12 that the peak pressures predicted by method I (Takezawa, Chuang, a.o.) and the present method show about the same deviations from the experimental values. Generally, the results obtained with method II (Margaret D. Ochi, M.K. Ochi, L.E. Motter) remained a good deal lower than the test results. It also became clear that the measured peak pressures for this case are relatively low in comparison with the peak pressures measured for heave and pitch with an angle between the bottom and water surface.

For these cases, it is obvious that the existing methods for prediction of bottom impact (I and II) deliver too low peak pressure values. The methods for predicting bow slamming III (Stavovy-Chuang) and IV (Kaplan-Malakhoff) produced values which are too high. Method III (Stavovy-Chuang) gives the best agreement with the test results.

It should, however, be remarked that application of both mentioned methods, to predict bow slamming for the cases considered is rather doubtful because of the very small angle (max. 2.3 degree) between the bottom and the water surface.

The proposed method provides results which show rather good agreement with the test results for these cases.

However, it is important to note that the results are strongly dependent on the choice of the sectional draught at which the hydrodynamic mass achieved the maximum velocity component perpendicular to the bottom.

As stated in 3, Figure 13 shows that no proportionaality constant could be established for all vertical velocities or for all frequencies of oscillation.

In Figure 13, the dimensionless peak pressures have been plotted on the basis of the circular frequency of oscillation.

This has the advantage that for a certain frequency, the influence of the sectional added mass and the rate of increase of added mass with depth are eliminated. According to the proposed theory, the slamming pressure for oscillation with the bottom parallel to the water surface is mainly determined by the second hydrodynamic term of equation (7) which shows the well-known relation between slamming pressure and impact velocity squared. For a certain frequency of oscillation, this means that the slamming pressure is proportional to the squared amplitude of oscillation.

Figure 13 shows that the experimental results more or less confirm this relationship for the cases of pure heave and pitch.

For heave oscillation with an angle between bottom and water surface, the third hydrodynamic term of equation (7) influenced by forward speed, becomes more important.

However, this term presents a linear relation between maximum impact pressure and amplitude of oscillation and so the relation between this pressure and the impact velocity becomes more complex for this mode of motions, as discussed in 4.3.

Experimental results such as those shown in Figure 13 give little indication of this linear relation.

Furthermore, Figure 13 clearly demonstrates that the dimensionless peak pressures also show the highest values for the most forward pressure gauge. This observation is in agreement with the proposed theory which states in equation (7) that the peak pressure is inversely proportional to the wetted width of the section.

7. Conclusions and recommendations

Based on analysis of the tests and proposed – and existing calculation methods for bottom impact slamming, the following conclusions and recommendations may be derived:

1. The bottom impact pressure in cases where there is forward speed appeared to be much higher if there is an angle between the bottom and water surface at the moment of impact with the water surface.
2. These high peak pressures cannot be explained by the well-known relation between slamming pressure and the squared vertical velocity of the ship with respect to the water and the rate of increase

of added mass with depth only. Also the acceleration of the added mass due to the development of a forward velocity component perpendicular to the bottom should be taken into account as follows from the proposed calculation method.

3. Photographs indicate that air inclusion for flat bottom impacts is so randomly distributed, that prediction is difficult and not worthwhile because the slamming pressure is usually reduced by the presence of air.
4. From the existing calculation procedures, method I (Takezawa, Chuang, a.o.) delivers the best results

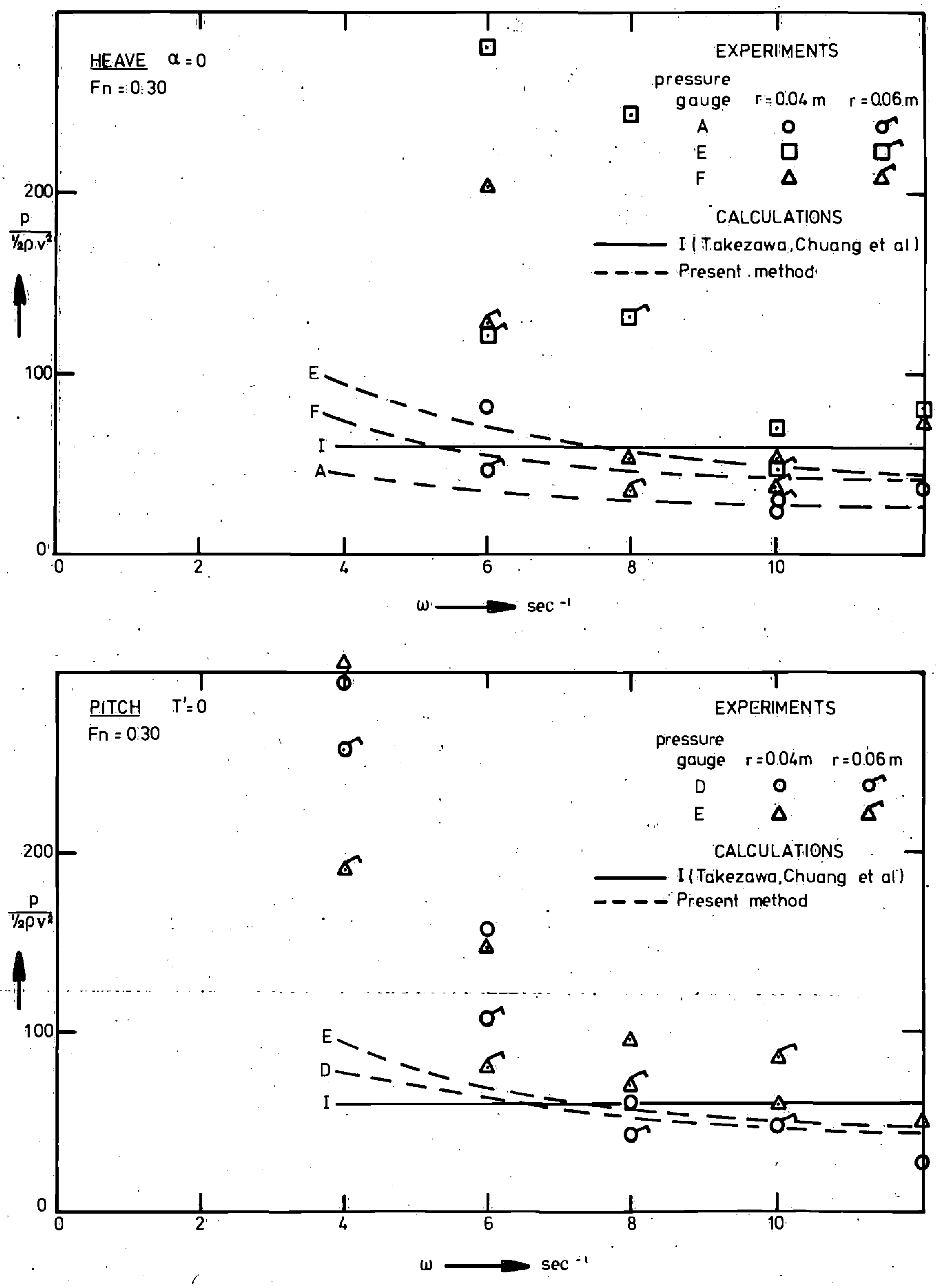

Figure 13. Dimensionless peak pressure in relation to frequency of oscillation.

for flat bottom impact pressures, but gives unreasonably low values for cases with forward speed if there is even a small angle (about 2 degrees) between the bottom and the water surface.

5. The existing calculation methods for bow slamming generally provide peak pressure values which are too high for cases with forward speed if there is even a small angle (about 2 degrees) between the bottom and water surface. Method III (Stavovy-Chuang) shows the best agreement with the experiments for this case.
6. The time in which the peak pressure develops for the case of forward speed with a small angle between the bottom and water surface appeared to be about four times shorter than for the case of pure flat bottom impact, while prediction up to now is hardly possible.
7. The results for the prediction of bottom impact peak pressures according to the proposed calculation method are rather satisfactory. The deviations from the experimental values in the case of pure bottom impact are comparable with those of method I (Takezawa, Chuang, a.o.).
   Extending the results to the situation of a ship moving in waves is possible and expedient. Bow slamming results can also be extended to thise case.
8. Further investigation is needed to determine the draught of a section at which the sectional added mass has achieved the forward velocity component perpendicular to the bottom or the hull.
9. The question remains of which frequency(ies) should be used for calculating the hydrodynamic mass.
10. Forced oscillation by PMM proved to be of great assistance to the experimental analyses of slamming phenomena.

8. Acknowledgement

Special thanks are due to the various members of the staff of the Delft Ship Hydromechanics Laboratory for their assistance in running these slamming experiments.
Particularly the author wishes to mention mr. C.W. Jorens, who developed and handled the greater part of the electronic instrumentation and mr. A.J. van Strien who perfomed the tests and worked out the measurements.

9. List of symbols

A	half area of the section with a draught $T' = 0.08\,T$
a_a	average acceleration perpendicular to the bottom due to forward speed
a_{max}	maximum acceleration perpendicular to the bottom due to forward speed
a_1, a_3, a_5	conformal transformation coefficients
B	breadth of the ship
b	half width of the section with a draught $T' = 0.08\,T$
C_B	blockcoefficient
F'	sectional hydromechanic force
Fn	Froude number
G	model's centre of gravity
g	acceleration of gravity
k, k_1	proportionality constant
LCB	longitudinal position of centre of buoyancy
L_{pp}	length between perpendiculars
m'	sectional added mass
N'	sectional damping
n	impact velocity exponent
p	slamming pressure, coefficient
p_i	impact pressure
p_p	planing pressure
q	coefficient
r	amplitude of oscillation
s	displacement of section perpendicular to bottom
T	design draught of model
T'	average draught at test condition
t	time
V	forward speed
V_A	forward speed component
v	impact velocity
$x\,y\,z$ $x_b y_b z_b$	right hand coordinate systems fixed to ship
y_w	half width of the cross section at the water surface
z	heave displacement
z_a	heave amplitude
α	angle between bottom and water surface
γ	angle at which bottom touches the water surface
ω	circular frequency of oscillation
ρ	density of water
θ	pitch angle
θ_a	pitch amplitude

10. References

1. Ochi, M.K. and Motter, L.E., 'Prediction of slamming characteristics and hull responses for ship design', SNAME 81, 1973, pp. 144-176.
2. Takezawa, S. and Hasegawa, S., 'On the characteristics of water impact pressures acting on a hull surface among waves', Journal of the Society of Naval Architects of Japan, Vol. 13, 1975.
3. Ochi, Margaret D. and Bonilla-Norat, J., 'Pressure-velocity relationship in impact of a ship model dropped onto the

water surface and in slamming in waves, NSRDC, report 3153, June 1970.

4. Ochi, M.K., 'Prediction of occurrence and severity of ship slamming at sea', 5th Symposium on Naval Hydrodynamics, Bergen, Norway, 1964.
5. Tasai, F., 'A study on the seakeeping qualities of full ships', Report of Research Institute for Applied Mechanics, Japan, Vol. XVI, No. 55, 1968.
6. Ochi, M.K., 'Model experiments on ship strength and slamming in regular waves', Trans. SNAME, Vol. 66, 1958.
7. Hagiwara, K. and Yuhara, T., 'Fundamental study on wave impact loads on ship bow' (1st report), Selected papers from Jour. Soc. Nav. Arch. of Japan, Vol. 14, 1976.
8. Wagner, H., 'Über Stoss- und Gleitvorgänge an der Oberfläche von Flüssigkeiten', Zeitschr. für Angewandte Mathematik und Mechanik, Band 12, Heft 4, 1932.
9. Kaplan, P. and Malakhoff, A., 'Hard structure slamming of SES craft in waves', AIAA/SNAME Advanced Marine Vehicles Conference, San Diego, April 1978.
10. Tick, L.J., 'Certain probabilities associated with bow submergence and ship slamming in irregular seas', Journal of Ship Research, Vol. 2, June 1958.
11. Ochi, M.K. and Motter, E., 'Prediction of extreme ship response in rough seas of the North Atlantic', International symposium on the Dynamics of Marine Vehicles in Waves, London, 1974.
12. Aertsen, G., 'Labouring of ships in rough seas', SNAME, Diamond Jubilee Spring Meeting 1968.
13. Verhagen, J.H.G., 'The impact of a flat plate on a water surface', Journal of Ship Research, December 1967, pp. 211-222.
14. Chuang, S.L., 'Experiments on flat-bottom slamming', Journal of Ship Research, March 1966, pp. 10-17.
15. Chuang, S.L., 'Experiments on slamming of wedge-shaped bodies', Journal of Ship Research, September 1967, pp. 190-198.
16. Chuang, S.L. and Milne, D.T., 'Drop tests of cones to investigate the three-dimensional effects of slamming', NSRDC report 3543, 1971.
17. Hagiwara, K. and Yuhara, T., 'Fundamental study of wave impact loads on ship bow (2nd report) – Effect of scale of the model on maximum impact pressure and equivalent static pressure', Naval Architecture and Ocean Engineering of the Society of Naval Architects of Japan, 1977, Vol. 15.
18. Johnson, Robert S., 'The effect of air compressibility in a first approximation to the ship slamming problem', Journal of Ship Research, March 1968, pp. 57-68.
19. Lewison, G.R.G., 'On the reduction of slamming pressure', RINA, Vol. 112, 1970.
20. Greenberg, Michael D., 'On the water impact of a circular cylinder', Therm Advanced Research, Inc. TAR-TR6701, May 1967.
21. Chuang, S., 'Investigation of impact of rigid and elastic bodies with water', NSRDC report 3248, February 1970.
22. Lewison, G.R.G., 'Slamming', National Physical Laboratory, Ship Report 138, March 1970.
23. Bosch, J.J.v.d., 'Slamming', Laboratorium voor Scheepsbouwkunde, Technische Hogeschool Delft, rapport no. 67, October 1970.
24. Kaplan, P. and Sargent, T.P., 'Further studies of computer simulation of slamming and other wave-induced vibratory structural loadings on ships in waves', Ship Structure Committee report 231, 1972.
25. Mansour, A. and d'Oliviera, J.M., 'Hull bending moment due to ship bottom slamming in regular waves', Journal of Ship Research, June 1975, pp. 80-92.
26. Stavovy, Alexander B. and Chuang, S.L., 'Analytical determination of slamming pressures for hig-speed vehicles in waves', Journal of Ship Research, December 1976, pp. 190-198.
27. Bishop, R.E.D. and Price, W.G., 'On the dynamics of slamming', RINA, Spring Meetings 1978.
28. Gerritsma, J. and Beukelman, W., 'Analysis of the modified strip theory for the calculation of ship motions and wave bending moments', International Shipbuilding Progress, Vol. 14, No. 156, 1967.
29. Frank, W. and Salvesen, N., 'The Frank close-fit motion computer program', NRSDC report 3289, June 1970.

Appendix

To achieve the vertical forward speed component V_A, the following relation between speed, acceleration and time has been assumed:

for speed : $v = \frac{1}{2} p\, t^2 - \frac{1}{3} q\, t^3$

for acceleration : $a = p\, t - q\, t^2$

in which p and q are coefficients and t = time. See Figure 14.

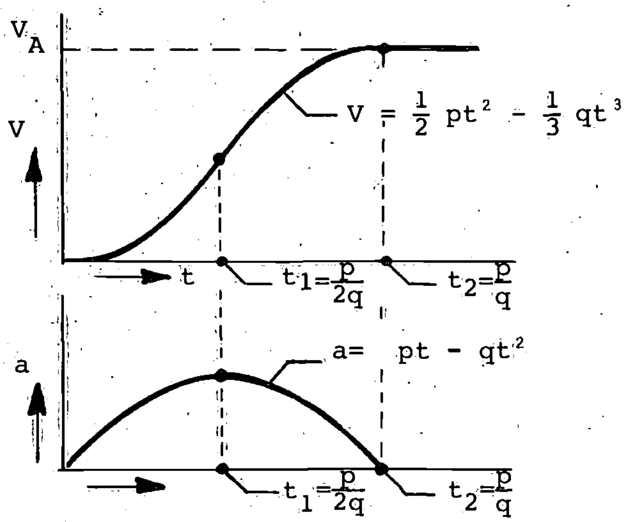

Figure 14. Assumed relation of speed and acceleration with time in which the pressure develops.

The time in which the velocity V_A for the sectional added mass will be achieved when $a = 0$ and amounts:

$$t_2 = \frac{p}{q}$$

The velocity at that time is

$$V = V_A = \frac{p^3}{6q^2}$$

The average acceleration during the time t_2 may be written as:

$$a_a = \frac{V_A}{t_2} = \frac{p^2}{6q}$$

The maximum acceleration will occur if $\frac{da}{dt} = 0$, so at the time

$$t_1 = \frac{p}{2q}$$

This maximum acceleration will then be:

$$a_{max} = \frac{p^2}{4q}$$

It now appears that this maximum acceleration is given by:

$$a_{max} = 1.5\, a_a$$

A NEW THEORY OF MINIMUM STABILITY, A COMPARISON WITH AN EARLIER THEORY AND WITH EXISTING PRACTICE

by

K. Jakić*

Summary

The author has already presented his new theory of minimum stability for the intact and damaged ship, and his own programmes for use on computers, at a Yugoslav and at two foreign symposiums.

To the best of the author's knowledge, only Russian scientists are studying this field, very intensely. They developed a theory that there are several possibilities to obtain a diagram of minimum stability, the most important of which are the 'diagram of minimum moment' and of 'minimum work'. It is becoming more and more important, and essential for a damaged ship, to take the trim into account in stability calculations, generally known in the world only to specialists. It thus seems to the author that even in discussions on the following presentations the very simple essence of that new theory, which is to take the trim into account in the best possible way, has not been understood.

Here we shall try to give an even simpler explanation and also a short description of the mentioned Russian theory, because the author considers that the new theory shows both the mentioned diagrams to be identical, and even represented by a third, which belongs to the second group of those Russian propositions, under the new name 'diagram with excluded component in the direction of the principal axis of maximum inertia'. In this way the solution is completely determined, which is very important. It seems to the author that the fact that several solutions formerly existed is one of the main reasons why these Russian results, over twenty years old, have not yet entered international stability regulations.

We will also make a comparison with principles applied in computation with trim in systems accessible to the author, like 'VIKING', 'COMPUTAS' etc. Those principles are not completely exact, but are, it seems, acceptable for practice to date.

1. Introduction

In computing the stability of a damaged ship the trim must be taken into account, and this is growing more and more important for the intact ship also. We may ask how this is to be done. Many years ago I came to the conclusion that on calm water the lever of the ship's statical stability, regardless of whether the ship is damaged or intact, obviously changes with the trim if the heel φ is unchanged, so there must be a trim for which the lever is minimum. Both these values are critical, and thus relevant. In these studies the concept of the complete lever, p, described in the following chapter, immediately became apparent.

At the beginning of 1974 the author published a work listed in the References under [5] (we have used square brackets to denote works listed in the References), where this phenomenon for the intact ship is treated grapho-analytically with the aid of a computer. Figure 1.1. was taken over from there. In it the minimum levers, p_{min}, appear as distinct absolute minimums. Figure 1.1. refers to the intact passenger ship treated in that work, but the same regularity was always obtained in calculations carried out on hunderds of different intact ships in the 'Ship Stability' student programmes at this Department.

The new theory describes the complete phenomenon analytically. It is thus possible to carry out all necessary calculations on a computer, for which the author

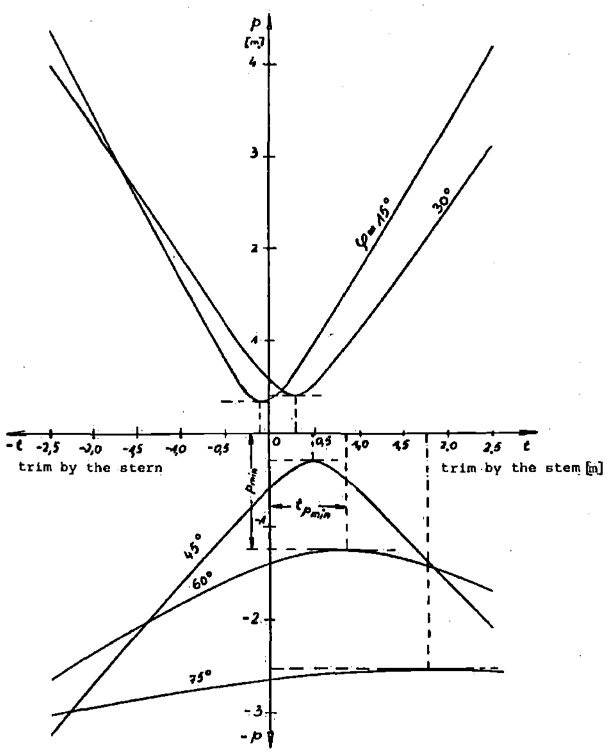

Figure 1.1. Dependence of complete levers of statical stability on ship's trim.

*) Department of Naval Architecture, Faculty of Mechanical Engineering and Naval Architecture, University of Zagreb, Yugoslavia.

TECHNISCHE HOGESCHOOL DELFT
AFDELING DER SCHEEPSBOUW- EN SCHEEPVAARTKUNDE
LABORATORIUM VOOR SCHEEPSHYDROMECHANICA

Rapport No. 479

BOTTOM IMPACT PRESSURES DUE TO FORCED OSCILLATION

W. Beukelman

Delft University of Technology
Ship Hydromechanics Laboratory
Mekelweg 2
Delft 2208
Netherlands

februari 1979.

Contents.

Abstract.

Forced oscillation tests about the water surface have been carried out with a segmented ship model to measure slamming pressures on two segments.
A calculation procedure based on a two-dimensional approach has been proposed.
These analytical results, together with those of other theories have been compared with the measurements.
The results of the proposed calculation method proved to be rather satisfactory.

1. Introduction.

The literature about tests and theories on slamming is rather extensive.

In most of the experiments, the object was to find a relation between the vertical impact velocity and the maximum slam pressure [1, 2, 3, 4, 5, 6]. A general form for this relation is presented by Margaret Ochi and José Bonilla-Norat in [3] as

$$p = kv^n$$

where: p = the impact pressure

v = the impact velocity

k and n are constants

Experimentally, these authors found that the pressure is proportional to the square of the velocity at impact and that the proportionality constant k is dependent on the section shape.

Others like Takezawa et al., M.K. Ochi, L.E. Motter [1, 2, 7] used a similar relation,

$$p = \tfrac{1}{2}\rho\, k_1 v^2$$

and established experimentally the coëfficient k_1 of the impact pressure dependent on the position considered as a flat bottom or stem front. For the pressure distribution on the surface of a wedge-shaped body the authors used the well-known formula of Wagner [8].

Remarkable model test results, together with theoretical results, are presented by P. Kaplan et al [9] for the case of bow slamming of SES craft in waves.

Most frequently used up to now is the procedure introduced by Tick [10] and Ochi [4] with respect to bottom impact slamming.

After some evaluations, Ochi et al [4, 11] stated two conditions required for bottom impact slamming to occur viz.:

a) Bow (fore foot) emergence

b) a certain magnitude of relative velocity between wave and ship bow.

The critical relative velocity below which slamming does not occur is called the "threshold velocity", denoted by $\dot{v}^*$.
Ochi showed by tests on a Mariner model that the threshold velocity is nearly constant with an average of 12 fps for a ship of 520 ft length. Aertssen [12] advised that the threshold value should be 50 percent greater for the Mariner, that is 18 fps.
Mostly the threshold velocity according to Ochi is accepted with an appropriate Froude scaling law for ships of different lengths.

To analyse the problem experimentally a series of drop tests with a flat plate [13, 14] or a wedge [7, 15, 16, 17] have been executed. Very often, the behaviour of the air layer between the falling body and the water surface has been taken into consideration [13, 18, 19, 20].
Chuang [21] showed that the effect of this compressible air causes a remarkable reduction of the acoustic pressure, which is frequently assumed.
Mathematical models have been developed to describe the cushioning effect of the air between the descending body and the water surface for instance by Verhagen [13] and Greenberg [20]. The predictions of Verhagen showed good agreement with experimental results. It is, however, rather complicated to apply these theories to the real problem of ship bottom impact because no account is taken of forward speed or of the three-dimensional flow caused by changes in the shape of the sections.

Model experiments in waves or full scale observations may statistically deliver rather good and useful results [1, 2, 3, 4, 6, 12, 22], but do not give a deeper insight in the phenomena slamming. This might be very important for establishment of design criteria.

Several authors have tried to formulate mathematical models describing slamming [13, 20, 22, 23, 24, 25, 26, 27].
The great majority of them accepted the rate of change of the momentum of the hull's added mass as the main cause of the arise of slamming forces. In this way they found, that the maximum slamming pressure is indeed proportional to the squared relative vertical impact velocity.
To calculate the hydrodynamic impact force, Kaplan [24] made use

of the well-known stripmethod, however, with a different way of treatment of the forward speed influence.
Kaplan [24], Ochi [6] and Lewison [22] also stated that the slamming pressure is proportional to the rate of change of the added mass with depth.
Stavovy and Chuang [26] determined slamming pressures for fast ships by a method based on the Wagner impact theory, the Chuang cone impact theory and experiments.
They stated that slamming pressures acting normal to the hull bottom may be separated into two components:

1. the <u>impact pressure</u> due to the normal component to the water surface of the relative velocity between the impact surface and the wave.

2. the <u>planing pressure</u> due to the tangential component to the water surface of the relative velocity between the impact surface and the wave.

The planing pressure is usually small compared to the impact pressure.

In the present work it was the intention to investigate mainly bottom impact slamming. To know more exactly the relationship between the vertical impact velocity and slamming pressure a choice had been made for experiments with a model forced oscillated in still water.
The bottom in which several pressure gauges were mounted was situated at or near the watersurface.
The measurements of the maximum slamming pressure have been compared with the results of some of the discussed methods and with the results of a proposed calculation procedure.

2. Description of the experiments.

The oscillation tests were carried out with a glass fibre reinforced polyester ship model of the Todd Series 60, $C_B = 0.70$ parent hull form. The same model has been used in the past for experiments described in [28]. The main particulars of the model are summarized in Table 1. The model consisted of seven separate segments connected to a continuous strong box girder above the model. See fig. 1.

For pure heaving without an angle between the bottom and the water surface three pressure gauges A, B and C were placed in the middle segment (no. 4) and three, D, E and F in segment no. 6 after the forward one, as denoted in figure 1.
For pitching and heaving with an angle between the bottom and the watersurface, all six pressure gauges were mounted in segment no. 6. See also figure 1. Each of the segments with the pressure gauges was connected to the box girder above the model by means of a force dynamometer. This provided a rough check on the pressure gauge readings by comparing them with the pressures calculated from the total force on the segment bottom.

The fore and aft leg of the oscillator were 0.5 m from the model's centre of gravity G.
Four modes of motions were carried out by the oscillator:

1. A <u>pure heaving motion</u> with zero angle between model bottom and water surface. In zero position of the oscillator the model bottom was situated on the still water surface.

2. A <u>pure pitching motion</u> around the model's centre of gravity in such a way that in the zero position of the oscillator the model bottom was also situated on the still water surface.

3. A <u>pitching motion around</u> the connection point of the <u>aft leg</u> and model in such a way that the model had a draught $T' = 0{,}02$ m in zero position of the oscillator.

4. A <u>heaving motion with an angle</u> of 2.3. degrees between model bottom and water surface. The draught of the model at the model's centre of gravity, so half way between the legs, was zero in the zero position of the oscillator.

The model was tested at two forward speeds, $Fn = 0.15$ and 0.30,

two amplitudes of oscillation, r = 0.04 and 0.06 m and five frequencies, ω = 4,6, 8, 10 and 12.
Photographs of the model-bottom at the moment of contact with the water surface are shown in fig. 2 for some cases. From these pictures it is clear that the air-bubbles do not exhibit a regular pattern.
Fig. 3 contains photographs taken of the oscilloscope illustrating some slamming pressures.

The peak values of the slamming pressures, measured from the UV-recorder are shown in fig. 10 -12 for the four modes of motion, both forward velocities except for pure pitch and the maximum amplitude of oscillation.
These peak pressures have been plotted on the basis of the impact velocity v as defined in eq. (22).
The time in which the peak pressure has been built up, the so-called rise-time, has been determined with the aid of the correlator and is shown in fig. 9 for the highest speed and both amplitudes of oscillation.

2.1. Instrumentation.

The slamming pressures have been measured by means of 6 semi conductor pressure transducers while at the same time forces have been measured on two segments as denoted in 2.
The characteristics of the pressure transducers were as follows:

- Manufacture : Druck Ltd.
- Type : PDCR 42
- Range : 69 kPa (10 psi)
- Acceleration sensitivity : for 69 kPa: 0.002% of full scale output/g
- Temperature drift and thermal shock : 0.02%/^{o}C/FSO
- Natural frequency (in air) : 15 kHz

The output signals of the pressure transducers, situated at the bottom of the segments, were amplified and recorded simultaneously on an analog instrumentation tape recorder and UV-recorder. The latter had been used for visual observation and preliminary deter~~mination of the peak values of the impact pressures.~~

Recording on the tape recorder took place at high speed (1.5 m/s or 60 ips) to ensure a sufficient bandwidth.
The block diagram of figure 4 shows the instrumentation set-up for the experiments. After the measurements the slamming signals were replayed one at a time and fed via a delay line to a correlator which was used in its signal recovery mode. (fig 4)
By using a mechanical oscillator there is an enormous ratio between the interval time of the oscillation and the width of the impact wave form. Only a small part of the cyclus has to be isolated. Therefore the signal is sent through an analog delay line to catch both the slamming wave form and a small piece of the signal preceeding the impact.
A trigger pulse generated by the slamming wave form at the input of the delay line triggered the correlator and after 20 ms the delayed wave form entered the correlator.
The principle of signal recovery is to examine a part of the signal following the trigger pulse and by repeating this observation to extract a coherent pattern. After each triggerpulse a series of 100 samples is taken and added to the corresponding samples of the previous series. In this way the coherent pattern is reinforced at each repetition while noise present in the signal is surpressed to a degree dependent on the number of pulses that had been averaged. After a summation of 128 repetitions the result had been normalised (divided by 128) and could be displayed and reflected on a X-Y recorder.
A digital storage oscilloscope was used to monitor the slamming signals. The results obtained with the correlator had to be carefully interpreted. A time jitter could occur between the triggerpulse and the peak of the slamming wave form due to the great difference in both shape and amplitude of the succeeding wave forms. As a result the peak value could be somewhat too small and the width of the impact wave form too large. However the energy contained under the pulse was still correct and represented the energy of an average impact wave form.

During the experiments photo's were taken of the model bottom to obtain an impression of the behaviour of air. See figure 2.
The camera shutter was opened when the model was in the near vicinity of the camera and an electronic flash was fired at the

first trigger pulse generated by an impact wave form. Therefore the photo's were made at almost the same moment that the impact took place.

3. Analysis of test results.

Occasionally, the measured local slamming pressures were compared with the pressures derived from the force-measurements on the segments. Although equality could not be expected, the agreement in the order of magnitude appeared to be satisfactory. The measurements showed that the impact pulses during one run could differ a great deal in shape. Using the method as described in 2.1., it was possible with the aid of a correlator to obtain an average pulse with satisfactory consistency.

A reasonable agreement could also be established between the values of the peak pressures obtained from the UV-recorder and those derived from the correlator, although it remains as stated in 2.1. that the peak values from the correlator are somewhat less reliable.
From the peak pressures measured by the UV-recorder and shown in fig. 10 - 12 it is clear that with respect to the longitudinal position of the pressure gauges the most forward one, E, delivered the highest values. This effect, which might be due to the higher impact velocities or to the smaller wetted width of the section will be discussed in 4.1. and 6.
The influence of the transverse position of the pressure gauges on the slamming pressures appeared to be negligible as shown in fig. 10 - 12.

According to expression (7) of the proposed theory, the pressures measured by A,B and F should be equal in the cases of pitching and heaving motions with an angle between bottom and water surface. From fig. 10 - 12, it is obvious that this fact was confirmed satisfactorily by experiments.

The effect of forward speed appeared to be remarkably small for the cases where the bottom was parallel to the water surface. Greater forward speed effects were measured for the other cases. These results also agree with the proposed theory, as will be discussed in 4.2.3. and 6.

For heave and pure pitch, the measured peak pressures have been non-dimensionalized as $p/\frac{1}{2}\rho\, v^2$ and plotted versus the frequency of oscillation for the various gauges and speeds as indicated in fig. 13. This dimensionless pressure also represents the well-known proportionality constant.
From the figures, however, it is clear that such a constant, proportional to the squared vertical velocity could not be established for all frequencies of oscillation.
For a certain frequency of oscillation there was a slight indication that the peak pressures are proportional to the squared amplitude of oscillation.
It was assumed that the value of the peak pressure was not significantly influenced by the elastic characteristics of the model-bottom. The oscillations in the pressure after the peak as shown in fig. 3 might have been due to the elasticity of the bottom material.

The amount of time required to obtain the peak pressure varied greatly with an average of about 4 à 5 ms for the case with the bottom parallel to the water surface. For heaving, with an angle between bottom and water surface, there was a large reduction of this rise-time to about 1 ms. This might have been due to the greater influence of the high accelerations of the added mass, which according to the proposed theory occurred as a consequence of the arise of the forward speed component.
This time, as denoted in (18) should be shorter than the rise-time.

The photographs (fig. 2) made of the model-bottom at the moment of impact with the water-surface show that the air layer is most significant when the bottom is parallel to the water surface. As soon as there is an angle between bottom and water surface a large reduction of the amount of trapped air can be established. Concerning this observation, it should be remarked that the distribution of the air about the model bottom seemed rather random, so no consistant pattern was observed.

Finally, it is worthwhile to stress the advantages of using a

PMM (Planar Motion Mechanism) for the analysis of slamming. Vertical speed, acceleration and angle with the water surface are perfectly adjustable, while the behaviour of air can be easily observed.

4. Proposed calculation method for determining slam pressures.

4.1. General.

It is essential for determining slam pressures to divide the velocities into two components: one component along the hull (or keel-line), and one component perpendicular to the hull. The velocities along the hull determine the so called planing pressure which is usually small and insiginificant in comparison with the impact pressure [26].

Therefore this impact pressure is mainly determined by the velocities normal to the hull. In the case of a ship with a flat bottom, the impact pressures on the bottom can be determined if the velocities normal to the bottom are known. This case will be considered here.

The calculation method is based on the strip theory as presented in [28]. The hydromechanic force per unit length on a strip of an oscillating ship in still water with respect to the coordinate system $x_b\ y_b\ z_b$ fixed to the ship at the center of gravity (fig. 5) will be

$$F' = F_1' + F_2' + F_3' \qquad (1)$$

in which:

$$F_1' = -2\rho\, g\, y_w s$$
$$F_2' = -N'\dot{s}$$
$$F_3' = -\frac{d}{dt}(m'\dot{s})$$

with:

- ρ = density of water
- g = acceleration of gravity
- y_w = half width of the cross-section at the moment of touching the water surface
- m' = the sectional added mass
- N' = the sectional damping
- s = the displacement of the strip into the z_b-direction, so perpendicular to the bottom.

For a pure heaving oscillation $z = z_a \cos\omega t$ about the waterline with the keel-line or bottom parallel to the waterline

$$s = z = z_a \cos \omega t \qquad (2)$$

while for a pure pitching oscillation $\theta = \theta_a \cos \omega t$ about the waterline

$$s = x_b \theta_a \cos\omega t \qquad (3)$$

x_b is the distance between the strip considered and the centre of gravity where the origin of the $x_b y_b z_b$ coordinate system is assumed to be located, see figure 5.

It is possible to write the sectional hydromechanic force of (1) as follows:

$$F' = -(2\rho g\, y_w s + N'\dot{s} + \frac{dm'}{dt}\dot{s} + m'\ddot{s})$$

$$= -(2\rho g\, y_w s + N'\dot{s} + \frac{dm'}{ds}\dot{s}^2 + m'\ddot{s}) \qquad (4)$$

The total slam-force on a strip may be expressed as:

$$F' dx_b = 2p\, y_w\, dx_b \qquad (5)$$

in which: p = the slam pressure

Substitution of (4) into (5) delivers the following expression for slam pressure:

$$p = -(\rho g s + \frac{N'}{2y_w}\dot{s} + \frac{dm'}{ds}\frac{1}{2y_w}\dot{s}^2 + \frac{m'}{2y_w}\ddot{s}) \qquad (6)$$

The first term of the right hand side may be neglected because of the very small displacement during the time that the maximum slam pressure is built up. So the general expression for the slam pressure may be written as:

$$p = -\frac{1}{2y_w}(N'\dot{s} + \frac{dm'}{ds}\dot{s}^2 + m'\ddot{s}) \qquad (7)$$

From (7) it appears that

1. the slam pressure mainly is composed of three hydro-dynamic terms.

2. the slam pressure is inversely proportional to the "wetted width", $2y_w$.

3. the second term is proportional to the squared vertical strip velocity.

Further remarks which can be made about the slam pressure are:

1. the first hydrodynamic term containing the sectional damping will deliver a small contribution to the total slam pressure because it is proportional to only the first power of the vertical strip velocity.

2. from the second hydrodynamic term, it appears that the increase of added mass with depth is very important.

3. the third hydrodynamic term may becomes very significant if the vertical strip acceleration is high. This may be the case if there is a component due to the forward velocity of the ship. This phenomenon will be considered further on.

4. the value which should be taken for the hydrodynamic mass is not clear. In this work the adjusted frequency of oscillation has been used, but there might also be reasons related to the transient character of slamming to start from infinite frequency or to consider a spectral value for the added mass.

4.2. Determination of speeds and accelerations.

At first the velocities and accelerations due to oscillations will be calculated and afterwards the influence of forward speed will be considered.

4.2.1. Heave oscillation.

For the heaving motion, the displacement of a strip is defined as:

$$s = z = z_a \cos \omega t \qquad (2)$$

from which follows:

$$\begin{aligned} &\text{the strip velocity} && \dot{s} = \dot{z} = -\omega z_a \sin\omega t \\ &\text{and the strip acceleration} && \ddot{s} = \ddot{z} = -\omega^2 z_a \cos\omega t \end{aligned} \qquad (8)$$

with: ω = circular frequency of oscillation
z_a = amplitude of heave oscillation

In the case of pure heaving with the bottom of the model at the water surface in the zero position of the oscillator, it is clear that at the moment of impact with the water surface the strip velocity will achieve a maximum value while the acceleration becomes zero. This means that the third hydrodynamic term of eq. (7), $\frac{m'\ddot{s}}{2y_w}$, does not contribute to the slam pressure for this case.
For heaving of the bottom about the waterline with a constant angle between bottom and watersurface, the situation is different.

If a point P on the bottom is situated at a distance z_o above the waterline in the zero position of the oscillator (fig. 7) there will be contact with the water surface if:

$$z = z_a \cos\omega t = -z_o = -x_b \, tg\alpha$$

or if $\text{arc}\left(\cos\omega t = \dfrac{-x_b \, tg\alpha}{z_a}\right) = \gamma$ and $\dot{s} < 0$ (9)

The velocity and acceleration perpendicular to the bottom due to oscillation for the section at P at the moment of contact with the watersurface are respectively:

$$\left.\begin{aligned} \dot{s} &= -z_a\omega \sin\gamma \cos\alpha \\ \ddot{s} &= -z_a\omega^2\cos\gamma \cos\alpha \end{aligned}\right. \qquad (10)$$

The angle α is small (2.3 degrees) and so it may be assumed that $\cos\alpha \approx 1$.

Another velocity component perpendicular to the bottom results from the forward speed viz.:

$$V_A = -V\sin\alpha \qquad (11)$$

This influence will be discussed in 4.2.3.

4.2.2. Pitch oscillation.

For the pitching motion the displacement of a strip may be expressed as:

$$s = x_b\theta = x_b\theta_a \cos\omega t \qquad (3)$$

from which follows:

$$\left.\begin{aligned} &\text{the strip velocity} && \dot{s} = -x_b\omega\theta_a \sin\omega t \\ &\text{and the strip acceleration} && \ddot{s} = -x_b\omega^2\theta_a \cos\omega t \end{aligned}\right\} \qquad (12)$$

For pitching around the aft leg with a certain draught T' of the model the situation is different. See fig. 8.

fig 8

If the fore leg has a displacement $z = z_a \cos \omega t$ the vertical displacement of a point P at the bottom will be

$$z' = z_a (x_b + 0.5) \cos\omega t \qquad (13)$$

The water surface will be contacted if

$$z' = T'$$

therefore holds:

$$\text{arc} \left(\cos \omega t = \frac{T'}{z_a (x_b + 0.5)}\right) = \gamma \text{ and } \dot{s} < 0 \qquad (14)$$

The velocity and acceleration perpendicular to the bottom due to oscillation for the section at P at the moment of contact with the water surface are respectively:

$$\left.\begin{array}{l} \dot{s} = - z_a (x_b + 0.5)\omega \sin\gamma \cos \theta_t \\ \ddot{s} = - z_a (x_b + 0.5)\omega^2 \cos\gamma \cos \theta_t \end{array}\right\} \qquad (15)$$

θ_t is the angle between the bottom and the watersurface when the point P contacts the water surface and may be characterized by:

$$\theta_t = \text{arc} \left(\text{tg } \theta_t = \frac{T'}{x_b + 0.5}\right) \qquad (16)$$

For this case θ_t is small (up to one degree) and so it may be assumed that $\cos \theta_t \simeq 1$.

Another velocity component perpendicular to the bottom results from the forward speed viz.:

$$V_A \quad = \quad - V \sin \theta_t \qquad (17)$$

4.2.3. Influence of forward speed.

For heaving and pitching with the bottom parallel to the water surface at the moment of contact there is no component of the forward speed normal to the bottom. If the bottom makes an angle α or θ_t with the water surface, the component V_A of the forward speed normal to the bottom, will arise for a particular strip as derived in 4.2.1. and 4.2.2.
If this component V_A develops within the time that the maximum slam pressure occurs the added mass of the strip will be subjected to very high accelerations.
It is reasonable to expect that the effect of these high accelerations on the added mass is dependent on the draught of the strip or wetted part of the section and for this reason also dependent on the strip velocity $\dot{s}$ due to oscillation.
The maximum value of the acceleration for the sectional added mass will be determined in accordance with the assumptions in the appendix.

The following calculation procedure with respect to the influence of the forward speed is proposed:

1. Determine the normal strip velocity V_A which should be achieved on account of the angle of the bottom with the water surface.

2. It is first assumed that the added mass has achieved the velocity V_A if the displacement of the strip $s \; = \; 0.00015$ m and the time in which this takes place is

$$t \quad = \quad \frac{0.00015}{\dot{s}} \qquad (18)$$

3. Next the average acceleration is determined by

$$a_a \quad = \quad \frac{V_A}{t} \qquad (19)$$

4. Furthermore, it is assumed that the peak pressure is dependent on the maximum acceleration. This maximum acceleration due to the forward speed component will be determined as proposed in the appendix

$$a_{max} = 1.5\ a_a \qquad (20)$$

5. Finally the total maximum acceleration of the sectional added mass perpendicular to the bottom is found to be:

$$\ddot{s}' = \ddot{s} + a_{max} \qquad (21)$$

4.3. Execution of the calculations.

To carry out the proposed calculations, it was first necessary to determine the sectional added mass and damping for several draughts and for the bottom of the model. The Frank-computer program [29] was used to make these calculations. For numerical reasons, it was necessary to introduce a slight deadrise in the bottom and a slight draught. A deadrise of 0.00002 m and a draught of the same value served as initial inputs. For small draughts (below 0.00004m) the variations in added mass and damping are negligable. All these calculations have been carried out for several sections after which added mass and damping have been determined by interpolations for the sections where the pressure-gauges were situated.
Afterwards the rate of change of added mass with depth, dm'/ds, has been determined in the same way and values have been graphically established for zero draught. See table 2 and 3. As an example, the results are shown in fig. 6., for pressure gauge E.
Calculations of the peak slam pressures have been executed in accordance with eq. (7) for the modes of motions considered with and without the forward speed influence as proposed in 4.2.3. Results are shown in table 4 and fig. 10 - 12 where the peak pressures are plotted on the basis of the impact velocity:

$$v = \dot{s}' = \dot{s} + V_A \qquad (22)$$

From the calculations it appears that:

1. The sectional damping given by the first hydrodynamic term of eq. (7) has very low values for all motions.

2. For oscillations with the model-bottom at the water surface in the zero position of the oscillator, only the second hydrodynamic term of eq. (7) has a significant value.

3. The rate of increase of added mass with depth dm'/ds for zero draught is very important for all motions, but not easily established and very sensitive.

4. The correction for the influence of forward speed might be very significant for the case of an angle between bottom and water surface at the moment of contact. It is strongly dependent on the value which has been taken for the section draught necessary to achieve the vertical forward speed component.
The correction of the forward speed as proposed in 4.2.3. influences only the third hydrodynamic term of eq. (7) containing the acceleration of the sectional added mass. However, there should also be an increasing influence on the second hydrodynamic term with the increase of the vertical forward speed component.
This influence was neglected in these calculations, but has been considered separately before with respect to the maximum value of the forward speed component without taking into account the influence of the accelerations as proposed in 4.2.3. In this way the peak slam pressures remain far too low, especially for the case of heaving with an angle of trim.
In fact, the problem is rather complex. Both influences are working together, however the one proposed in 4.2.3. appeared to be a great deal stronger.

4.4. Units.

All units in this paper are presented according to the "Système Internationale d'Unités" (SI).
For convenience the following conversion factors with respect to the former technical or kg (force)-m-sec units and the related

English units are given for:

force : $1\ N = 1\ kg\ m\ s^{-2}$ (SI)
$= 0.1019\ kgf$ (technical units)
$= 0.225\ lb$ (English units)

length : $1\ m = 3.28\ ft$, $= 39.37\ in$ (English units)

pressure : $1 kPa = 1000\ Nm^{-2} = 1000\ kg\ m^{-1}\ s^{-2}$ (SI)
$= 101.937\ kgf/m^2$ (technical units)
$= 0.145\ psi$ (English units)

mass : $1\ kg = 1\ Ns^2\ m^{-1}$ (SI)
$= 0.1019\ kgf\ s^2\ m^{-1}$ (technical units)

5. Other calculation methods.

As discussed in the introduction, most of the formula's used to determine slamming pressures are based on a relation between the squared vertical velocity and the slamming pressure. There is a scattering in the value of the proportionality constant for most of the authors [1, 2, 3, 4, 5, 6, 7, 22]. However, it is possible to distinguish roughly two groups for the case of pure flat bottom impact where the angle between the bottom and water surface is almost zero. The first group found a proportionality constant $k_1 \approx 60$ for this case, mostly by experimental methods. Proponents of this method include Takezawa [2] Lewison [19], Chuang [14] and Verhagen [13].
The peak slamming pressures are calculated and denoted in figure 10 - 12 as:

$$p_I = 30\ \rho v^2 \qquad (23)$$

with p_I in N/m^2

The second group also stated a proportional relation between the slamming pressure and the squared vertical velocity for bottom

impact. To this group belong among others Margaret D. Ochi [3], who found that the proportionality constant is dependent on the width and the area of a section considered with a draught equal to 0.08 times the design draught T.
The peak pressure may be expressed, after some corrections for the dimensions, as

$$p_{II} = 1480 \frac{b^2}{A} v^2 \qquad (24)$$

with p_{II} in N/m^2

and b = half width of the section with a draught $T' = 0.08\ T$
A = half area of the section with a draught $T' = 0.08\ T$
T = design draught of the section.

As another respresentative of the second group may be mentioned M.K. Ochi and L.E. Motter [1]. The peak pressure is written by the following expression:

$$p_{IIa} = \tfrac{1}{2}\rho\, k_1\, v^2 \qquad (25)$$

in which k_1 is a function of the hull section shape below one tenth of the design draught T.

$$k_1 = \exp(1.377 + 2.419\, a_1 - 0.873\, a_3 + 9.624\, a_5) \qquad (26)$$

a_1, a_3 and a_5 are the conformal transformation coefficients of the section with a draught of 0.1 T when a 3-parameter transformation is applied.

The pressures calculated according to method II (Margaret D. Ochi) and method IIa (M.K. Ochi and L.E. Motter) have been determined for the sections situated at the different pressure gauges and these results are also shown in fig. 10 - 12. If there is a small angle (up to about 3 degrees) between the bottom of the model and the water surface, the forward velocity component is added to the impact velocity due to oscillation. This means that the velocities normal to the bottom or keel have been taken into account and not the pure vertical velocities.

For the case of an angle between the model-bottom and the water-surface it is interesting to make use of the expressions to determine bow slamming pressures for high speed vehicles as presented by Stavovy-Chuang [26] and Kaplan - Malakhoff [24].
As stated in the introduction Stavovy - Chuang define two pressure components viz.:

1. the <u>impact pressure</u> p_i due to the normal velocity component, so perpendicular to the bottom for the case considered and written in the present notation as:

$$p_i = \frac{k_1}{\cos^4\alpha} \rho\, 144\, (\dot{s} \cos \alpha + V \sin \alpha)^2 \qquad (27)$$

   in which k_1 is dependent on the angle α.
   For this case $k_1 = 0.8374$.

2. the <u>planing pressure</u> due to the tangential velocity component

$$p_p = \tfrac{1}{2} \rho (V \cos \alpha + \dot{s} \sin \alpha)^2 \qquad (28)$$

   The total slamming pressure according to [26] has been calculated and denoted as:

$$p_{III} = p_i + p_p \qquad (29)$$

   in figures 11 and 12 for the different pressure gauges.

Kaplan - Malakhoff [24] determine the slamming pressure with the equivalent planing velocity and it is denoted here as:

$$p_{IV} = \tfrac{1}{2} \rho (V + \dot{z} \cot \alpha)^2 \qquad (30)$$

The results are also shown in figure 12 however, for heaving with an angle only. For pitching around the aft-leg with a draught $T' = 0.02$ m the angle between model-bottom and water surface achieved a value of about one degree, which delivered unreliably high values for slamming pressure when the expression of Kaplan-Malakhoff [24] was applied.

6. Comparison of experimental- and analytical results.

In comparing experimental and analytical results, it should be kept in mind, that perfect agreement cannot be expected because the high sensitivity of slamming phenomena reduces the accuracy of experimental results. This is especially true for the peak values because the very short time in which a peak develops requires a steep slope in the pressure curve up to the peak. For this reason it was difficult to obtain an accurate recording of the pressure variations. Moreover, there might have been other disturbances which influenced the peak pressure such as local air-inclusion, variable influence due to the local elasticity of the material, vibrations of the model or towing carriage, etc.

On the other hand, the analytical methods also show some sensitive parameters which are not easily determined such as:

the rate of increase of added mass with depth for almost zero draught, the choice of the draught which should be taken into account, the angle between hull or bottom and water surface etc.

All analytical methods take account of only the most important parameters which influence slamming.

It is hardly possible and perhaps not always necessary to include local influences and disturbances as mentioned before.

With respect to bottom impacts which occurred during pure heave and pitching motions about the water surface, it can be observed from fig. 10 - 12 that the peak pressures predicted by method I (Takezawa, Chuang, e.a.) and the present method show about the same deviations from the experimental values. Generally, the results obtained with method II (Margaret D.Ochi, M.K. Ochi, L.E. Motter) remained a good deal lower than the test results. It also became clear that the measured peak pressures for this case are relatively low in comparison with the peak pressures measured for heave and pitch with an angle between the bottom and water surface.

For these cases, it is obvious that the existing methods for prediction of bottom impact (I and II) deliver too low peak pressure values. The methods for predicting bow slamming III (Stavovy - Chuang) and IV (Kaplan - Malakhoff) produced values which are too high. Method III (Stavovy - Chuang) gives the best agreement with the test results.

It should, however, be remarked that application of both mentioned methods, to predict bow slamming for the cases considered is rather doubtful because of the very small angle (max. 2.3 degree) between the bottom and the water surface.
The proposed method provides results which show rather good agreement with the test results for these cases.
However, it is important to note that the results are strongly dependent on the choice of the sectional draught at which the hydrodynamic mass achieved the maximum velocity component perpendicular to the bottom,
As stated in 3, fig. 13 shows that no proportionality constant could be established for all vertical velocities or for all frequencies of oscillation.
In fig. 13, the dimensionless peak pressures have been plotted on the basis of the circular frequency of oscillation.
This has the advantage that for a certain frequency, the influence of the sectional added mass and the rate of increase of added mass with depth are eliminated. According to the proposed theory, the slamming pressure for oscillation with the bottom parallel to the water surface is mainly determined by the second hydrodynamic term of eq. (7) which shows the well-known relation between slamming pressure and impact velocity squared. For a certain frequency of oscillation, this means that the slamming pressure is proportional to the squared amplitude of oscillation.
Fig. 13 shows that the experimental results more or less confirm this relationship for the cases of pure heave and pitch.
For heave oscillation with an angle between bottom and water surface, the third hydrodynamic term of eq. (7) influenced by forward speed, becomes more important.
However, this term presents a linear relation between maximum impact pressure and amplitude of oscillation and so the relation between this pressure and the impact velocity becomes more complex for this mode of motions, as discussed in 4.3.
Experimental results such as those shown in fig. 13 give little indication of this linear relation.
Furthermore, fig. 13 clearly demonstrates that the dimensionless peak pressures also show the highest values for the most forward pressure gauge. This observation is in agreement with the proposed theory which states in eq. (7) that the peak pressure is

inversely proportional to the wetted width of the section.

7. Conclusions and recommendations.

Based on analysis of the tests and proposed - and existing calculation methods for bottom impact slamming, the following conclusions and recommendations may be derived:

1. The bottom impact pressure in cases where there is forward speed appeared to be much higher if there is an angle between the bottom and water surface at the moment of impact with the water surface.

2. These high peak pressures cannot be explained by the well-known relation between slamming pressure and the squared vertical velocity of the ship with respect to the water and the rate of increase of added mass with depth only. Also the acceleration of the added mass due to the development of a forward velocity component perpendicular to the bottom should be taken into account as follows from the proposed calculation method.

3. Photographs indicate that air inclusion for flat bottom impacts is so randomly distributed, that prediction is difficult and not worthwhile because the slamming pressure is usually reduced by the presence of air.

4. From the existing calculation procedures, method I (Takezawa, Chuang, e.a.) delivers the best results for flat bottom impact pressures, but gives unreasonably low values for cases with forward speed if there is even a small angle (about 2 degrees) between the bottom and the water surface.

5. The existing calculation methods for bow slamming generally provide peak pressure values which are too high for cases with forward speed if there is even a small angle (about 2 degrees) between the bottom and water surface. Method III (Stavovy - Chuang) shows the best agreement with the experiments for this case.

6. The time in which the peak pressure develops for the case of forward speed with a small angle between the bottom and water surface appeared to be about four times shorter than for the case of pure flat bottom impact, while prediction up to now is hardly possible.

7. The results for the prediction of bottom impact peak pressures according to the proposed calculation method are rather satisfactory. The deviations from the experimental values in the case of pure bottom impact are comparable with those of method I (Takezawa, Chuang, e.a.)
Extending the results to the situation of a ship moving in waves is possible and expedient. Bow slamming results can also be extended to this case.

8. Further investigation is needed to determine the draught of a section at which the sectional added mass has achieved the forward velocity component perpendicular to the bottom or the hull.

9. The question remains of which frequenc(y)(ies) should be used for calculating the hydrodynamic mass.

10. Forced oscillation by PMM proved to be of great assistance to the experimental analyses of slamming phenomena.

8. Acknowledgement.

Special thanks are due to the various members of the staff of the Delft Ship Hydromechanics Laboratory for their assistance in running these slamming experiments.
Particularly the author wishes to mention mr. C.W. Jorens, who developed and handled the greater part of the electronic instrumentation and mr. A.J. van Strien who performed the tests and worked out the measurements.

9. List of symbols.

A	half area of the section with a draught $T' = 0.08\ T$
a_a	average acceleration perpendicular to the bottom due to forward speed
a_{max}	maximum acceleration perpendicular to the bottom due to forward speed
a_1, a_3, a_5	conformal transformation coefficients
B	breadth of the ship
b	half width of the section with a draught $T' = 0.08\ T$
C_B	blockcoefficient
F'	sectional hydromechanic force
Fn	Froude number
G	model's centre of gravity
g	acceleration of gravity
k, k_1	proportionality constant
LCB	longitudinal position of centre of buoyancy
L_{pp}	length between perpendiculars
m'	sectional added mass
N'	sectional damping
n	impact velocity exponent
p	slamming pressure, coëfficient
p_i	impact pressure
p_p	planing pressure
q	coëfficient
r	amplitude of oscillation
s	displacement of section perpendicular to bottom
T	design draught of model
T'	average draught at test condition
t	time

V	forward speed
V_A	forward speed component
v	impact velocity
$x\ y\ z$, $x_b y_b z_b$	right hand coordinate systems fixed to ship
y_w	half width of the cross section at the water surface
z	heave displacement
z_a	heave amplitude
α	angle between bottom and water surface
γ	angle at which bottom touches the water surface
ω	circular frequency of oscillation
ρ	density of water
θ	pitch angle
θ_a	pitch amplitude

10. References.

[1] Ochi, M.K. and Motter, L.E.,
Prediction of slamming characteristics and hull responses for ship design.
SNAME 81, 1973 p.p. 144 - 176.

[2] Takezawa, S. and Hasegawa, S.,
On the characteristics of water impact pressures acting on a hull surface among waves,
Journal of the Society of Naval Architects of Japan,
Vol 13, 1975.

[3] Ochi, Margaret D. and Bonilla-Norat, José,
Pressure-velocity relationship in impact of a ship model dropped onto the water surface and in slamming in waves,
NSRDC, report 3153, June 1970.

[4] Ochi, M.K.,
Prediction of occurrence and severity of ship slamming at sea,
5th Symposium on Naval Hydrodynamics,
Bergen, Norway, 1964.

[5] Tasai, F.,
A study on the seakeeping qualities of full ships
Report of Research Institute for Applied Mechanics,
Japan, Vol. XVI, No. 55, 1968.

[6] Ochi, M.K.,
Model experiments on ship strength and slamming in regular waves,
Trans. SNAME, vol. 66, 1958.

[7] Hagiwara, K. and Yuhara, T.,
Fundamental Study of Wave Impact Loads on Ship Bow (1st report)
Selected Papers from Jour. Soc. Nav. Arch. of Japan,
Vol. 14 (1976).

[8] Wagner, H.,
Uber Stoss- und Gleitvorgänge an der Oberfläche von Flüssigkeiten,
Zeitschr. für Angewandte Mathematik und Mechanik, Band 12, Heft 4, 1932.

[9] Kaplan, P. and Malakhoff, A.,
Hard structure slamming of SES Craft in waves.
AIAA/SNAME Advanced Marine Vehicles Conference, San Diego, april 1978.

[10] Tick, L.J.
Certain probabilities associated with bow subemergence and ship slamming in irregular seas,
Journal of Ship Research, vol. 2, June 1958.

[11] Ochi, M.K. and Motter, E.,
Prediction of extreme ship responses in rough seas of the North Atlantic,
International Symposium on the Dynamics of Marine Vehicles in Waves, London, 1974.

[12] Aertsen, G.
Labouring of ships in rough seas,
SNAME, Diamond Jubilee Spring Meeting 1968.

[13] Verhagen, J.H.G.,
The impact of a flat plate on a water surface,
Journal of Ship Research, December 1967, p.p. 211 - 222.

[14] Chuang, S.L.,
Experiments on flat-bottom slamming,
Journal of Ship Research, March 1966, p.p. 10 - 17.

[15] Chuang, S.L.,
Experiments on slamming of wedge-shaped bodies,
Journal of Ship Research, September 1967, p.p. 190 - 198.

[16] Chuang, S.L. and Milne, D.T.,
Drop tests of cones to investigate the three-dimensional effects of slamming,
NSRDC report 3543, 1971.

[17] Hagiwara, K. and Yuhara, T.,
Fundamental study of wave impact loads on ship bow (2nd report)
- Effect of scale of the model on maximum impact pressure and equivalent static pressure,
Naval Architecture and Ocean Engineering of the Society of Naval Architects of Japan, 1977, vol. 15.

[18] Johnson, Robert S.,
The effect of air compressibility in a first approximation to the ship slamming problem,
Journal of Ship Research, March 1968, p.p. 57 - 68.

[19] Lewison, G.R.G.,
On the reduction of slamming pressure,
RINA, vol. 112, 1970.

[20] Greenberg, Michael D.,
On the water impact of a circular cylinder,
Therm Advanced Research, Inc. TAR-TR6701, May 1967.

[21] Chuang, S.,
Investigation of impact of rigid and elastic bodies with water,
NSRDC Report 3248, Febr. 1970.

[22] Lewison, G.R.G.
Slamming,
National Physical Laboratory, Ship Report 138, March 1970.

[23] Bosch, J.J. v.d.,
Slamming
Laboratorium voor Scheepsbouwkunde, Technische Hogeschool Delft, rapport no. 67, October 1970.

[24] Kaplan, P. and Sargent, T.P.,
Further studies of computer simulation of slamming and other wave-induced vibratory structural loadings on ships in waves,
Ship Structure Committee report 231, 1972.

[25] Mansour, A. and d'Oliviera, J.M.,
Hull bending moment due to ship bottom slamming in regular waves,
Journal of Ship Research, June 1975, p.p. 80 - 92.

[26] Stavovy, Alexander B. and Chuang, S.L.,
Analytical determination of slamming pressures for high-speed vehicles in waves,
Journal of Ship Research, december 1976, p.p. 190 - 198.

[27] Bishop, R.E.D. and Price, W.G.,
On the dynamics of slamming,
RINA, Spring Meetings 1978.

[28] Gerritsma, J. and Beukelman, W.,
Analysis of the modified strip theory for the calculation of ship motions and wave bending moments,
International Shipbuilding Progress, Vol. 14, no. 156, 1967.

[29] Frank, W. and Salvesen, N.,
The Frank close-fit ship motion computer program,
NRSDC report no. 3289, June 1970.

Appendix.

To achieve the vertical forward speed component V_A, the following relation between speed, acceleration and time has been assumed:

$$\text{for speed}: \quad v = \tfrac{1}{2}\, p\, t^2 - \tfrac{1}{3}\, q\, t^3$$
$$\text{for acceleration}: \quad a = p\, t - q\, t^2$$

in which p and q are coëfficients and t = time. See fig. 14.

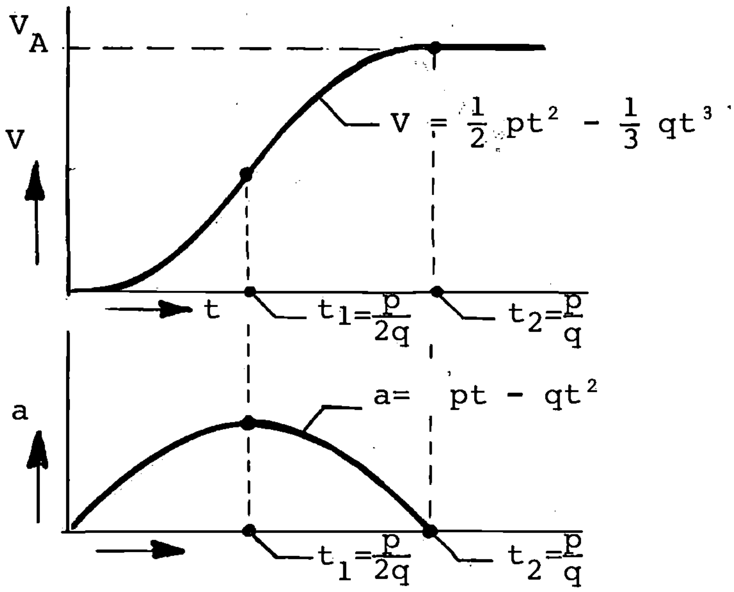

Fig.14 Assumed relation of speed and acceleration with time in which the pressure develops.

The time in which the velocity V_A for the sectional added mass will be achieved when a = 0 and amounts:

$$t_2 = \frac{p}{q}$$

The velocity at that time is

$$V = V_A = \frac{p^3}{6q^2}$$

The average acceleration during the time t_2 may be written as:

$$a_a = \frac{V_A}{t_2} = \frac{p^2}{6q}$$

The maximum acceleration will occur if $\frac{da}{dt} = 0$, so at the time

$$t_1 = \frac{p}{2q}$$

This maximum acceleration will then be:

$$a_{max} = \frac{p^2}{4q}$$

It now appears that this maximum acceleration is given by:

$$a_{max} = 1.5\ a_a$$

TABLE 1 Main particulars of ship model.

Length between perpendiculars (L_{pp})	2.258	m
Breadth (B)	0.322	m
Draught (design) (T)	0.129	m
Draught (used for test condition) (T')	0.040	m
Volume of displacement (design)	0.0657	m^3
Volume of displacement (test condition)	0.0181	m^3
Block coëfficient (design) (C_B)	0.700	
LCB forward of $L_{pp}/2$ (design)	0.011	m
LCB forward of $L_{pp}/2$ (test condition)	0.035	m

TABLE 2 Sectional hydrodynamic characteristics for pure heave.

ω	SECTION AT PRESSURE GAUGE											
	A		B		C		D		E		F	
	y_w=0.124m		y_w=0.124m		y_w=0.124m		y_w=0.089m		y_w=0.034m		y_w=0.072m	
	N'	$\frac{dm'}{ds}$	N'	$\frac{dm'}{ds}$	N'	$\frac{dm'}{ds}$	N'	$\frac{dm'}{ds}$	N'	$\frac{dm'}{ds}$	N'	$\frac{dm'}{ds}$
s^{-1}	$\frac{Ns}{m^2}$	$\frac{Ns^2}{m^3}$	$\frac{Ns}{m^2}$	$\frac{Ns^2}{m^3}$	$\frac{Ns}{m^2}$	$\frac{Ns^2}{m^3}$	$\frac{Ns}{m^2}$	$\frac{Ns^2}{m^3}$	$\frac{Ns}{m^2}$	$\frac{Ns^2}{m^3}$	$\frac{Ns}{m^2}$	$\frac{Ns^2}{m^3}$
4	148	-4542	150	-4179	150	-4316	72	-6377	16	-3051	59	-5042
6	169	-3836	171	-3257	170	-3473	86	-5435	21	-2354	71	-4179
8	175	-3237	177	-3012	176	-3090	92	-4365	23	-1874	77	-3365
10	171	-3110	173	-2796	173	-2914	94	-3875	25	-1648	79	-2992
12	162	-3090	163	-2815	163	-2914	93	-3689	26	-1511	79	-2835

TABLE 3 : SECTIONAL HYDRODYNAMIC CHARACTERISTICS FOR PITCH AND HEAVE WITH AN ANGLE.

ω	SECTION AT PRESSURE GAUGE (S)											
	A, B, F			C			E			D		
	y_w =0.0722 m			y_w =0.053 m			y_w = 0.034 m			y_w = 0.089 m		
	N'	m'	$\frac{dm'}{ds}$	N'	m'	$\frac{dm'}{ds}$	N'	m'	$\frac{dm'}{ds}$	N'	m'	$\frac{dm'}{ds}$
s^{-1}	$\frac{Ns}{m^2}$	$\frac{Ns^2}{m^2}$	$\frac{Ns^2}{m^3}$	$\frac{Ns}{m^2}$	$\frac{Ns^2}{m^2}$	$\frac{Ns^2}{m^3}$	$\frac{Ns}{m^2}$	$\frac{Ns^2}{m^2}$	$\frac{Ns^2}{m^3}$	$\frac{Ns}{m^2}$	$\frac{Ns^2}{m^2}$	$\frac{Ns^2}{m^3}$
4	59	16	-5042	38	10	-4052	16	5	-3051	72	19	-6377
6	71	12	-4179	46	8	-3276	21	4	-2354	86	14	-5435
8	77	10	-3365	50	6	-2619	23	3	-1874	92	12	-4365
10	79	9	-2992	52	6	-2325	25	3	-1648	94	11	-3875
12	79	8	-2835	52	5	-2178	26	2	-1511	93	10	-3689

blanco cijfer

TABLE 4 : CALCULATED PRESSURES

FOR GAUGE E; r = 0.04 m; y_w = 0.034 m

mode of motion	ω	$-\frac{N'}{2y_w}\dot{s}$	$-\frac{dm'}{ds}\frac{\dot{s}^2}{2y_w}$	v=0.706 m/s		v=1.412 m/s		$-\frac{m'}{2y_w}\ddot{s}'$ kPa			p kPa		
				$t.10^3$	a_{max}	$t.10^3$	a_{max}	V= 0	V= 0.706	V= 1.412	V= 0	V= 0.706	V= 1.412
	s^{-1}	kPa	kPa	s	m/s^2	s	m/s^2	m/s	m/s	m/s	m/s	m/s	m/s
PURE HEAVE (T' = 0 m)	4	0.04	1.15	-	-	-	-	-	-	-	1.19	1.19	1.19
	6	0.07	1.99	-	-	-	-	-	-	-	2.06	2.06	2.06
	8	0.11	2.82	-	-	-	-	-	-	-	2.93	2.93	2.93
	10	0.15	3.87	-	-	-	-	-	-	-	4.02	4.02	4.02
	12	0.19	5.10	-	-	-	-	-	-	-	5.29	5.29	5.29
PITCH (T' = 0 m)	4	0.05	1.74	-	-	-	-	-	-	-	1.79	1.79	1.79
	6	0.09	3.02	-	-	-	-	-	-	-	3.11	3.11	3.11
	8	0.14	4.27	-	-	-	-	-	-	-	4.41	4.41	4.41
	10	0.18	5.88	-	-	-	-	-	-	-	6.06	6.06	6.06
	12	0.23	7.74	-	-	-	-	-	-	-	7.97	7.97	7.97
PITCH (T' = 0.02 m)	4	0.04	1.45	0.83	-20	0.83	- 41	0.02	1.40	2.91	1.51	2.89	4.40
	6	0.08	2.52	0.56	-30	0.56	- 52	0.04	1.62	3.36	2.64	4.22	5.96
	8	0.13	3.56	0.42	-40	0.42	- 83	0.06	1.80	3.69	3.75	5.49	7.38
	10	0.17	4.99	0.33	-50	0.33	-104	0.08	1.95	4.01	5.14	7.01	9.07
	12	0.21	6.45	0.28	-59	0.28	-124	0.10	2.12	4.33	6.76	8.78	10.99
HEAVE WITH (T'=0 m) α =2.3°	4	0.03	0.53	1.37	-31	1.37	- 62	-0.03	2.10	4.31	0.53	2.66	4.87
	6	0.05	0.91	0.92	-46	0.92	- 93	-0.06	2.38	4.90	0.90	3.34	5.86
	8	0.08	1.29	0.69	-61	0.69	-124	-0.08	2.58	5.35	1.29	3.95	6.72
	10	0.10	1.78	0.56	-75	0.56	-154	-0.11	2.78	5.76	1.77	4.66	7.64
	12	0.13	2.35	0.46	-91	0.46	-186	-0.15	2.97	6.19	2.33	5.45	8.67

TABLE 5 : CALCULATED PRESSURES

FOR GAUGE E; $r = 0.06$ m; $y_w = 0.034$ m.

mode of motion	ω	$-\frac{N'}{2y_w}\dot{s}$	$-\frac{dm'}{ds}\frac{\dot{s}^2}{2y_w}$	v=0.706 m/s $t.10^3$	v=0.706 m/s a_{max}	v=1.412 m/s $t.10^3$	v=1.412 m/s a_{max}	$-\frac{m'}{2y_w}\ddot{s}'$ kPa V= 0 m/s	$-\frac{m'}{2y_w}\ddot{s}'$ kPa V= 0.706 m/s	$-\frac{m'}{2y_w}\ddot{s}'$ kPa V= 1.412 m/s	p kPa V= 0 m/s	p kPa V= 0.706 m/s	p kPa V= 1.412 m/s
	s^{-1}	kPa	kPa	s	m/s^2	s	m/s^2						
PURE HEAVE (T' = 0 m)	4	0.06	2.58	-	-	-	-	-	-	-	2.64	2.64	2.64
	6	0.11	4.47	-	-	-	-	-	-	-	4.58	4.58	4.58
	8	0.17	6.33	-	-	-	-	-	-	-	6.50	6.50	6.50
	10	0.22	8.70	-	-	-	-	-	-	-	8.92	8.92	8.92
	12	0.27	11.49	-	-	-	-	-	-	-	11.76	11.76	11.76
PITCH (T' = 0 m)	4	0.07	3.92	-	-	-	-	-	-	-	3.99	3.99	3.99
	6	0.14	6.78	-	-	-	-	-	-	-	6.92	6.92	6.92
	8	0.21	9.59	-	-	-	-	-	-	-	9.80	9.80	9.80
	10	0.27	13.19	-	-	-	-	-	-	-	13.46	13.46	13.46
	12	0.34	17.43	-	-	-	-	-	-	-	17.77	17.77	17.77
PITCH (T' = 0.02 m)	4	0.07	3.63	0.53	- 31	0.53	- 66	0.02	2.22	4.61	3.72	5.92	8.31
	6	0.13	6.30	0.35	- 47	0.35	- 98	0.04	2.54	5.29	6.47	8.97	11.72
	8	0.20	8.90	0.26	- 63	0.26	-131	0.06	2.80	5.79	9.16	11.90	14.89
	10	0.26	12.25	0.21	- 78	0.21	-164	0.08	3.04	6.29	12.59	15.55	18.80
	12	0.32	16.16	0.18	- 94	0.18	-196	0.10	3.30	6.78	16.58	19.78	23.26
HEAVE WITH (T'=0 m) α=2.3°	4	0.05	1.95	0.72	- 59	0.72	-119	-0.03	4.05	8.29	1.97	6.05	10.29
	6	0.10	3.40	0.48	- 88	0.48	-179	-0.06	4.63	9.50	3.44	8.13	13.00
	8	0.15	4.80	0.36	-117	0.36	-238	-0.08	5.05	10.37	4.87	10.00	15.32
	10	0.20	6.61	0.29	-146	0.29	-298	-0.11	5.44	11.21	6.70	12.25	18.02
	12	0.24	8.74	0.24	-176	0.24	-358	-0.15	5.85	12.06	8.83	14.83	21.04

TABLE 6 : CALCULATED PRESSURES
FOR GAUGE F AND GAUGES A, B (PITCH AND
HEAVE WITH AN ANGLE); r = 0.04 m; y_w = 0.072 m.

mode of motion	ω	$-\frac{N'}{2y_w}\dot{s}$	$-\frac{dm'}{ds}\frac{\dot{s}^2}{2y_w}$	v=0.706 m/s		v=1.412 m/s		$-\frac{m'}{2y_w}\ddot{s}'$ kPa			p kPa		
				$t.10^3$	a_{max}	$t.10^3$	a_{max}	V= 0	V= 0.706	V= 1.412	V= 0	V= 0.706	V= 1.412
	s^{-1}	kPa	kPa	s	m/s^2	s	m/s^2	m/s	m/s	m/s	m/s	m/s	m/s
PURE HEAVE (T' = 0 m)	4	0.07	0.89	-	-	-	-	-	-	-	0.96	0.96	0.96
	6	0.12	1.67	-	-	-	-	-	-	-	1.79	1.79	1.79
	8	0.17	2.38	-	-	-	-	-	-	-	2.55	2.55	2.55
	10	0.22	3.32	-	-	-	-	-	-	-	3.54	3.54	3.54
	12	0.26	4.52	-	-	-	-	-	-	-	4.78	4.78	4.78
PITCH (T' = 0 m)	4	0.07	1.03	-	-	-	-	-	-	-	1.10	1.10	1.10
	6	0.13	1.91	-	-	-	-	-	-	-	2.04	2.04	2.04
	8	0.19	2.74	-	-	-	-	-	-	-	2.91	2.91	2.91
	10	0.24	3.82	-	-	-	-	-	-	-	4.06	4.06	4.06
	12	0.28	5.21	-	-	-	-	-	-	-	5.49	5.49	5.49
PITCH (T' = 0.02 m)	4	0.06	0.80	0.99	- 20	0.99	- 43	0.04	2.22	4.73	0.90	3.08	5.59
	6	0.11	1.49	0.66	- 30	0.66	- 64	0.06	2.54	5.39	1.66	4.14	6.99
	8	0.17	2.14	0.50	- 39	0.50	- 85	0.09	2.82	5.96	2.40	5.13	8.27
	10	0.21	2.97	0.40	- 49	0.40	-106	0.12	3.13	6.62	3.30	6.31	9.80
	12	0.25	4.06	0.33	- 59	0.33	-127	0.17	3.49	7.34	4.48	7.80	11.65
HEAVE WITH (T'=0 m) α =2.3°	4	0.05	0.60	1.15	- 37	1.15	- 75	-0.04	4.00	8.20	0.61	4.65	8.85
	6	0.10	0.11	0.77	- 55	0.77	-112	-0.07	4.51	9.23	1.14	5.72	10.44
	8	0.14	1.60	0.57	- 73	0.57	-149	-0.10	4.98	10.24	1.64	6.72	11.98
	10	0.18	2.22	0.46	- 92	0.46	-186	-0.14	5.47	11.27	2.26	7.87	13.67
	12	0.22	3.02	0.38	-110	0.38	-223	-0.19	6.00	12.41	3.05	9.24	15.65

TABLE 7 : CALCULATED PRESSURES FOR GAUGE F AND GAUGES A, B (PITCH AND HEAVE WITH AN ANGLE); r = 0.06 m; y_w = 0.072 m.

mode of motion	ω	$-\frac{N'}{2y_w}\dot{s}$	$-\frac{dm'}{ds}\frac{\dot{s}^2}{2y_w}$	v=0.706 m/s t.10^3	v=0.706 m/s a_{max}	v=1.412 m/s t.10^3	v=1.412 m/s a_{max}	$-\frac{m'}{2y_w}\ddot{s}'$ kPa V=0 m/s	$-\frac{m'}{2y_w}\ddot{s}'$ kPa V=0.706 m/s	$-\frac{m'}{2y_w}\ddot{s}'$ kPa V=1.412 m/s	p kPa V=0 m/s	p kPa V=0.706 m/s	p kPa V=1.412 m/s
	s^{-1}	kPa	kPa	s	m/s^2	s	m/s^2						
PURE HEAVE (T' = 0 m)	4	0.10	2.01	-	-	-	-	-	-	-	2.11	2.11	2.11
	6	0.18	3.75	-	-	-	-	-	-	-	3.93	3.93	3.93
	8	0.26	5.37	-	-	-	-	-	-	-	5.72	5.72	5.72
	10	0.33	7.46	-	-	-	-	-	-	-	7.79	7.79	7.79
	12	0.39	10.18	-	-	-	-	-	-	-	10.57	10.57	10.57
PITCH (T' = 0 m)	4	0.11	2.31	-	-	-	-	-	-	-	2.42	2.42	2.42
	6	0.19	4.32	-	-	-	-	-	-	-	4.51	4.51	4.51
	8	0.27	6.18	-	-	-	-	-	-	-	6.45	6.45	6.45
	10	0.36	8.56	-	-	-	-	-	-	-	8.92	8.92	8.92
	12	0.42	11.70	-	-	-	-	-	-	-	12.12	12.12	12.12
PITCH (T' = 0.02 m)	4	0.10	2.10	0.61	- 32	0.61	- 69	0.04	3.55	7.60	2.24	5.75	9.80
	6	0.19	3.89	0.41	- 48	0.41	-103	0.06	4.04	8.62	4.14	8.12	12.70
	8	0.26	5.57	0.31	- 64	0.31	-137	0.09	4.49	9.56	5.92	10.32	15.39
	10	0.33	7.74	0.25	- 80	0.25	-171	0.12	4.91	10.61	8.19	12.98	18.68
	12	0.40	10.58	0.20	- 96	0.20	-206	0.17	5.55	11.77	11.15	16.53	22.75
HEAVE WITH (T'=0 m) α =2.3°	4	0.09	1.72	0.68	- 62	0.68	-127	-0.04	6.82	13.91	1.77	8.63	15.72
	6	0.17	3.21	0.45	- 93	0.45	-190	-0.07	7.71	15.76	3.31	11.09	19.14
	8	0.24	4.57	0.34	-125	0.34	-253	-0.10	8.58	17.39	4.71	13.39	22.20
	10	0.30	6.36	0.27	-155	0.27	-316	-0.14	9.35	19.18	6.52	16.01	25.84
	12	0.36	8.68	0.23	-186	0.23	-379	-0.19	10.31	21.19	8.85	19.35	30.23

TABLE 8 : CALCULATED PRESSURES

FOR GAUGE D; $r = 0.04$ m; $y_w = 0.089$ m.

mode of motion	ω	$-\frac{N'}{2y_w}\dot{s}$	$-\frac{dm'}{ds}\frac{\dot{s}^2}{2y_w}$	v=0.706 m/s		v=1.412 m/s		$-\frac{m'}{2y_w}\ddot{s}'$ kPa			p kPa		
				$t.10^3$	a_{max}	$t.10^3$	a_{max}	V= 0 m/s	V= 0.706 m/s	V= 1.412 m/s	V= 0 m/s	V= 0.706 m/s	V= 1.412 m/s
	s^{-1}	kPa	kPa	s	m/s^2	s	m/s^2						
PURE HEAVE (T' = 0 m)	4	0.07	0.92	-	-	-	-	-	-	-	0.99	0.99	0.99
	6	0.12	1.76	-	-	-	-	-	-	-	1.88	1.88	1.88
	8	0.17	2.51	-	-	-	-	-	-	-	2.68	2.68	2.68
	10	0.21	3.48	-	-	-	-	-	-	-	3.69	3.69	3.69
	12	0.25	4.78	-	-	-	-	-	-	-	5.03	5.03	5.03
PITCH (T' = 0 m)	4	0.07	0.90	-	-	-	-	-	-	-	0.97	0.97	0.97
	6	0.11	1.73	-	-	-	-	-	-	-	1.84	1.84	1.84
	8	0.17	2.47	-	-	-	-	-	-	-	2.64	2.64	2.64
	10	0.21	3.41	-	-	-	-	-	-	-	3.62	3.62	3.62
	12	0.24	4.70	-	-	-	-	-	-	-	4.84	4.84	4.84
PITCH (T' = 0.02 m)	4	0.06	0.68	1.10	- 19	1.10	- 39	0.03	2.09	4.15	0.77	2.83	4.89
	6	0.10	1.29	0.73	- 29	0.73	- 58	0.06	2.39	4.73	1.45	3.78	6.12
	8	0.14	1.84	0.55	- 38	0.55	- 77	0.09	2.68	5.27	2.07	4.66	7.25
	10	0.18	2.56	0.44	- 48	0.44	- 96	0.12	2.98	5.85	2.86	5.72	8.59
	12	0.22	3.50	0.37	- 58	0.37	-115	0.16	3.35	6.53	3.88	7.07	10.25
HEAVE WITH (T'=0 m) $\alpha = 2.3^o$	4	0.06	0.70	1.08	- 39	1.08	- 79	-0.03	4.14	8.46	0.73	4.90	9.22
	6	0.10	1.33	0.72	- 59	0.72	-119	-0.06	4.68	9.59	1.37	6.11	11.02
	8	0.15	1.89	0.54	- 78	0.54	-157	-0.09	5.16	10.60	1.95	7.20	12.64
	10	0.19	2.63	0.44	- 97	0.44	-198	-0.12	5.69	11.71	2.70	8.51	14.53
	12	0.22	3.61	0.36	-117	0.36	-238	-0.16	6.31	13.00	3.67	10.14	16.83

TABLE 9 : CALCULATED PRESSURES

FOR GAUGE D; r = 0.06 m; y_w = 0.089 m.

mode of motion	ω	$-\frac{N'}{2y_w}\dot{s}$	$-\frac{dm'}{ds}\frac{\dot{s}^2}{2y_w}$	v=0.706 m/s		v=1.412 m/s		$-\frac{m'}{2y_w}\ddot{s}'$ kPa			p kPa		
				$t.10^3$	a_{max}	$t.10^3$	a_{max}	V= 0	V= 0.706	V= 1.412	V= 0	V= 0.706	V= 1.412
	s^{-1}	kPa	kPa	s	m/s^2	s	m/s^2	m/s	m/s	m/s	m/s	m/s	m/s
PURE HEAVE (T' = 0 m)	4	0.10	2.07	-	-	-	-	-	-	-	2.17	2.17	2.17
	6	0.18	3.96	-	-	-	-	-	-	-	4.14	4.14	4.14
	8	0.25	5.66	-	-	-	-	-	-	-	5.91	5.91	5.91
	10	0.31	2.85	-	-	-	-	-	-	-	8.16	8.16	8.16
	12	0.37	10.75	-	-	-	-	-	-	-	11.12	11.12	11.12
PITCH (T' = 0 m)	4	0.10	2.03	-	-	-	-	-	-	-	2.13	2.13	2.13
	6	0.18	3.89	-	-	-	-	-	-	-	4.07	4.07	4.07
	8	0.25	5.56	-	-	-	-	-	-	-	5.81	5.81	5.81
	10	0.31	7.72	-	-	-	-	-	-	-	8.03	8.03	8.03
	12	0.37	10.58	-	-	-	-	-	-	-	10.95	10.95	10.95
PITCH (T' = 0.02 m)	4	0.09	1.80	0.67	- 31	0.67	- 63	0.03	3.38	6.75	1.92	5.27	8.64
	6	0.16	3.45	0.45	- 47	0.45	- 94	0.06	3.87	7.69	3.67	7.48	11.30
	8	0.24	4.92	0.34	- 63	0.34	-125	0.09	4.32	8.55	5.25	9.48	13.71
	10	0.29	6.86	0.27	- 78	0.27	-157	0.12	4.81	9.50	7.27	11.96	16.65
	12	0.35	9.40	0.22	- 94	0.22	-188	0.16	5.38	10.58	9.91	15.31	20.33
HEAVE WITH (T'=0 m) α=2.3°	4	0.09	1.84	0.66	- 63	0.66	-129	-0.03	6.78	13.83	1.90	8.71	15.76
	6	0.17	3.53	0.44	- 55	0.44	-194	-0.06	7.65	15.64	3.64	11.35	19.34
	8	0.24	5.04	0.33	-127	0.33	-258	-0.09	8.47	17.33	5.19	13.75	22.61
	10	0.29	7.00	0.26	-159	0.26	-323	-0.12	9.39	19.21	7.17	16.68	26.50
	12	0.35	9.59	0.22	-190	0.22	-388	-0.16	10.38	21.30	9.78	20.32	31.24

List of figures.

Fig. 15 Dimensionless peak pressure in relation to frequency of oscillation.

Fig. 16 Assumed relation of speed and acceleration with time in which the pressure develops.

TABLE 4 : CALCULATED PRESSURES
FOR GAUGE E; r = 0.04 m; y_w = 0.034 m

TABLE 5 : CALCULATED PRESSURES
FOR GAUGE E; r = 0.06 m; y_w = 0.034 m.

TABLE 6 : CALCULATED PRESSURES
FOR GAUGE F AND GAUGES A, B (PITCH AND
HEAVE WITH AN ANGLE); r = 0.04 m; y_w = 0.072 m.

TABLE 7 : CALCULATED PRESSURES
FOR GAUGE F AND GAUGES A, B (PITCH AND
HEAVE WITH AN ANGLE); r = 0.06 m; y_w = 0.072 m.

TABLE 8 : CALCULATED PRESSURES
FOR GAUGE D; r = 0.04 m; y_w = 0.089 m.

TABLE 9 : CALCULATED PRESSURES
FOR GAUGE D; r = 0.06 m; y_w = 0.089 m.

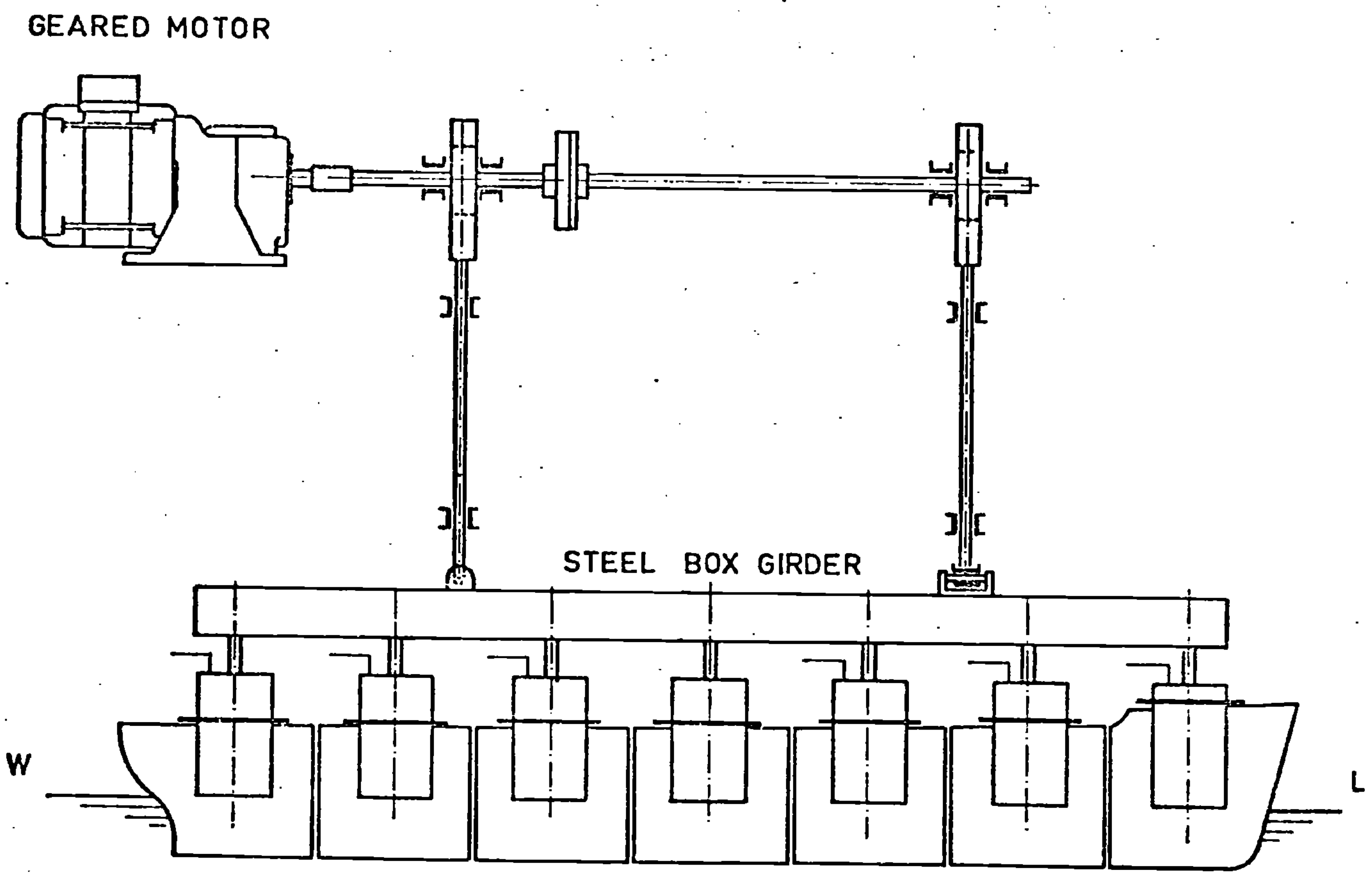

Fig. 1 Arrangement of oscillation tests.

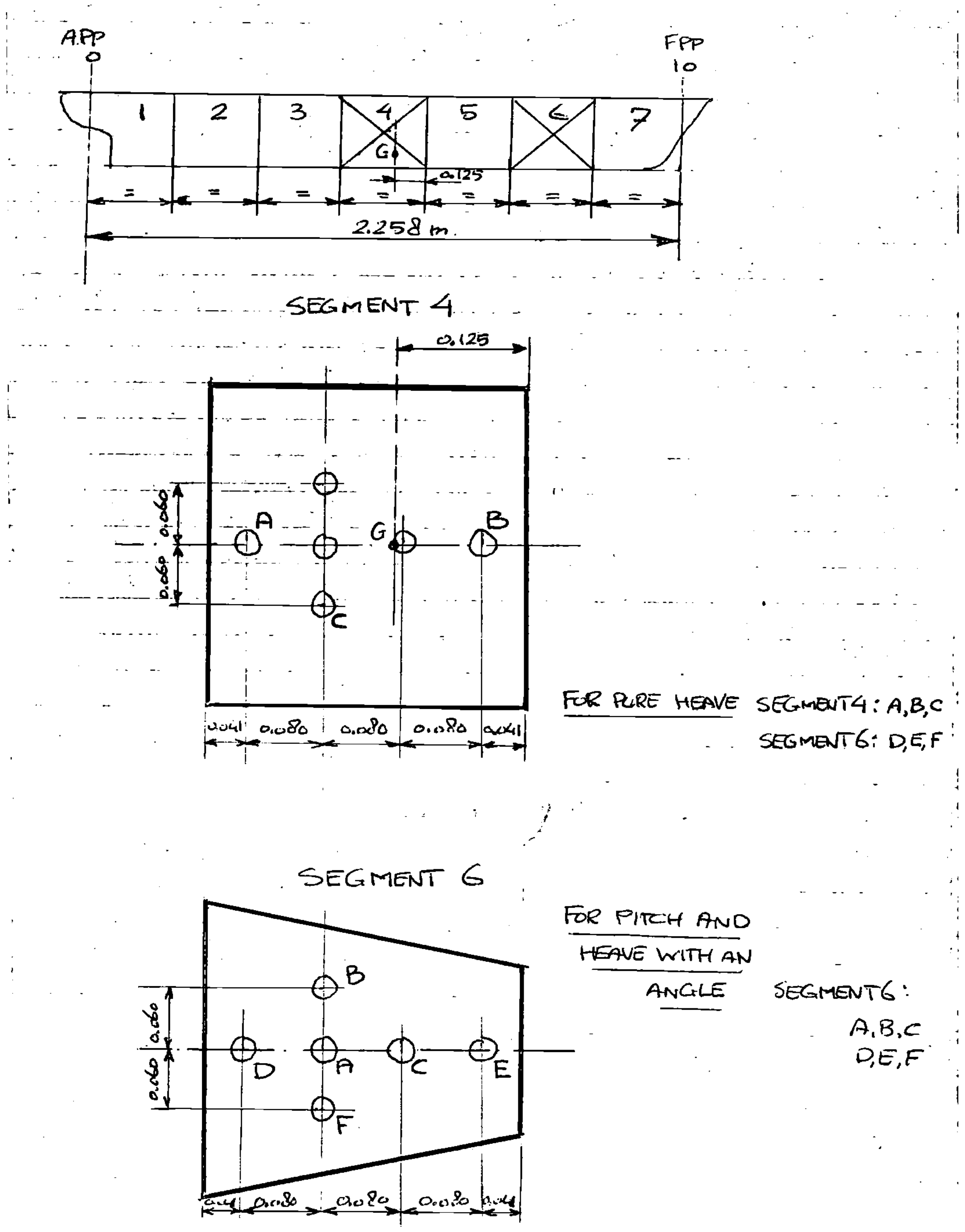

Fig. 2 Place of pressure gauges in the segments for the different modes of oscillation.

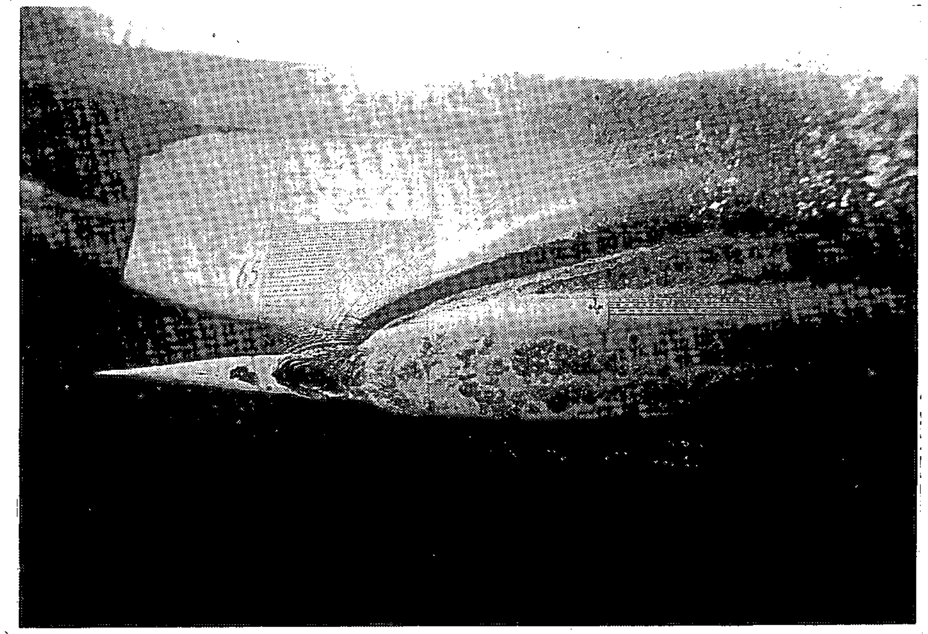

Heave Fn = 0.25; ω = 8; r = 0.06 m
T = 0; α = 0

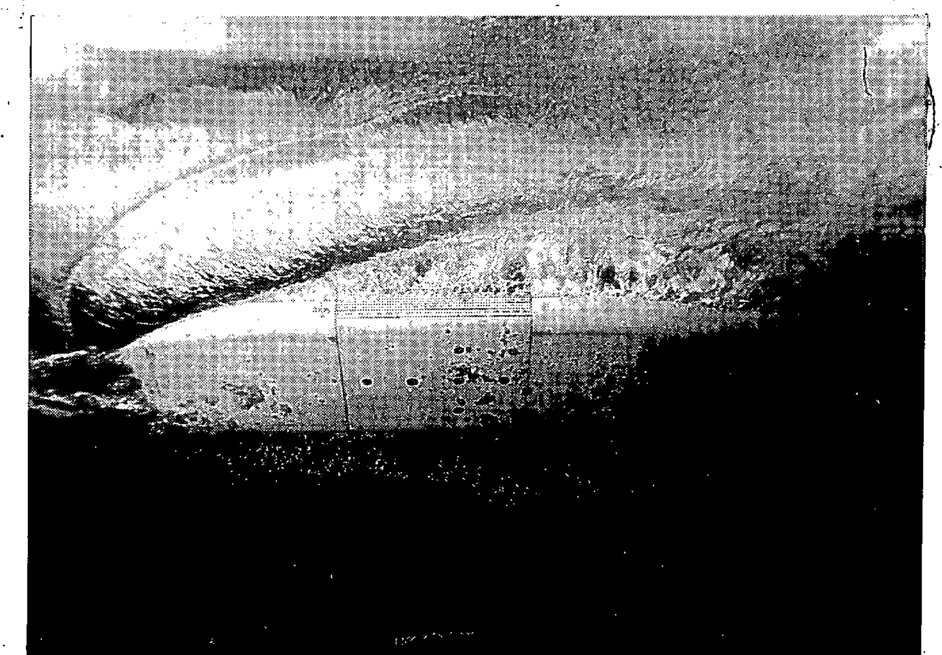

Pitch Fn = 0.25; ω = 8; r = 0.06 m
T' = 0.02 m

Fig. 2 Photographs of the model bottom showing air inclusion.

Heave
T=0 α=0
Pressure
gauge C

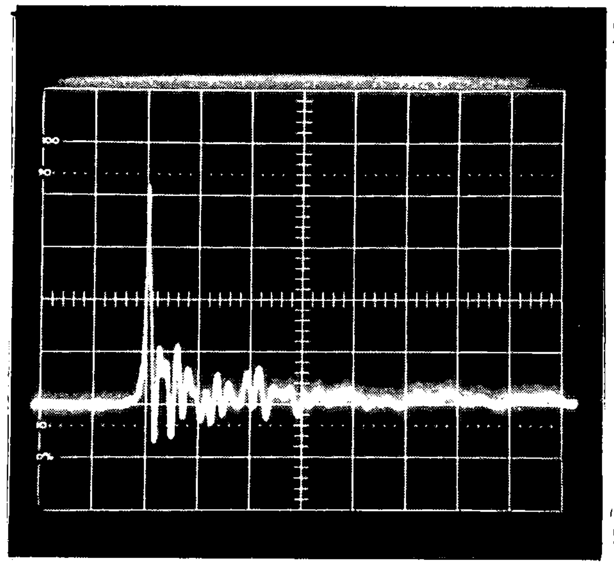

[Fn = 0.15; ω = 6; r = 0.04 m

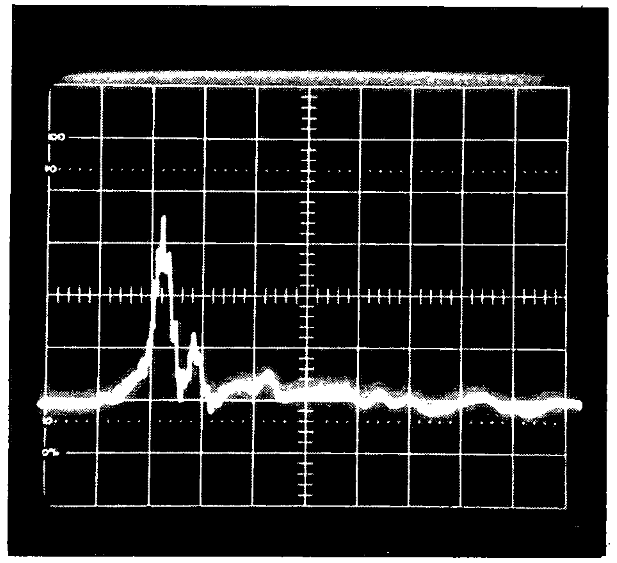

[Fn = 0.25; ω = 12; r = 0.04 m

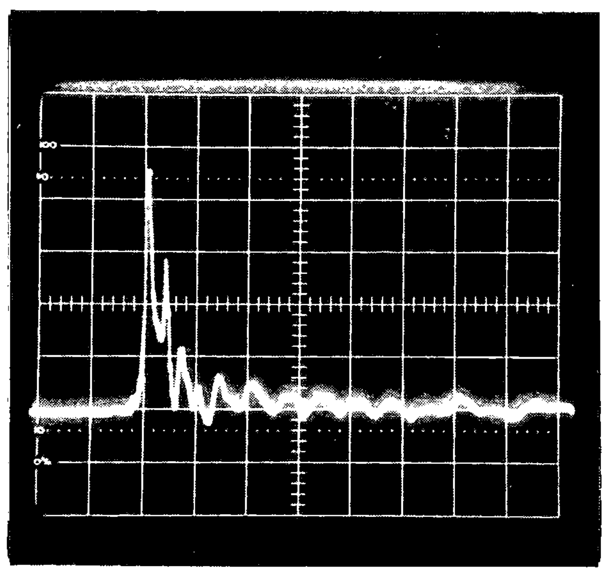

[Fn = 0.20; ω = 10; r = 0.04 m

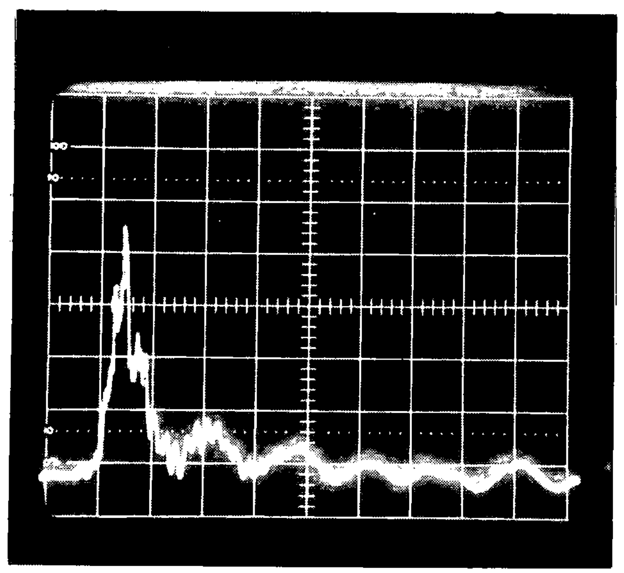

[Fn = 0.20; ω = 10; r = 0.06 m

Fig. 3 Photographs of slamming pressure taken from the oscilloscope.

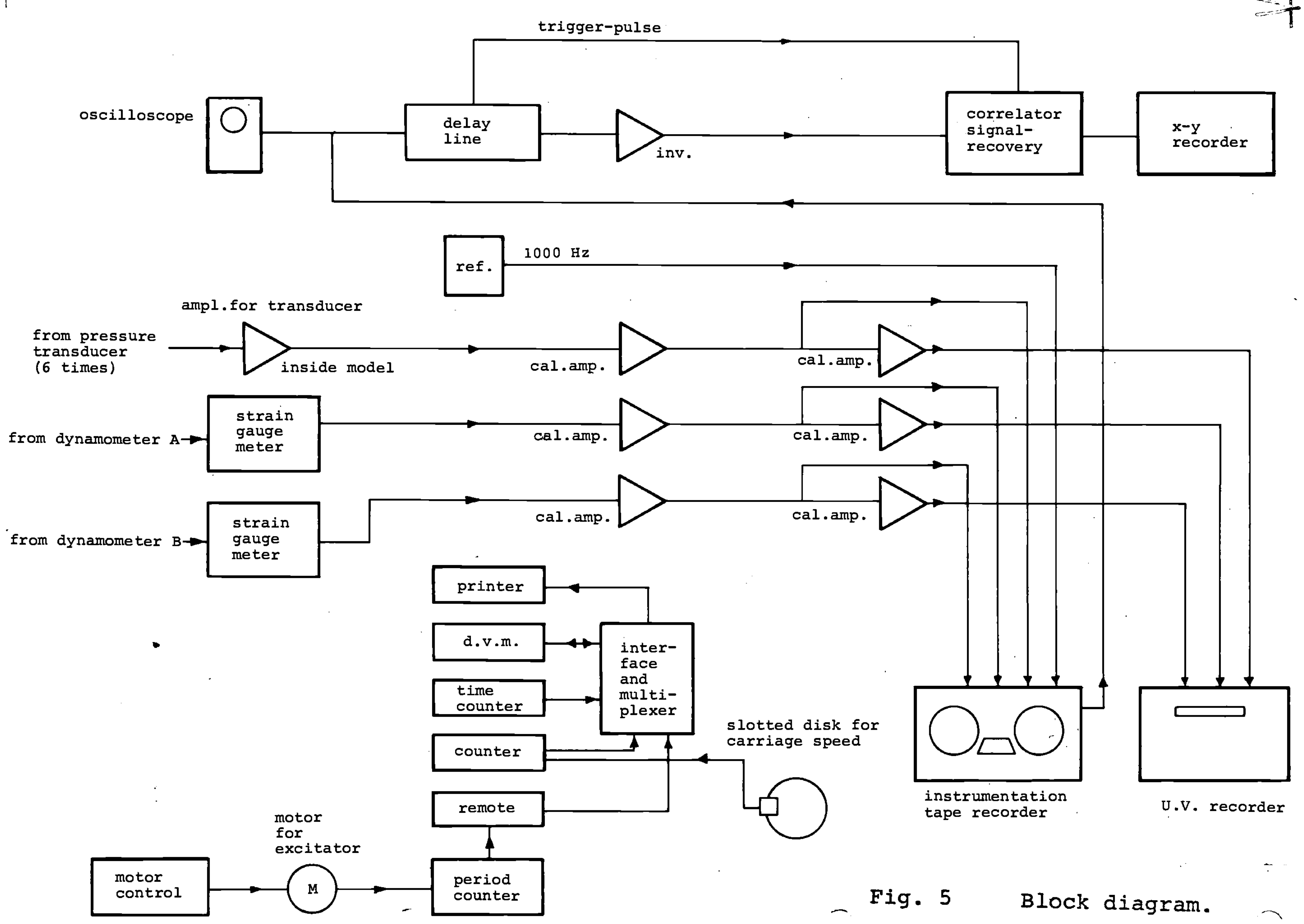

Fig. 5 Block diagram.

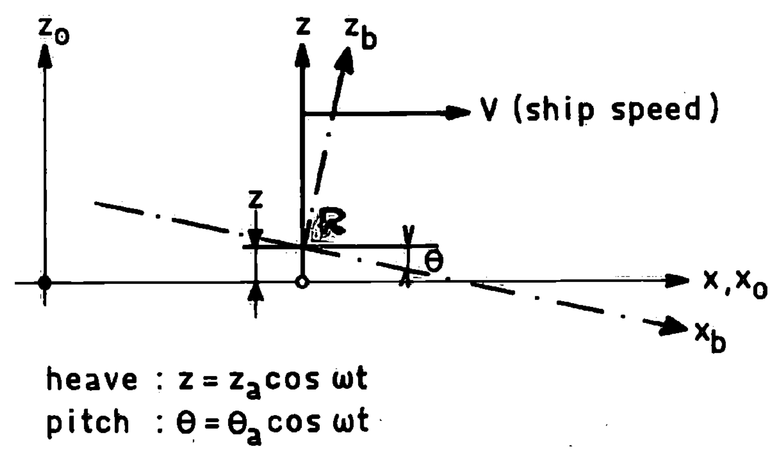

Fig. 6 Coordinate systems.

6

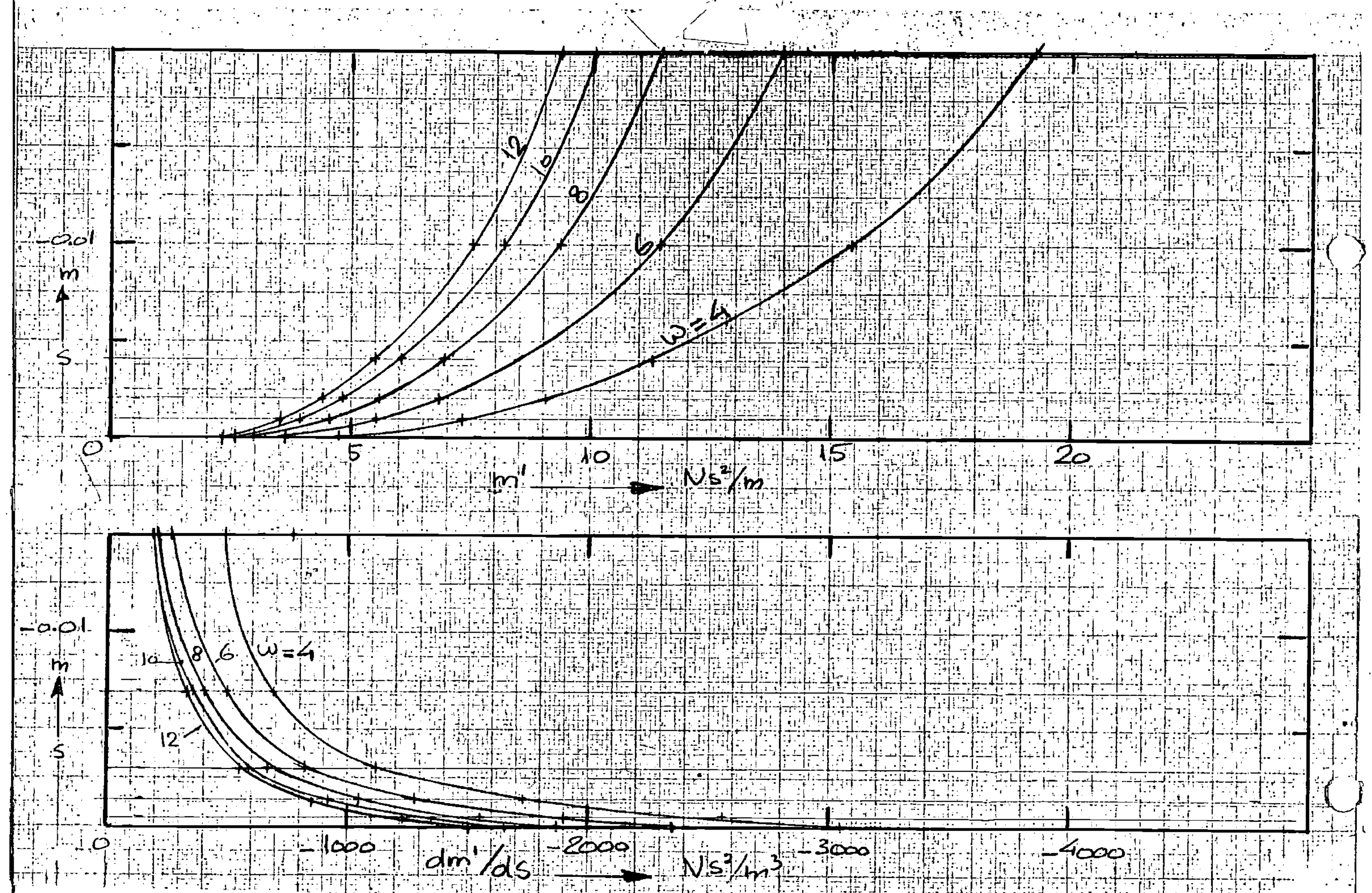

Fig. 7 Added mass and rate of change of added mass with depth per unit length for the section at pressure gauge E.

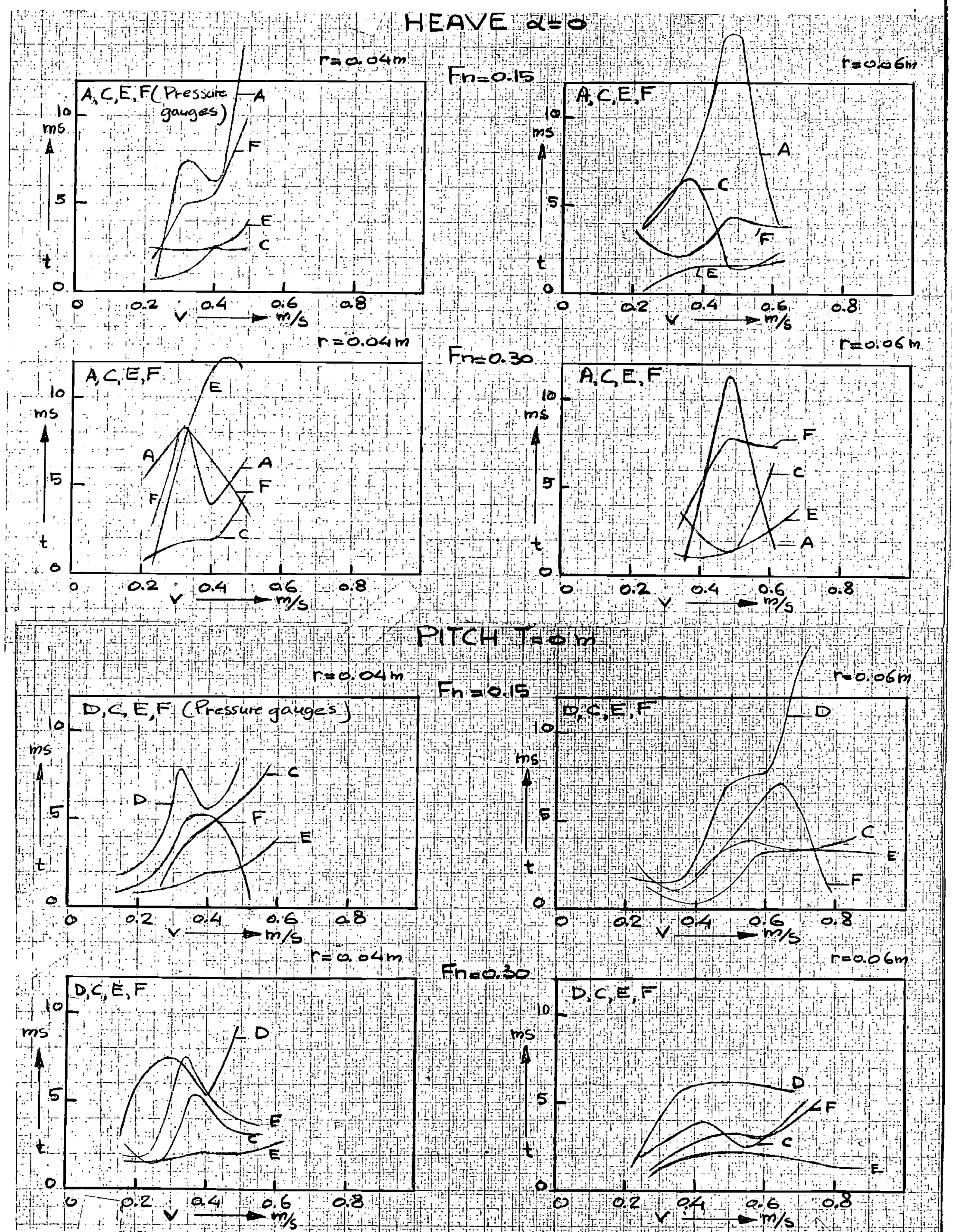

Fig. 10a Time in which peak pressures develop.

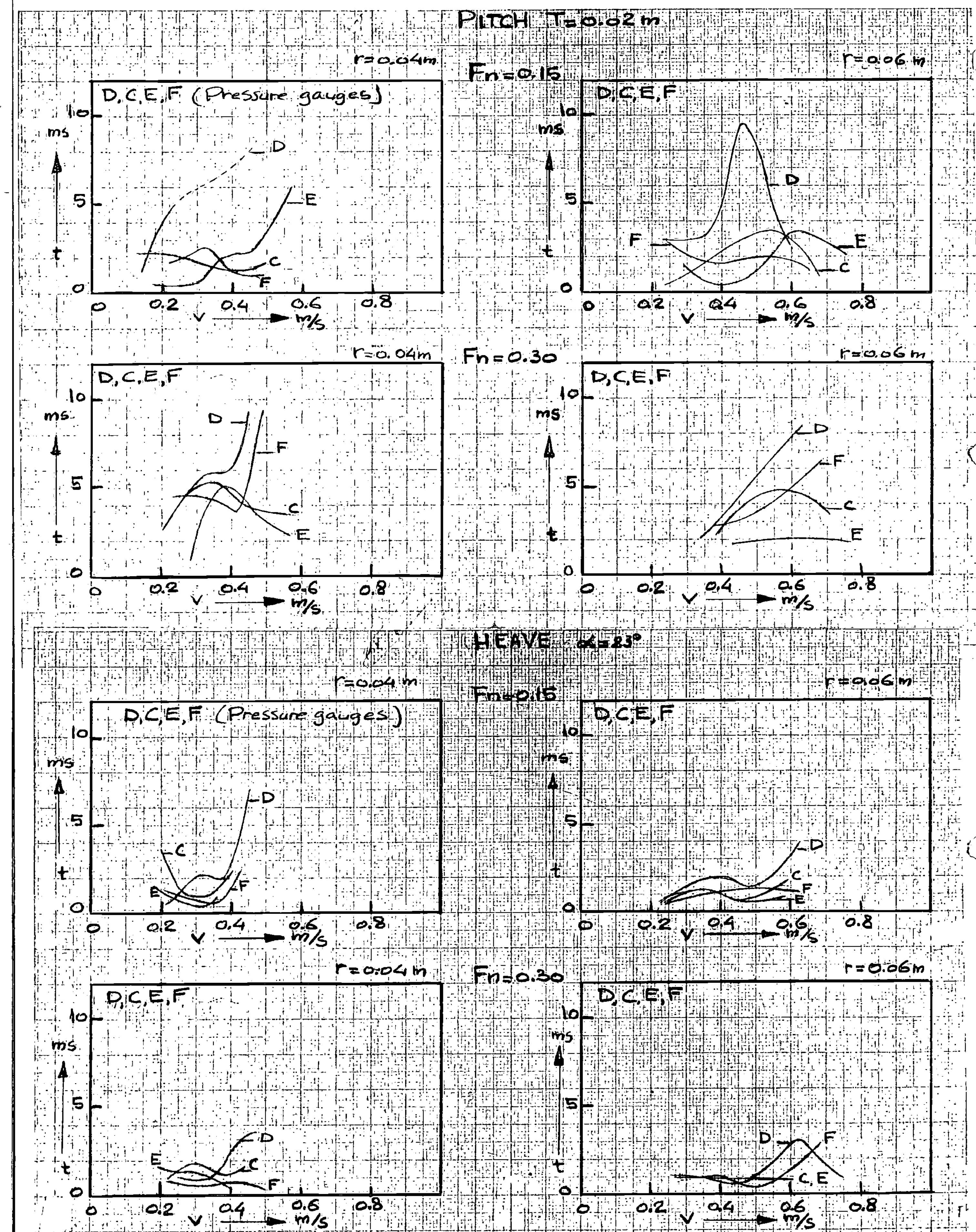

Fig. 10 b Time in which peak pressures develop.

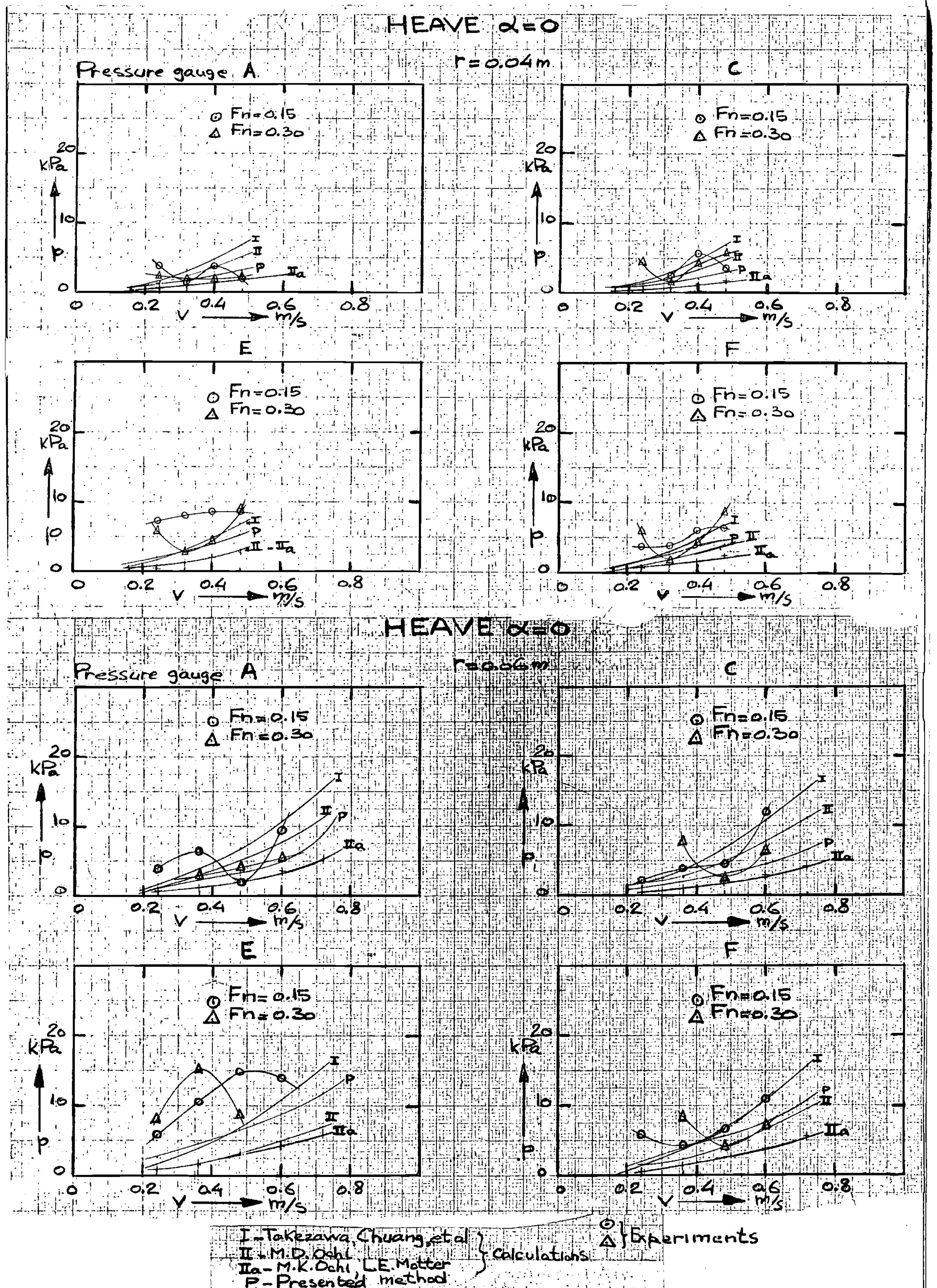

Fig. 11 Test- and calculation results of peak pressures for pure heave.

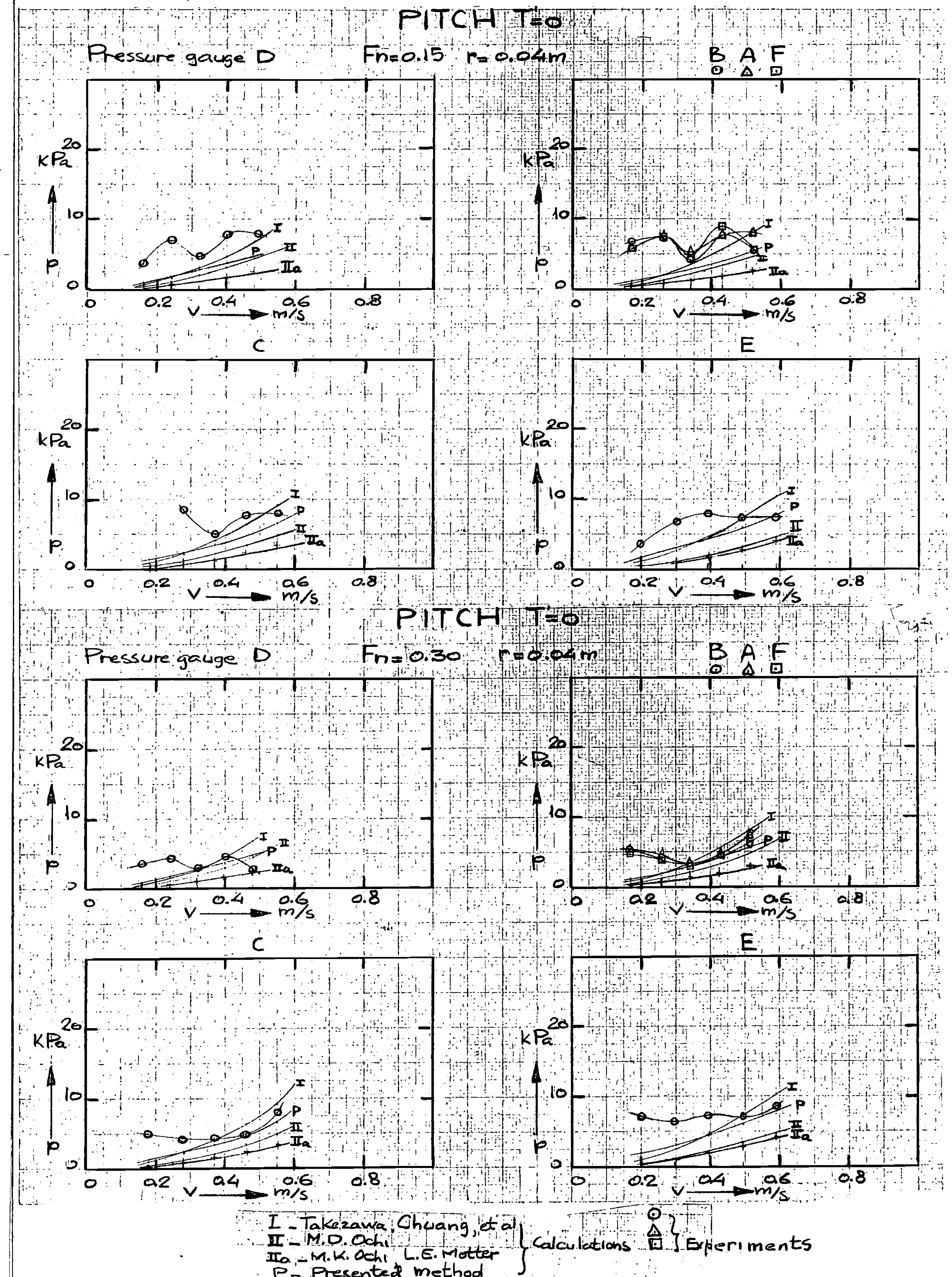

Fig. 12 a Test- and calculation results of peak pressures for pitch about the water surface.

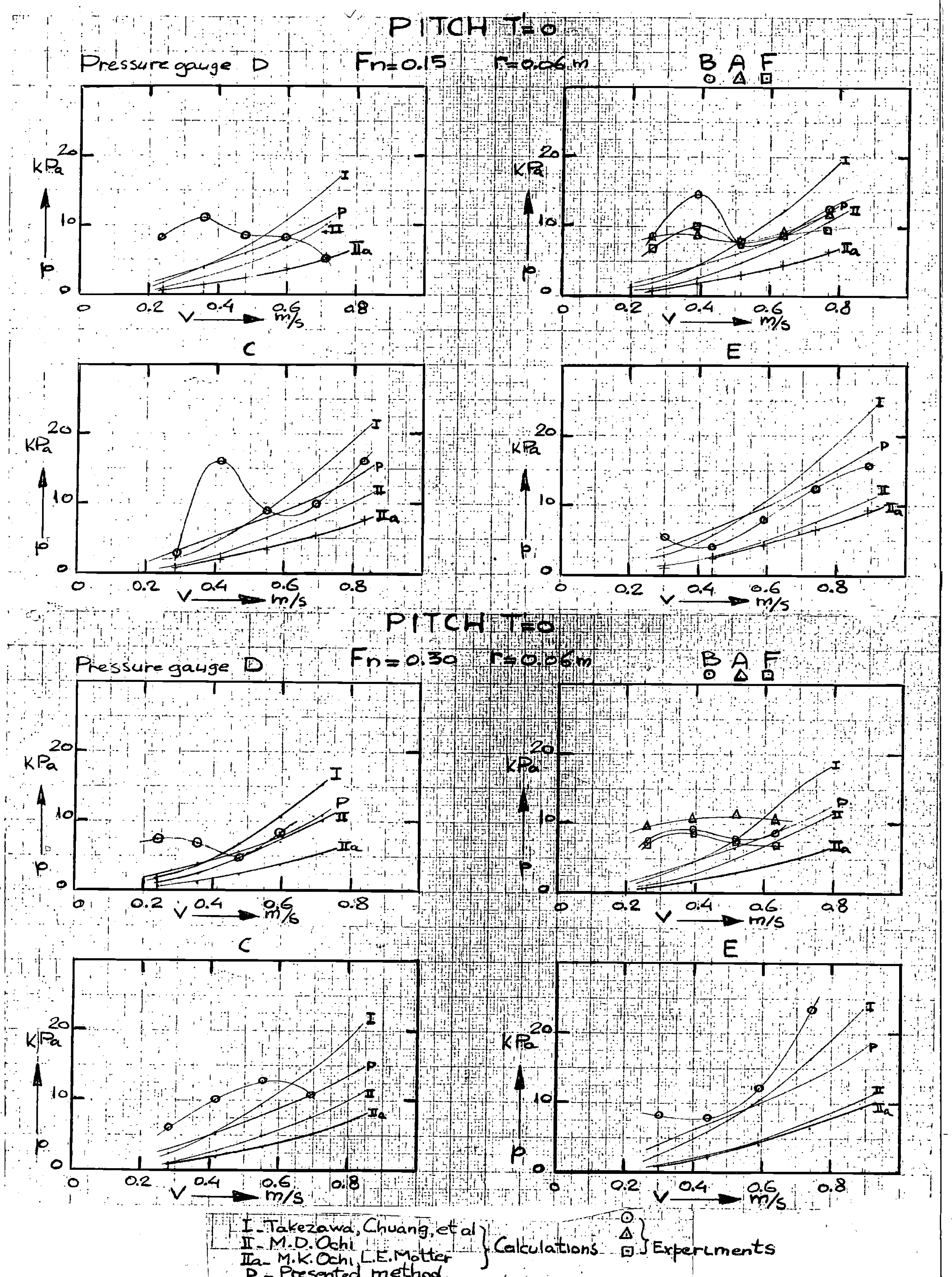

Fig. 12 b Test- and calculation results of peak pressures for pitch about the water surface.

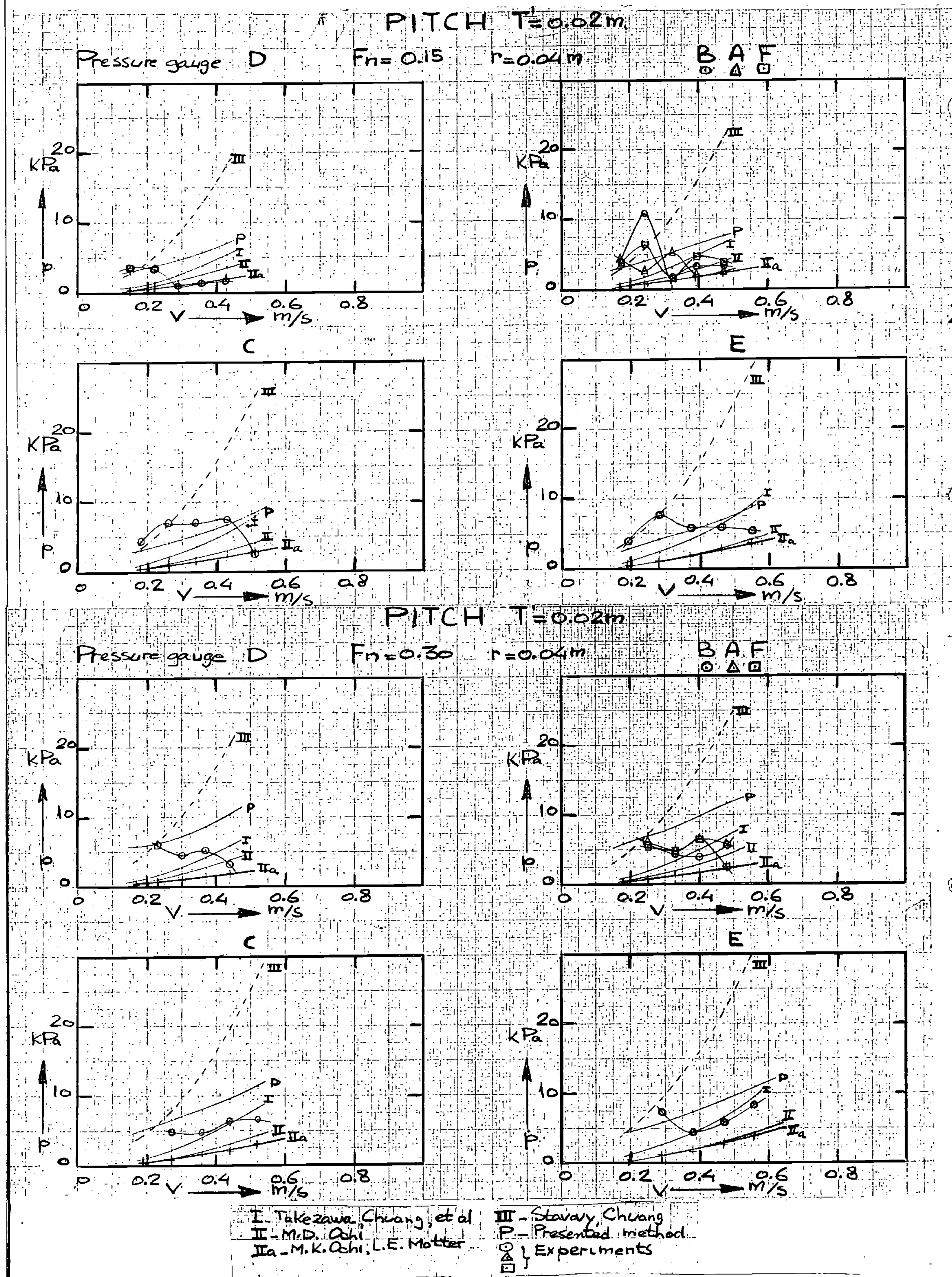

Fig. 13[a] Test- and calculation results of peak pressures for pitch around the aft leg with T' = 0.02 m.

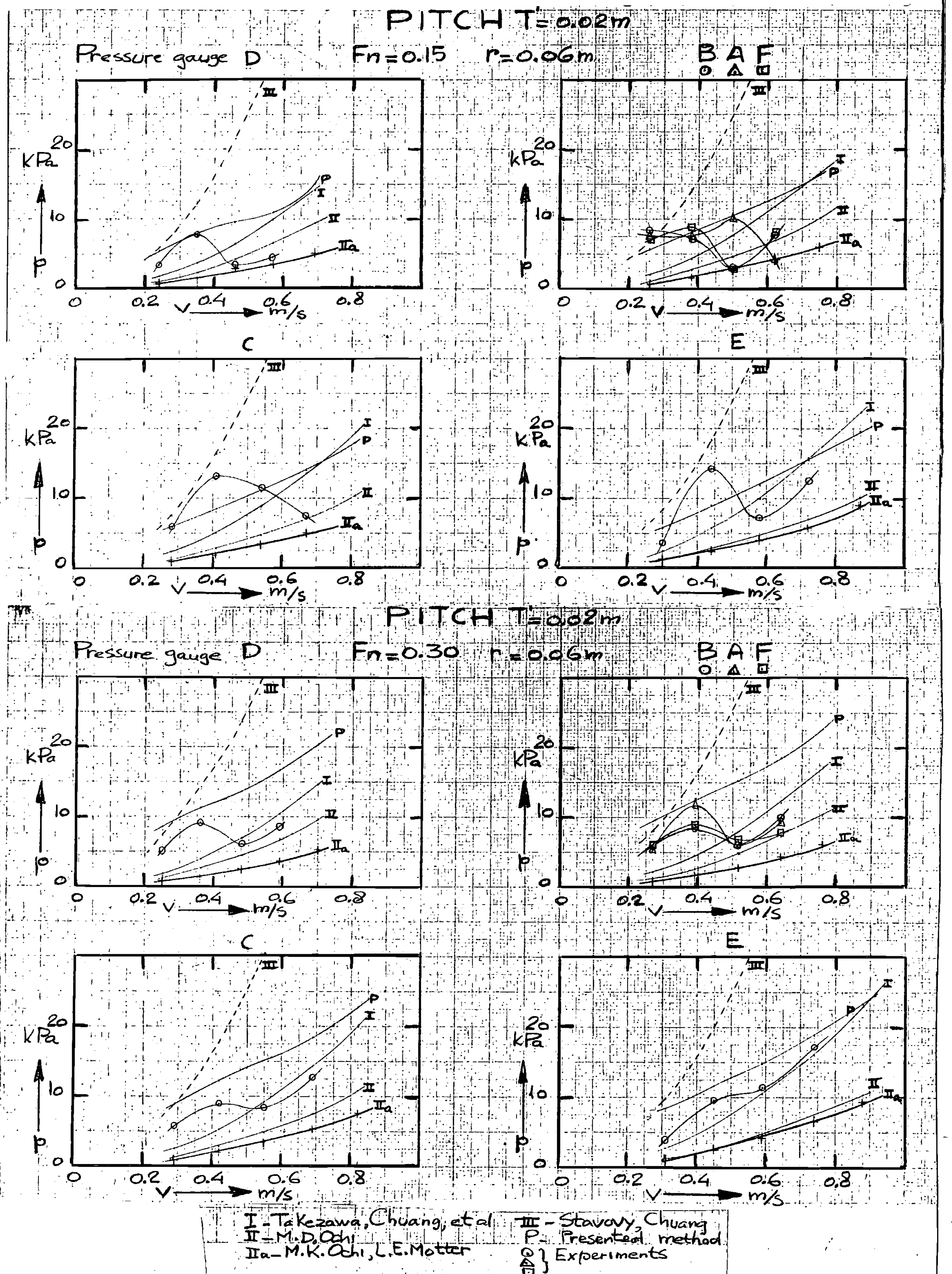

Fig. 13 b Test- and calculation results of peak pressures for pitch around the aft leg with T' = 0.02 m.

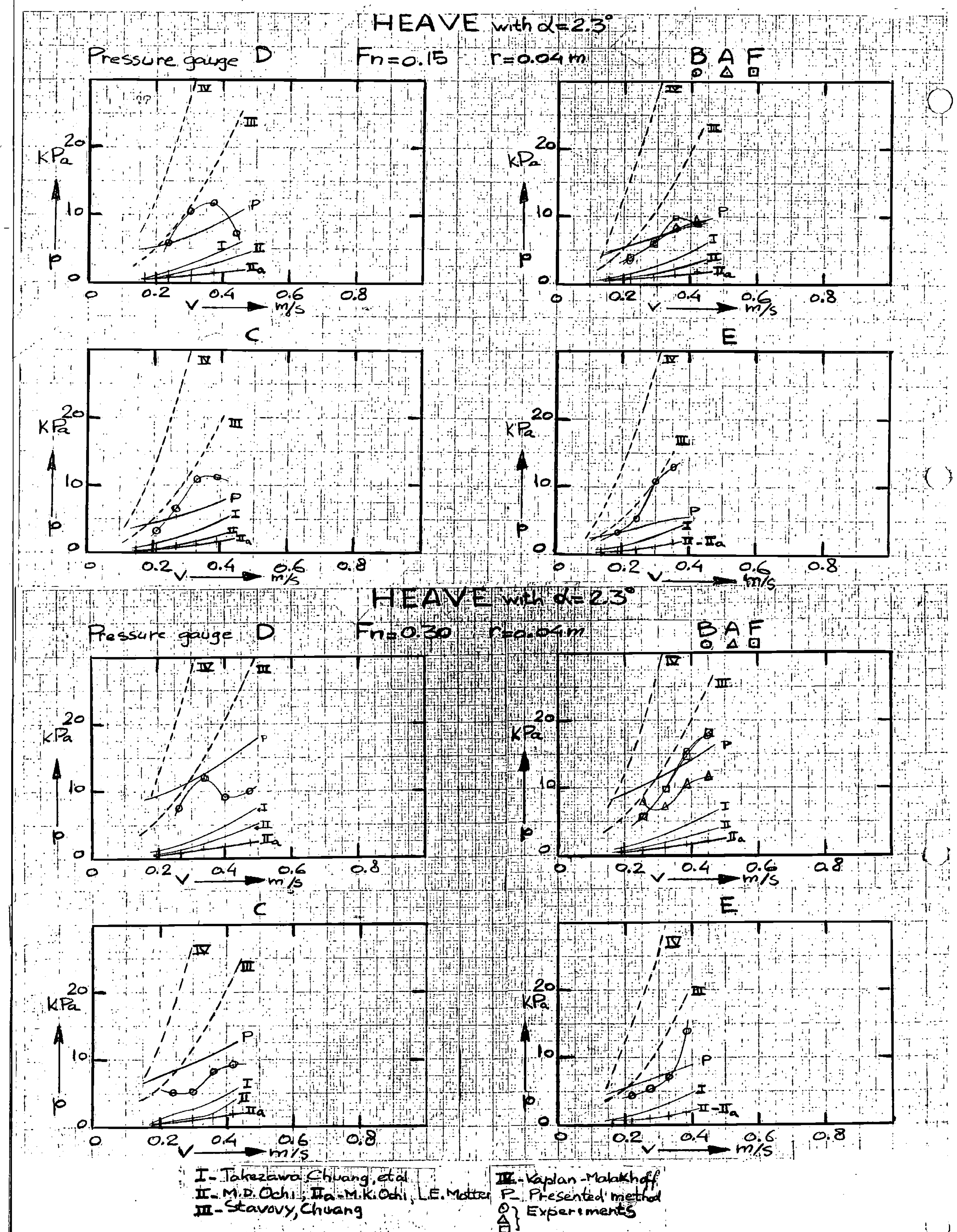

Fig. 14 a Test- and calculation results of peak pressures for heave with an angle between bottom and water surface.

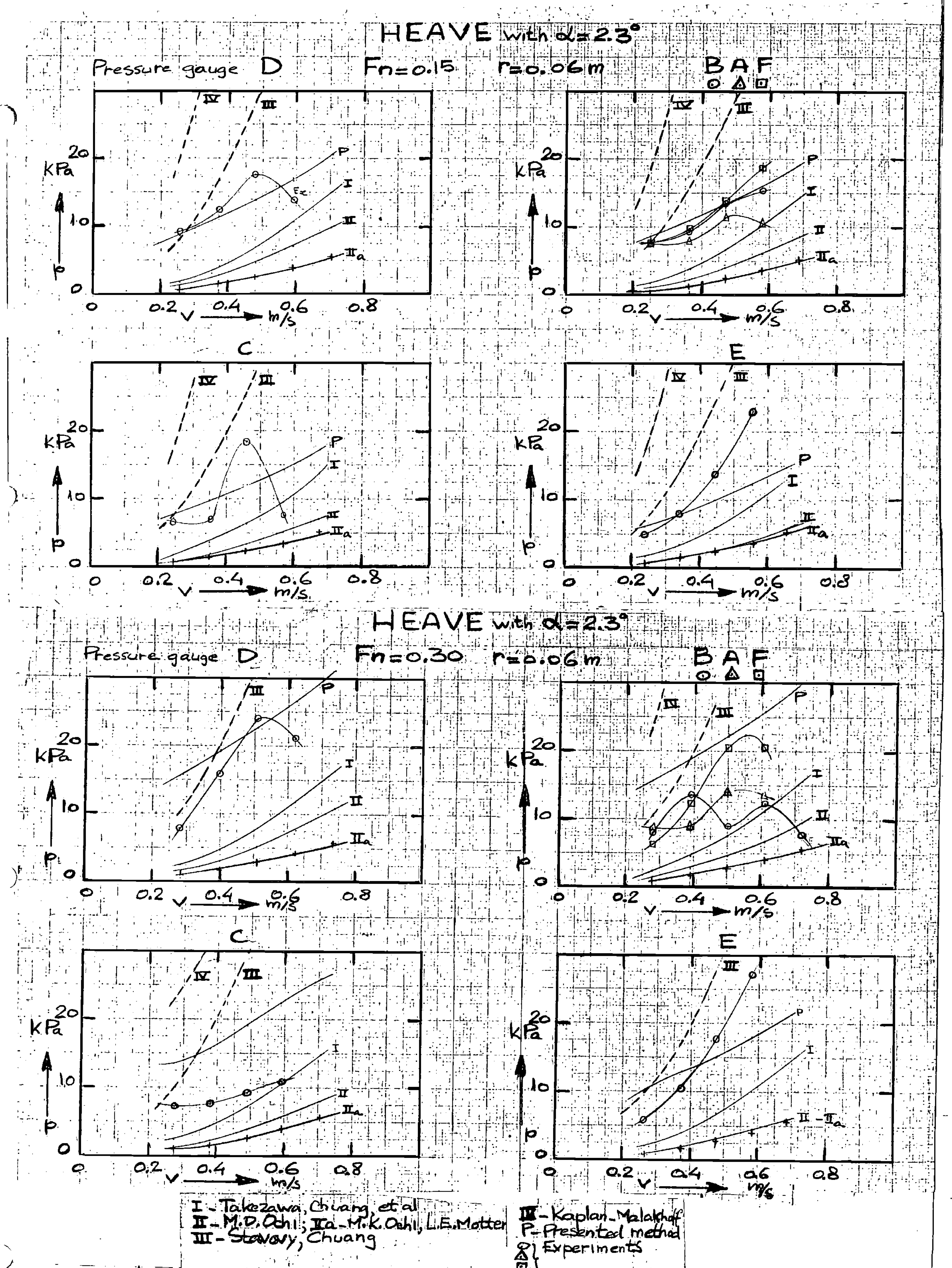

Fig. 14 b Test- and calculation results of peak pressures for heave with an angle between bottom and water surface.

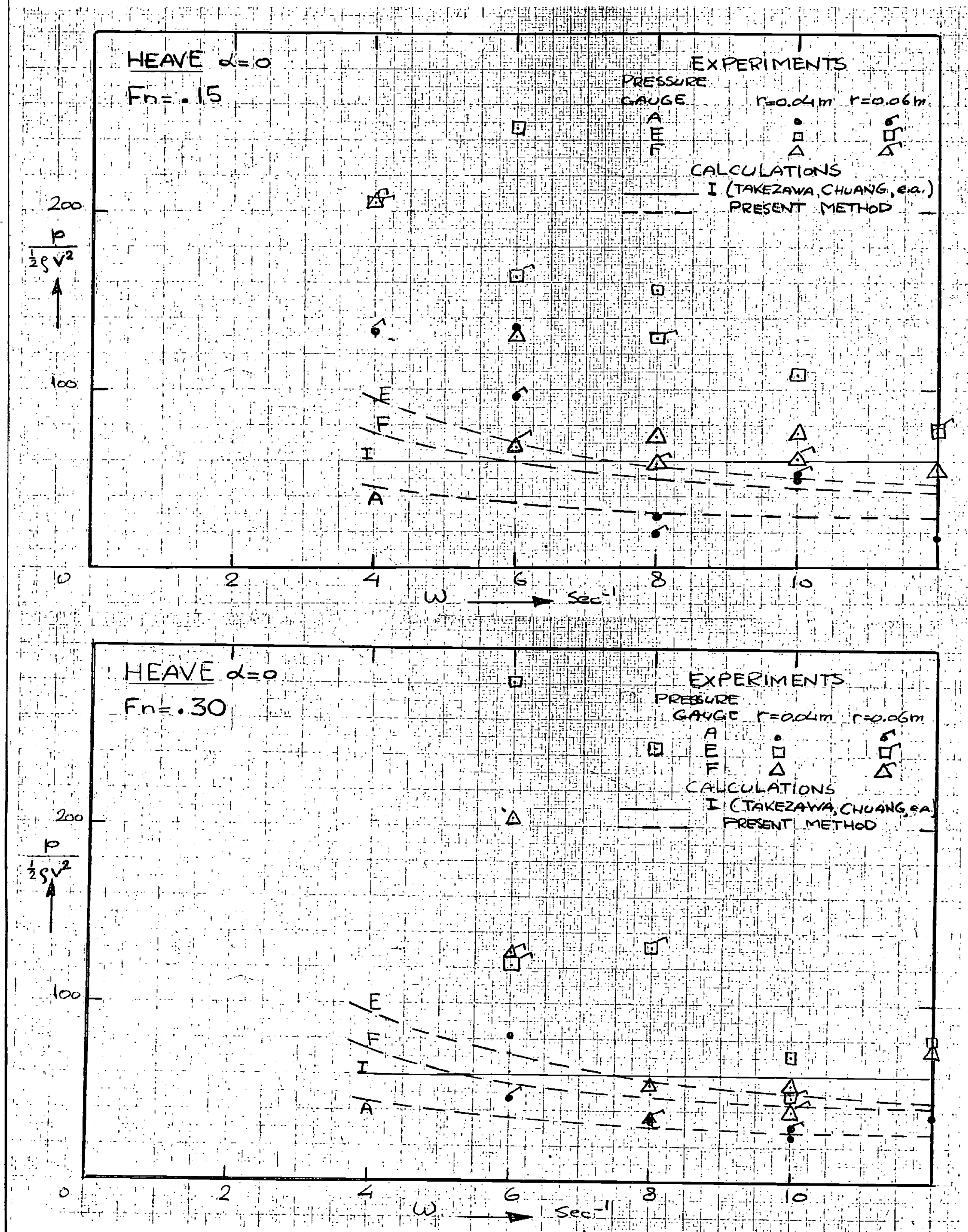

Fig. 15 a Dimensionless peak pressure in relation to frequency of oscillation.

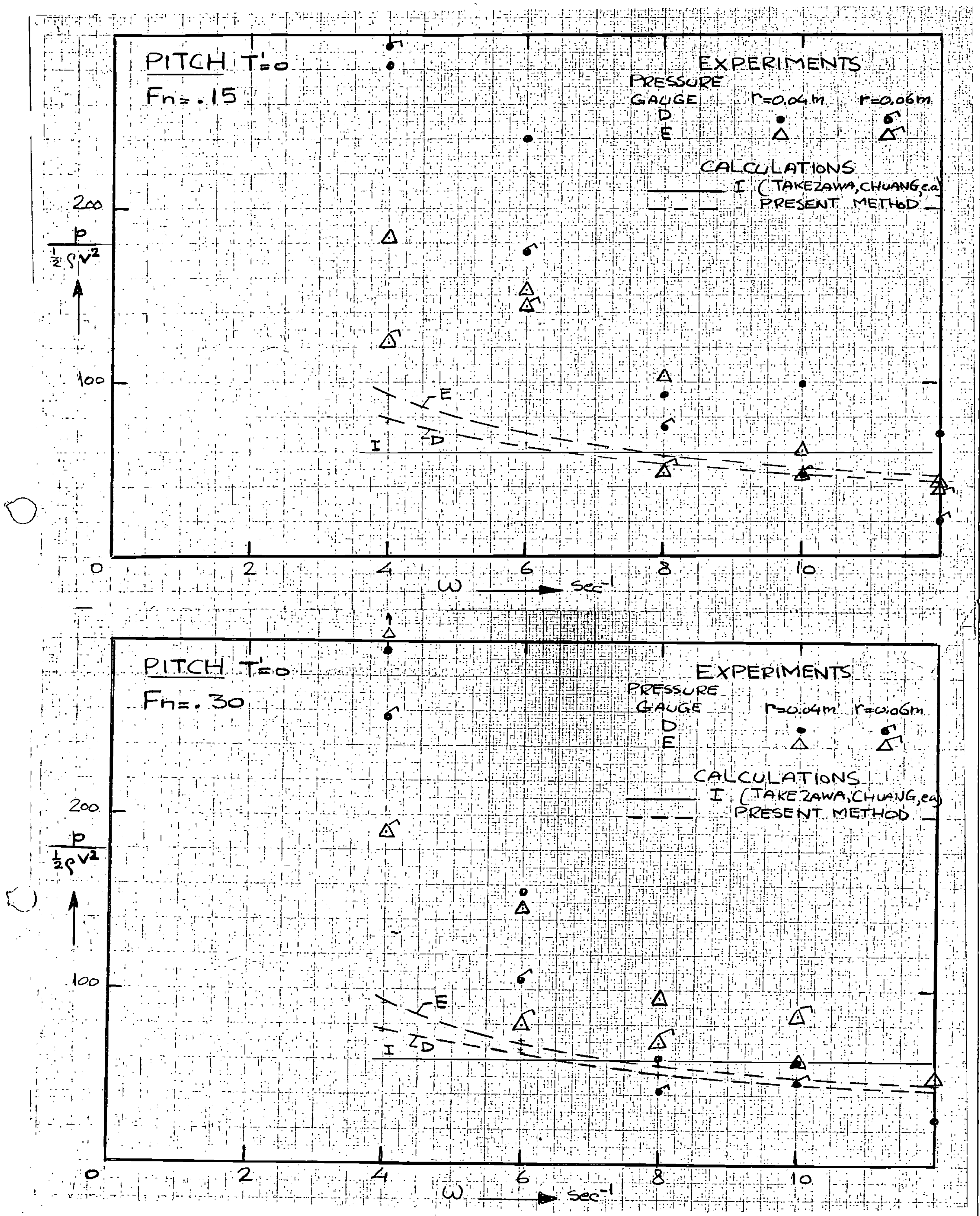

Fig. 15 b Dimensionless peak pressure in relation to frequency of oscillation.

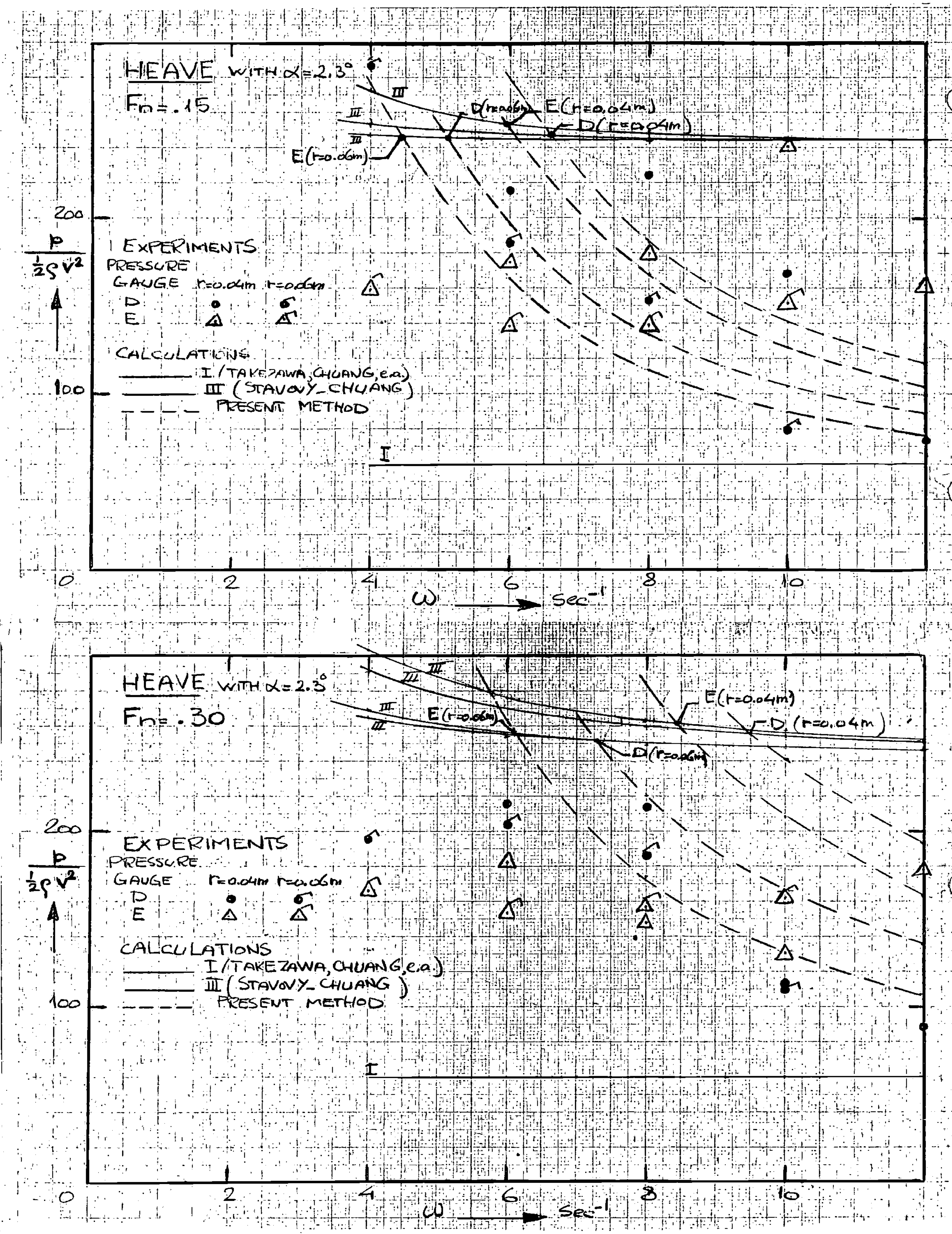

Fig. 15 C Dimensionless peak pressure in relation to frequency of oscillation.